T.R.

EGE UNIVERSITY

Graduate School of Applied and Natural Science

SYNTHESIS OF SILICA NANO PARTICLES, THEIR USAGE IN AUTOMOTIVE HYBRID COATINGS AND EVALUATION OF THEIR PERFORMANCES

Necati GÜDÜMCÜOĞLU

Supervisor: Prof. Dr. Şerife Ş. HELVACI

Chemical Engineering Department

İzmir

2019

Necati GÜDÜMCÜOĞLU tarafından yüksek lisans tezi olarak sunulan "Synthesis of silica nano particles, their usage in automotive hybrid coatings and evaluation of their performances-Silika nano taneciklerinin üretimi, otomotiv hibrit kaplamalarında kullanılması ve performanlarının değerlendirilmesi"başlıklı bu çalışma EÜ Lisansütü Eğitim ve Öğretim Yönetmeliği ile EÜ Fen Bilimleri Enstitüsü Eğitim ve Öğretim Yönergesi'nin ilgili hükümleri uyarınca tarafımızdan değerlendirilerek savunmaya değer bulunmuş ve 11.09.2019 tarihinde yapılan tez savunma sınavında aday oy birliği/oy ~~çokluğu~~ ile başarılı bulunmuştur.

Jüri Üyerleri:		**İmza**
Jüri Başkanı	: Prof. Dr. Şerife Şeref HELVACI	
Raportör Üye	: Prof. Dr. Günseli ÖZDEMİR	
Üye	: Prof. Dr. Sacide Alsoy ALTINKAYA	

EGE ÜNİVERSİTESİ FEN BİLİMLERİ ENSTİTÜSÜ

ETİK KURALLARA UYGUNLUK BEYANI

EÜ Lisansüstü Eğitim ve Öğretim Yönetmeliğinin ilgili hükümleri uyarınca Yüksek Lisans Tezi / Doktora Tezi olarak sunduğum "Silika Nano Taneciklerinin Üretimi, Otomotiv Hibrit Kaplamalarında Kullanılması ve Performanslarının Değerlendirilmesi" başlıklı bu tezin kendi çalışmam olduğunu, sunduğum tüm sonuç, doküman, bilgi ve belgeleri bizzat ve bu tez çalışması kapsamında elde ettiğimi, bu tez çalışmasıyla elde edilmeyen bütün bilgi ve yorumlara atıf yaptığımı ve bunları kaynaklar listesinde usulüne uygun olarak verdiğimi, tez çalışması ve yazımı sırasında patent ve telif haklarını ihlal edici bir davranışımın olmadığını, bu tezin herhangi bir bölümünü bu üniversite veya diğer bir üniversitede başka bir tez çalışması içinde sunmadığımı, bu tezin planlanmasından yazımına kadar bütün safhalarda bilimsel etik kurallarına uygun olarak davrandığımı ve aksinin ortaya çıkması durumunda her türlü yasal sonucu kabul edeceğimi beyan ederim.

11.09.2019

Necati GÜDÜMCÜOĞLU

ÖZET

SİLİKA NANO TANECİKLERİNİN ÜRETİMİ, OTOMOTİV HİBRİT KAPLAMALARINDA KULLANILMASI VE PERFORMANSLARININ DEĞERLENDİRİLMESİ

GÜDÜMCÜOĞLU, Necati

Yüksek Lisans Tezi, Kimya Mühendisliği Anabilim Dalı Tez Danışmanı: Prof. Dr. Şerife Ş. HELVACI

Eylül 2019, 112 sayf

Tez kapsamında otomotiv boya uygulamaları için yüzeyi modifiye edilmiş nano taneciklerin kullanıldığı organik-inorganik hibrit kaplamaların geliştirilmesi ve değerlendirilmesi amaçlanmaktadır. Bu amaç doğrultusunda farklı organic yüzey kaplama kimyasalları ile yüzey modifikasyonları yapılmıştır. Yüzeyi uygun şeklide modifiye edilmiş nano boyuttaki (<100nm) silica taneleri ile Otomotiv sektöründe kullanımı olan iki bileşenli (2K) düşük sıcaklıkta film oluşturma özelliğne sahip transparan kaplamanın (verniğin) geliştirilmesi hedeflenmiştir.

Nano boyuttaki silika taneleri "sol-gel" methodu baz alınarak TEOS'dan üretilmiştir. Yapılan deney tasarımı sonucunda metanol içinde inorganik silika konsantrasyonu 9.54% ve tanecik boyutu 67nm solüsyonun stabil olarak üretimi gerçekleşmiştir.

Üretimi başarı ile gerçekleştirilen içeriği bahsedilen solüsyonun inorganik silika taneciklerinin yüzeyleri farklı fonksiyon grupları içeren silan kimyaları ile modifiye edilmiştir. Yüzeyi modifiye edilen tanelerin karakterizasyonu FTIR, TGA ve SEM analizleri ile yapılmıştır. Yapılan değerlendirmeler sonucunda silika(katı):silan oranının 1:0.5 optimize olduğu görülmüştür.

Bu doğrultuda yüzeyi etkin şekilde kaplanmış olan silika taneleri ile otomotiv sektöründe kullanılacak olan hibrit transparan sonkat kaplamasının, (verniğin) formülasyon tasarımı yapılmıştır. Geliştirilen hibrit transparan sonkat kaplamasının reolojisi, film oluşturma kinetiği, film oluşturma öncesi ve sonrası viskoelastik davranışları ile yüzey fizikokimyası karakterize edilmiştir. Elde edilen sonuçlar doğrultusunda 100 katı bağlayıcıda 1.75 birim katı silika içeriğinin verniğin performansına olumlu etki ettiği ve çizilme direncini referansına göre 80% iyileştirdiği tespit edilmiştir.

Anahtar kelimeler: Sol-gel, silika, yüzeyi modifiye edilmiş nano silika taneleri, Otomotiv, vernik, çizilme direnci,

ABSTRACT

SYNTHESIS OF SILICA NANO PARTICLES, THEIR USAGE IN AUTOMOTIVE HYBRID COATINGS AND EVALUATION OF THEIR PERFORMANCES

GÜDÜMCÜOĞLU, Necati

Master of Science Thesis, Chemical Engineering
Department Supervisor: Prof. Dr. Şerife Ş. HELVACI

September 2019, 112 pages

The aim of the thesis is to develop and evaluate organic-inorganic hybrid coatings using modified nanoparticles for automotive paint applications. For this purpose, surface modifications were performed with different organic surface treatment chemicals. By using surface treated nanoscale (<100nm) silica particles, development of 2K and low bake temperature needed hybrid transparent coating i.e.,clearcoat formulation was tried to design.

Nanoscale silica particles were produced from TEOS based on the “sol-gel” method. As a result of the experimental design, the inorganic silica particle concentration and particle sizes in methanol were obtained as 9.54% and 67nm respectively in addition to being stable.

The surfaces of the inorganic silica particles of the solution, whose production was successfully carried out, were modified with silane chemicals containing different functional groups. Characterization of surface modified silica particles was performed by FTIR, TGA and SEM analyzes. As a result of the evaluations, it was found that optimum silica (solid): silane ratio is 1: 0.5.

As a result, by using surface treated nanoscale silica particles, hybrid transparent topcoat i.e., clearcoat formulation were designed for automotive industry. The rheology of the developed hybrid clearcoat, kinetics of its film

formation, its viscoelastic behavior before and after film formation and its surface physicochemistry were characterized. According to performance evaluation results, 1.75 per hundred resin usage of surface treated silica provided a positive effect on the performance of the hybrid clearcoat and improved its scratch resistance by 80%.

Key Words: Sol-gel, silica, surface modified nano silica particles, automotive, clearcoat, scratch resistance

PREFACE

Organic-inorganic hybrid coatings using modified nanoparticles for automotive paint applications is so critic to enhance overall performances. By using surface treated nanoscale (<100nm) silica particles, 2K and low bake temperature needed hybrid transparent coating i.e.,clearcoat formulation was designed.

I would like to thank my supervisor Prof. Dr. Şerife Ş. HELVACI for her guidance and support throughout this MSc thesis.

İZMİR

11/09/2019

Necati GÜDÜMCÜOĞLU

To my lovely pregnant wife …

Table of Contents

Table of Contents (continued)

Table of Contents (continued)

Table of Contents (continued)

List of Figures

List of Figures (continued)

List of Figures (continued)

List of Figures (continued)

List of Figures (continued)

List of Tables

1. INTRODUCTION

Polymeric materials are commonly used in everywhere and application area increases day to day. Nevertheless, sometimes performance of polymeric materials is needed to be enhanced. Regarding to automotive industry, nowadays organic-inorganic coating systems become more and more popular. Although they have been investigated for a long time, depending on customer expectation, enhancement on coating systems is always desired.

Organic-inorganic systems are called as hybrid composite materials or systems. The basic idea of all performed investigations is to combine the unique properties of inorganic structures (hardness, thermal stability, etc.,) with the unique properties of the organic structures (flexibility, dielectric, processability, etc.). Nevertheless, inorganic structures cannot be distributed homogeneously in the organic phases because of differences in their surface polarity. According to this reason, the surfaces of the inorganic structures are modified or covered by related and suitable chemicals that can match the organic polymeric phase.

In order to enhance the properties of organic coatings especially for automotive coatings, hybrid technology can provide desired properties if inorganic part of system is considerably in nano size which is less than 100nm and suitable surface modified. Because visual and protective performance properties of coating systems are so vital in automotive industry. Incorporation of inorganic nanoparticles into the coating system must not affect the performance of coating system negatively.

The most important point of this thesis is to produce nano-sized and surface modified inorganic structures or particles which can be homogeneously dispersed in different organic coating chemicals used in the automotive coatings industry, to produce organic-inorganic hybrid coatings and to evaluate their performances.

In this thesis, scratch resistance of clear coat used in automotive industry is tried to be improved. Clear coat formulation in automotive industry is applied on the basecoat which contains color and effect pigments (metallic or pearlescent). Clear coat is the top coat that contacts with air. It is commonly formulated with two

components. The fist component is paint (coating) and the second component is described as its hardener.

Clear coats should provide excellent levelling, high gloss, surface appearance, high exterior durability and high chemical and physical resistances as long as its service life. However there are some factors that can affect the mentioned desired properties. UV and IR radiation of sun light, scratch traces and marks, humidity, condensations of water are some critical factors. Although clear coat formulations are designed considering such factors, always there are some limitations on anti-scratch properties. Only polymeric structures do not give enough scratch resistance due to their mechanical properties. The best way is incorporation of inorganic nano particles to organic polymer matrix.

The combination of toughness of organic polymeric substances and hardness of inorganic particles can increase the scratch resistances of clear coat formulation. Alumina and silica nano particles (<100nm) are widely used to improve scratch and abrasion resistance of coating systems. If these particles are untreated, their surfaces are hydrophilic because of –OH on their chemical structure. In automotive coating, hydrophilic properties are commonly not desired. Moreover, addition of hydrophilic nanoparticles to semi or nonpolar coating systems changes their rheological properties generally, increases their viscosity. Especially for clear coat, increase in application viscosity is not acceptable in order to maintain surface leveling and gloss after spray application.

For scratch resistance clear coat formulation, in order to overcome incompatibility issues between nanoparticles and clear coat formulations, hydrophilic characteristic of such particles has to be converted to suitable affinity of organic structure of the clear coat. Surface treatments of nanoparticles can be done with basic or acidic surface affinic agents or suitable silane chemicals

Regarding surface affinities, isoelectric point (IEP) of nanoparticles is needed. If IEP of nanoparticles is less than 7, their surfaces are acidic. Then, basic surface treatment agents has to be used.

Regarding silane chemistries, the commonly used ones are trialkoxysilane. In addition silanes which have different organic functional groups such as epoxy,

amine, vinyl, methacryl etc. functional groups can be chosen depending on chemistry and polarity of coating system. Clear coat formulations are medium polar and considering their film formation chemistries, isocyanate hydroxyl reactions are commonly used in automotive industry. Then, amine, vinyl, methacryl, isocyanate, hydroxyl functional groups can be chosen.

The formation of chemical bond between organic polymers and inorganic particles is considered reasonably in order to maintain suitable chemical film formation. Especially for scratch resistance property of clear coat, location of nanoparticles in film formation is so critical and it should be carefully evaluated.

In this thesis, only silica nanoparticles have been used to improve scratch resistance of clear coat due to their transparency index. Because transparency index of SiO_2 particle is similar to the polymeric structure of the clear coat formulations. SiO_2 nano particles have been tried to synthesize via anhydrous "sol-gel" technique. For "sol-gel" technique, solvent selection has been done. The surfaces of SiO_2 particles have been modified by appropriate chemicals. Modified and unmodified nano SiO_2 particles have been characterized by Fourier-transform infrared spectroscopy (FTIR), **scanning electron microscope** (SEM), **Thermogravimetric analysis** (TGA), and Dynamic light scattering (DLS). Finally, organic-inorganic hybrid clear coat formulation has been improved according to expectations automotive industry.

2. THEORY and LITERATURE SURVEY

2.1. Synthesis of Silica Nano Particles via "Sol-Gel" Technology

Sol-gel technology is widely used to synthesize different kind of materials. With this technology, materials can be produced at desired properties and their properties can be modified in addition to being in low cost. Although sol-gel technique has been used in years, nowadays with innovation in nanotechnology, functional nanoscale particles in addition to microscale particles can also be produced. Therefore, inorganic nanoparticles can be combined with organic materials, then these mixtures are called as hybrid materials.

The nanoscale (<100nm) nature of the substances can provide the new functions and properties. Even if they are outside of nanoscale, depending on functional expectation, they may be also useful but this case is not so common.

The "Sol-gel" technology is so important for production of nanoscale particles. Actually, there are two ways to obtain nanoscale particles. The first one is "*top-down*" process. In this process, bigger structures are tried to be broken down to smaller structures by special~~ly~~ designed energy-intensive milling machines. In order to maintain grinded small particles as stable, their new freshly formed surfaces due to grinding have to be covered by special additives as soon as after they are opened. It is known that required amount of additive is a reasonably high. Disadvantages of top-down processes are high energy consumption, long grinding time and possible contamination coming from mill. The second one is "*bottom-up*" process: "*Sol-gel*" and "*Aerosil*" processes can be considered as "*bottom-up*" process. "*Aerosil"*, nanoscale particle manufacturing, process requires high temperature such as 1000-2500°C which is also called as *pyrogenic process*. However in "sol-gel" process, nanoscale particles are produced from atoms, ions, or molecules at low temperature. These are chosen according to desired properties of nanoscale particles. Basic disadvantage of "*bottom-up*" process is rough sedimentation. In this process, sedimentation tendency of particles should carefully be controlled (Jonschker, 2014).

The "Sol-gel" process begins with the formation of the suspension, continues with the gel formation of the suspension (formation of controlled enlarged granules)

and ends with the solvent extraction from gelled suspension if it is required. Sometimes, solvent extraction is not need. In the system, solvent can be used as carrier of particles. The reagent used in particle production identify the chemical and physical properties of the solid-gel in the colloidal structure in the suspension (Zou et al., 2008).

To produce particles at low temperature starting from soluble precursors, the sol-gel process is mainly preferred. The sol-gel process can be used for not only synthesis nanoparticles and organic-inorganic hybrid structures but also in coating formulations.

The sol-gel method depending on the reagents, used according to method and technique, can be evaluated in two groups as colloidal and polymeric (alkoxide). In both methods, the reagent is dissolved in a suitable solvent: Water is used in colloidal sol-gel method and, alcohol in polymeric one. The hydrolyze reaction is accelerated by using a reactive substance(catalysts, activators) such as acidic (hydrochloric acid etc.) or basic (ammonia etc.) material; and the reactive substance itself forms a network by giving a condensation reaction. The particle formation continues until to reach the required time and temperature. The increase in viscosity is directly related to the degree of network formation. Particle formation differs according to the amount and type of acid and base activators used (Collins, 2012).

The reactions taking place in the sol-gel method depend on the amount and composition of the reagents used, the type of solvent, the amount of water present in the medium and the time given for hydrolysis with water, the chemistry of used catalyst, the pH and concentration of the medium, the order of reaction entities, the mixing time, the mixing efficiency, and the reaction temperature (Niderberger and Pinna, 2009).

2.2. Sol-Gel Process: Hydrolysis and Condensation Reactions

The basic chemical principles of sol to gel transformation for the production of silica based materials are condensation reactions which are the conversion of silanol (Si-OH) and alkoxy (Si-OR) to siloxane (Si-O-Si) compounds. Commonly, SiO_4 tetrahedral structures are used to obtain stable network. This stable network

can be optimized when the number of siloxane bonds are maximized and the number of silanol and alkoxy groups are minimized.

Commonly, aqueous solution type of silicates and silicon alkoxides such as tetramethoxysilane (TMOS) or tetraethoxysilane (TEOS) precursors are used. Aqueous solution of silicates may contain some monomeric silicate impurities and their stability highly depends on pH and temperature. Therefore, some of zinc, titanium, alumina etc. type of alkoxides and TMOS/TEOS are used as reactive substances in nano particles produced by sol -gel method (Mittal, 2011).

The hydrolysis and condensation reactions of sol-gel process can be identified by such reactions as stated in Figure 2.1.

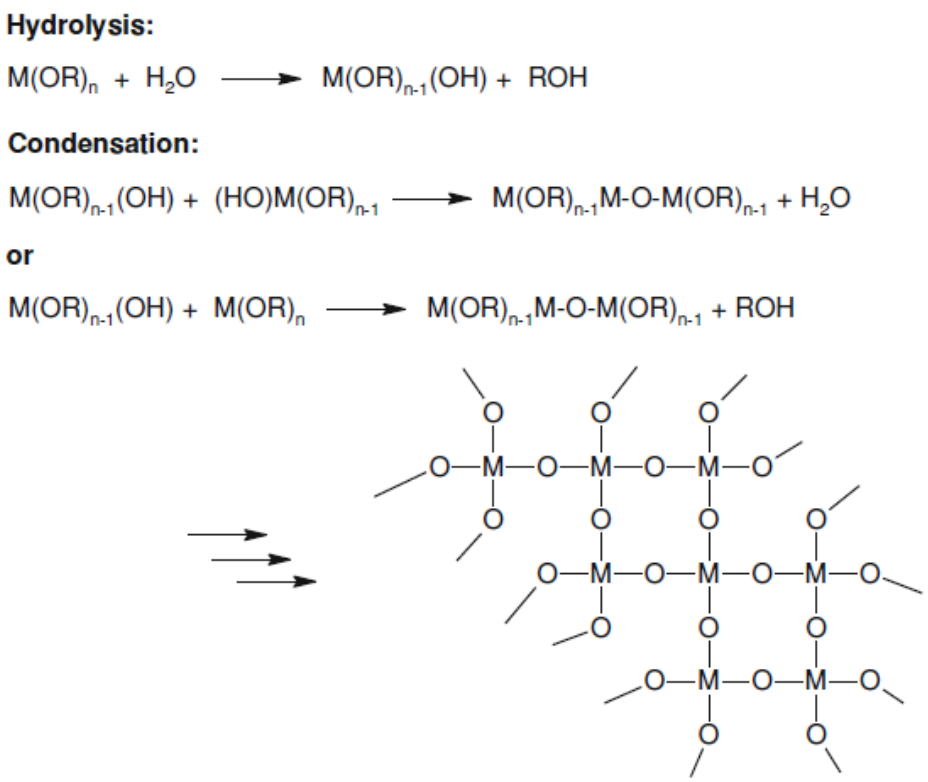

Figure 2.1 The bottom-up chemical reaction in "sol-gel" process and network formation. (Levy and Zayad, 2015)

Hydrolysis reactions of silicon alkoxides are generally so slow. Therefore, suitable catalyst type has to be used to accelerate the reactions. It can be either acidic or basic type. It is also known that catalyst type affects the final structure of "sol-gel" derived network. Generally, although, by using acidic type catalysts, network

structure becomes polymer-like expanded, basic ones gives more particle/grain – like structure. The basic differences can be seen in Figure 2.2.

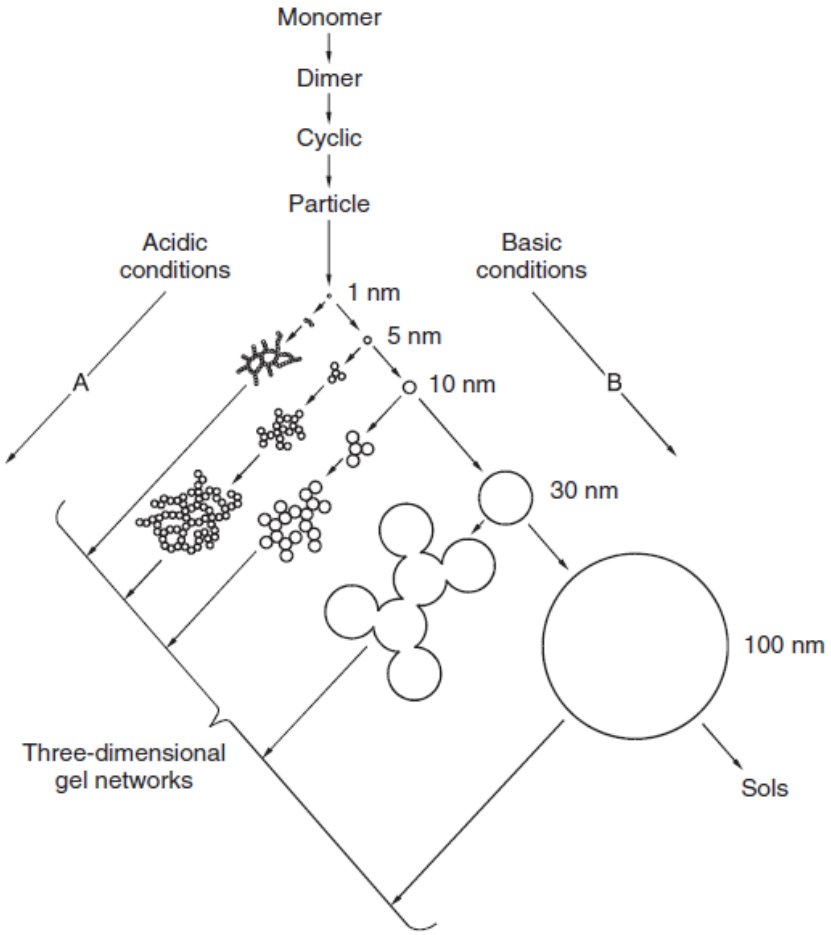

Figure 2.2.Network and structure formations of "sol-gel" technique in presence of basic and acidic conditions (Levy and Zayad, 2015)

In acidic condition, at initial step, alkoxy groups propagate much faster than in which basic condition, and these groups are substituted by water as seen in Figure 2.3. However in basic conditions, the poly-condensation reaction is much faster and it is inversely proportional to number of alkoxy group. In this case, the mechanism is related to interaction between nucleophilic anion and silicon atom of the alkoxysilane. Hydrolysis reaction occurs via negatively charged intermediate. It continues at chain ends and also occurs at inner centers of oligomers. Therefore, small, highly branched, dense and almost spherical structures are formed. In Figure 2.4, condensation and hydrolysis rates are illustrated depending on pH of the medium.

Generally, in such “sol-gel” bottom-up techniques, relatively simple acid and bases are used such as HCl and NH_4OH, respectively. Sol-gel transition is changed by selection of catalyst type.

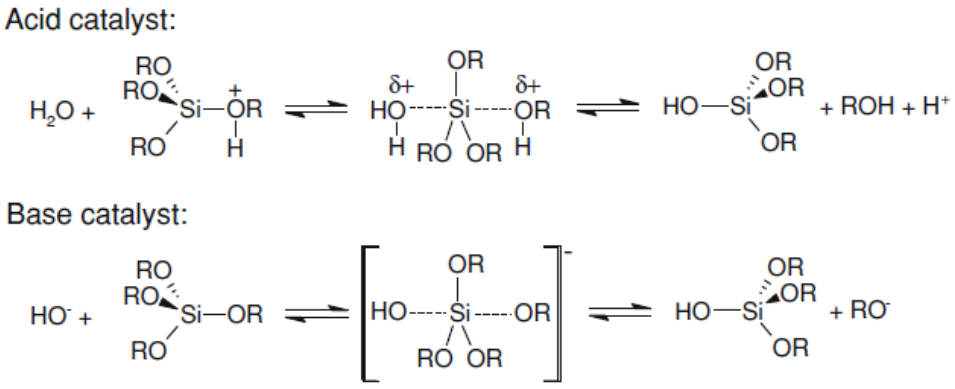

Figure 2.3 Mechanisms of silanol group formation in the presence of acidic and basic catalysts (Levy and Zayad , 2015)

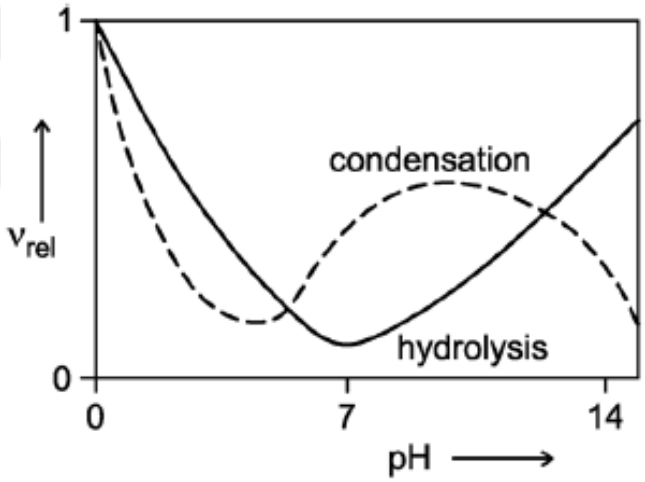

Figure 2.4. Condensation and hydrolysis rates of silicon alkoxides at different reaction pH. (Levy and Zayad, 2015)

In addition to selection of catalyst type, “sol-gel” transition technique depends on temperature, solvent types, pH, amount of precursor and water. The final solid particle has many polar hydroxyl groups, and can be stabilized by hydrogen bonds to the continuous (solvent) phase. Regarding to solvent selection, stability of particles synthesized by “sol-gel” method has to be carefully controlled.

Although aqueous “sol-gel” process are more common, there are also “sol-gel” processes in which protic and aprotic polar solvents can be used.

Polar protic solvents are capable of hydrogen bonding because they contain at least one hydrogen atom connected directly to an electronegative atom (such as O-H or N-H bonds). Polar protic solvents are water, ethanol, methanol, ammonia, acetic acid, and others.

Polar aprotic solvents contain no hydrogen atoms connected directly to an electronegative atom and they are not capable of hydrogen bonding. These are acetone, dimethyl sulfoxide, DMF (N,N-dimethylformamide), acetonitrile, HMF (hydroxymethylfurfural), crown ethers and others.

For polar aprotic sol-gel transition, generally higher temperature are required. Crystalline nanoparticles can be generated via usage of polar aprotic solvents. In the preparation of nanocomposites, it is a seldom used method, due to the mentioned temperature restrictions.

For polar protic sol-gel transition, condensation reactions have to be catalyzed at low temperature. It is known that some of catalyst may contain water. Especially for NH_4OH, it is inevitable due to its solubility nature. In addition water is essential to initiate condensation reaction of sol to gel process. Regarding nature of chemistry, if ternary system stays in miscible zone, sol to gel efficiency is enhanced. Therefore, related phase diagrams should be examined carefully.

In TEOS-alcohol-water ternary phase diagram given in Figure 2.5, Miscibility zone is divided by red line in the figure. As it is seen in Figure 2.5., miscibility zone inversely proportional with TEOS content. (Innocenzi, 2016).

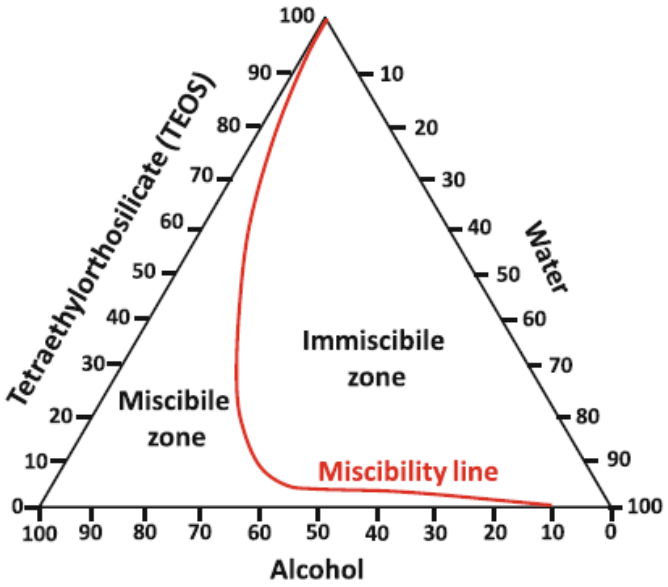

Figure 2.5. TEOS-alcohol-water ternary phase diagram. Continuous phase consists of 95%EtOH+5%H2O (Innocenzi, 2016).

As it is stated before, water is an essential component in the sol-gel synthesis. It is one of the critical parameters to be controlled in the process. It affects poly-condensation kinetics. Water is required to start hydrolysis. Sol to gel transition is strongly dependent on the stoichiometric molar ratio of water to alkoxy. Although this ratio is recommended to be 4, a ratio of 2 is enough for conversion of TEOS into oxide. If amount of water is increased, rate of poly-condensation is also expected to enhance. But, it is not really true. When amount of water is increased while keeping amount of solvent as constant, concentration of the precursor (TEOS) is reduced. When concentration of the precursor is reduced, efficiency of sol to gel conversion is negatively affected (Innocenzi, 2016). The effect of molar ratio of water to TEOS on gelation time can also be seen in Figure 2.6: When H2O: TEOS molar ratio increases up to 4, the required time to obtain the same gel structure decreases. An increase in the concentration of TEOS (a decrease of molar ratio of ethanol to TEOS from 3 to 1) results in a negative effect on rate of gelation

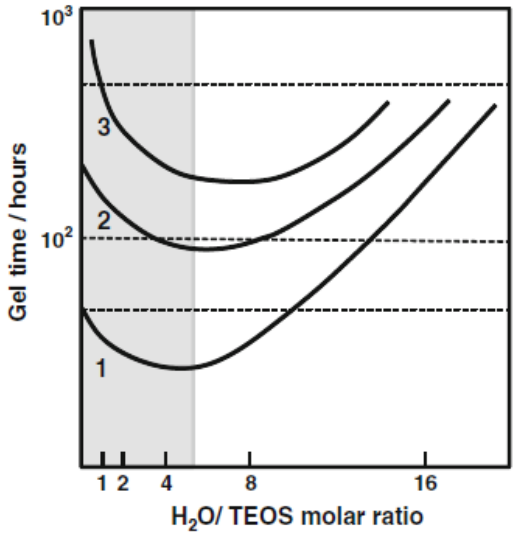

Figure 2.6 Effect of H2O:TEOS and Ethanol: TEOS molar ratios on gelation time (molar ratio of ethanol: TEOS: 1, 2 and 3.) (Innocenzi, 2016).

2.3. Usage of Nano Particles Usage in Automotive Hybrid Coatings

In view of the characteristics of organic coatings used in the automotive industry, the use of nano-sized inorganic materials such as SiO_2, TiO_2 and ZnO is appropriate. Nano-sized SiO_2 particles (particle size below 100 nm) give scratch and corrosion resistance properties to the organic coating formulations. The transparency of SiO_2 particle is similar to the polymeric structure of the organic coating (the refractive index, which is 1.46, is very close to the organic binders) (Fernando and Sung, 2009). In addition, these nano-particles improve the mechanical properties such as tensile, break, compress, toughness, strength, conductivity, chemical-moisture resistance, adhesion to the surface, etc. of the organic coatings in which they are used (Sprenger, 2016).

Nano-sized SiO_2 and MgO particles have a function of artificial anodes with their high surface electrons in the corrosion mechanism (Kar et al., 2015). The nano-sized ZnO exhibits properties of transparency and absorptivity in the visible and UV wavelengths, respectively. ZnO particles absorb the harmful UV light when they are used in organic coating formulations. Therefore, the life time of organic coatings enhance (Fernando and Sung, 2009). Nano-sized TiO_2 particles are used

in self-cleaning organic coating formulations by reason of their high photocatalytic and hydrophilic properties (Zhang et al., 2005). TiO_2 nanoparticles can have super hydrophobic property with silane-functional perfluoropolyether organic binder (Mishra, 2017).

2.4. Treatment, Grafting and Covering of Nano Silica Surfaces

Surface of silica particles are highly polar, therefore they may have poor interactions with their surroundings, formed by organics such as polymers in coating formulations. Mentioned polymers have partially polar characteristics. Due to this polarity difference, surface of silica particles have to be treated and covered to adjust their surface polarity to surrounding medium or coating formulations. For this purpose, silane coupling agents or wetting and dispersing additives can be used.

Surfaces of the nano-sized particles produced by the "sol-gel" method are modified according to chemistry of the organic coating formulation. Silane based chemicals are suitable modification materials for SiO_2. These chemicals include epoxy, vinyl, isocyanate, carboxyl, amine, and alkyl functional groups (Innocenzi, 2016).

2.4.1. Agents for Surface Treatments - Silanes

Silane surface treatment agents are substances which consist of special functional groups which are appropriate for inorganic or organic materials. Silane surface treatment agents act as a simple bridge which provide special bonds from organic to inorganic materials each other. It is the main and desired characteristic, making silane surface treatment agents beneficial and essential for the mechanical strength and adhesion performance and modification of resin and surface enhancements. (Moriguchi et al, 2013)

A general schematic formulation of a silane coupling agent given in Figure 2.7 typically shows two classes of active reactive sides: "-X" represents the reactive hydrolysable group, such as vinyl, epoxy, amino, mercapto, vinyl, hydroxyl,

isocyanate etc., that forms chemical bonds with organic materials such as reactive polymers, having suitable reactant counterparts, in organic coatings. Reaction mechanism on organic materials improves wettability, compatibility and makes chemical bonds with network to be formed organic film coating. "-OR" is other reactive side, such as methoxy and ethoxy groups, which forms chemical bonds with inorganic materials (fillers, extenders and pigments). Features of hydrolyzable silyl groups vary from their chemistry. Whereas, hydroxylation rate of methoxy type is fast, the one of ethoxy type is slow (Brochier et al, 2011). Also, Hydrolysis rate of amine functional silane group with that of methoxy group is compared in Figure 2.8 and it is seen that hydrolysis rate of methoxy type is much quicker than its ethoxy type.

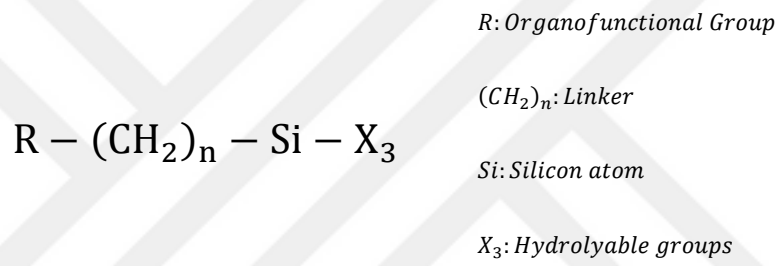

Figure 2.7 *Schematic representation of silane chemistry (Moriguchi et al, 2013)*

After hydrolysis of alkoxy groups, silanol groups are formed. These silanol groups can give strong hydrogen bond with the hydroxyls on the substrate as shown in Figure 2.9. As a results silane surface treatment agents can easily react with inorganic materials if there are enough number of active hydroxyl ends on their surfaces. Glass, silica and alumina materials have large number of hydroxyl groups on their surfaces therefore their reactivity to silanol groups is also high. Silane chemistry is not only used as coupling/treatment agents but also is used as adhesion promoters for such metal, alumina and glass substrates where adhesion performance of organic coatings is not so easy (Moriguchi et al, 2013).

Hyrolysis rate of silanes are also affected by pH of solution. As it is mentioned before in Figure 2.8., generally, silanes having methoxy groups ($-OCH_3$) have higher reactivity than ones having ethoxy groups ($-OC_2H_5$). In acidic conditions, dimethoxy types will hydrolyze the fastest, with respect to by the

trimethoxy, diehoxy and triethoxy types. Nevertheless, in basic conditions the reactivity order changes from the fastest to the slowest as following; trimethoxy, dimethoxy, triehoxy and diethoxy respectively. Hydrolytic properties are illustrated in Figure 2.10.

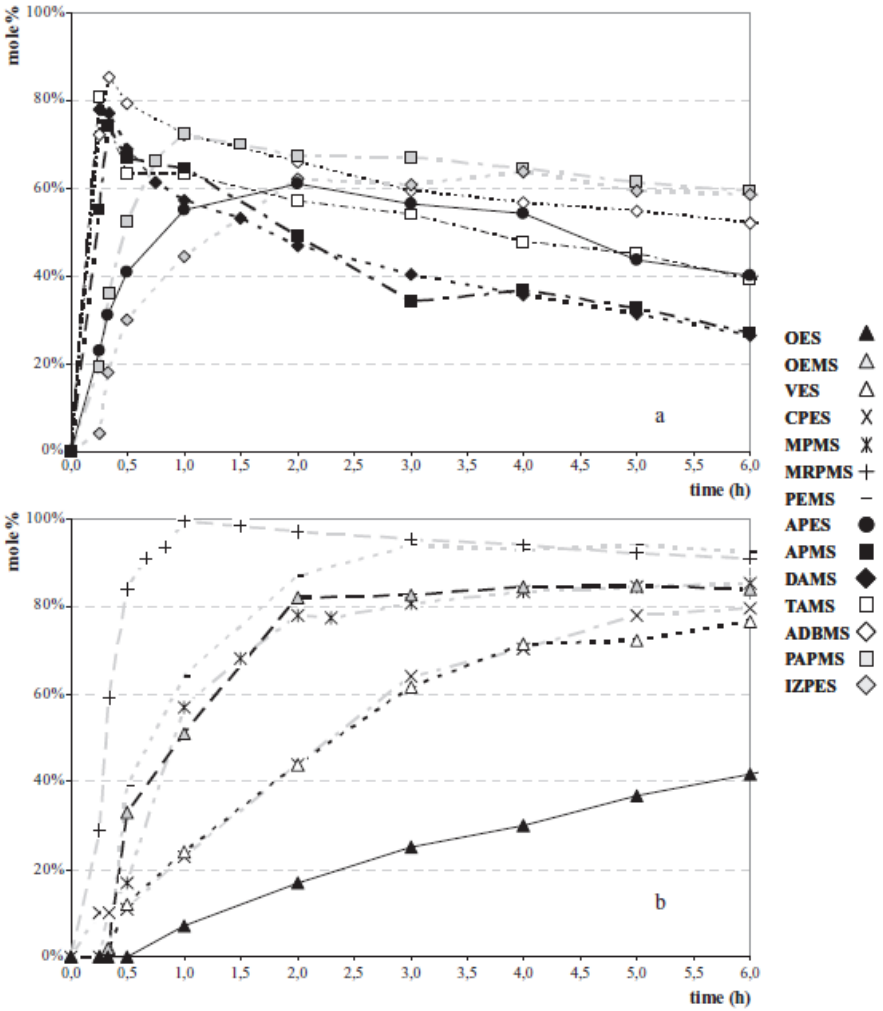

Figure 2.8 Comparison of hydrolysis rate of silanes having different functional groups. Silanes having a) amine and b) other functional groups (Brochier et al, 2011)

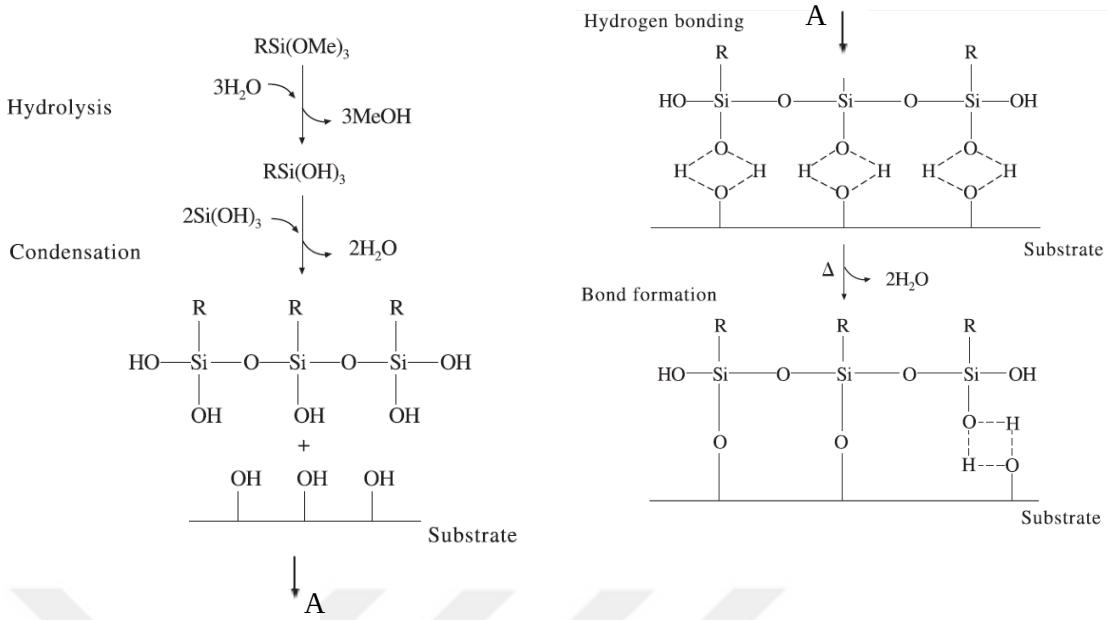

Figure 2.9 Hydrolic Deposition of Silanes (Arkles, 2006)

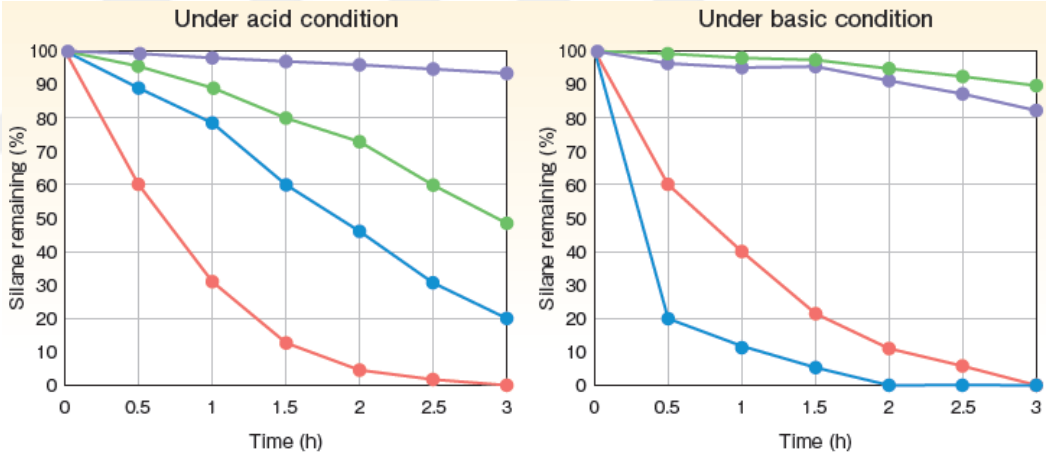

Figure 2.10 Hydrolytic properties of alkoxy groups of silanes at acidic and basic conditions. (orange:dimethoxy, blue:trimethoxy, green:diethoxy,purple:triethoxy) (Arkles, 2006)

2.4.2. Wetting and Dispersing Additives

In physical chemistry, wetting phenomena refer to the displacement of air, and adhered/absorbed water or contaminated impurities, from the surface layer of organic or inorganic particles and aggregates in the solution of polymers, additives and organic solvents. Total of them is called as *organic coating formulation in automotive industry*.

In order to maintain desired wetting performance, the surface tension of organic coating formulation has to be lower than the surface free energy of the pigment. This is necessary for all inorganic and organic pigments. At this point, the rate of wetting is so critical and can vary depending on different chemistry of wetting additives, which should be chosen to let the organic coating formulation to penetrate through into the pigment aggregates.

The rate of wetting is related to the viscosity of the carrier medium (polymer, additive and solvent), the stirring rate, and the surface tension. Surface tension difference in aqueous media (67-72mN/m) is higher than in solvent borne one (20-30 mN/m). In this case, suitable surfactant blends can be used to accelerate wetting procedure rate.

Wetting and separation of organic and inorganic microscale particles are essential steps. In organic solvent systems, there can be rarely a problem. On the contrary, stabilization of particles to be wetted can frequently be challenging problem. If the dispersion of particles could not be stabilized, the particles inside the dispersion can attach to each other and be flocculated. Flocculation can be considered as a type of aggregation but flocs formed do not come together like status of the aggregates in the dry powders. Flocculation is a reversible step, so the flocs can be unflocculated by applying considerably low shear stresses.

The wetting of the particle agglomerates by the binder or solvent solution is affected by many factors such as surface affinity (treatment), and surface free energy (polarity) differences of particles.

The penetration speed of the liquid phase, V into the gap within the agglomerates can be mathematically expressed

$$V = \frac{dl}{dt} = \left(\frac{r}{2l\eta}\right)(\sigma cos\theta) \qquad (2.1)$$

by Washburn equation. In this equation, l, t, r, σ, μ and θ is penetration depth, time, capillary radius between the particles, surface tension of the liquid phase, viscosity of liquid phase and contact angle, respectively.

Regarding first term ($\frac{r}{2l\mu}$), for loosely packed particle agglomerates (r is large), low viscosity of liquid phase is favorable. However, in organic coating formulation, viscosity reduction is limited due to application expectation in customer lines. (Zeno et al, 2007)

The second term ($\gamma\cos\theta$) in the equation includes wetting properties of wetting additives such as are the surface tension of the penetrating liquid and the contact angle. It has to be taken into account that they are not independent from each other. Having high surface tension together with low contact angle is not possible. In practice, wetting additives are used to decrease the surface tension as far as necessary to make the contact angle close to zero to penetrate completely (Streitberger and Dössel, 2008).

Characteristics of wetting agents can be classified according to chemical structure of surfactants. Generally a surfactant molecule consists of two functional (active) groups as polar (hydrophilic) and nonpolar (hydrophobic). As a result of such combination, such compounds become interface-active. In other word, the wetting additives can easily migrate to the particle/binder solution interface. Therefore, wetting and incompatibility issues can be solved. From a chemical point of view, wetting additives can be classified as either being ionic or being non-ionic. Generally non-polar part is represented by hydrocarbon chains whereas polar one is for particle affinic side. (Streitberger and Dössel, 2008)

The reason of flocculation in the medium is due to the attractive “London-van der Waal” forces occurring between the particles. These forces are only reasonable effective only in small distances. However, the “Brownian” molecular motions of particles result to come particles together and collide and create flocculation. In order to stabilize a system against flocculation due mentioned “Brownian” molecular motion, between the particles, reasonable repelling forces must be provided. (Streitberger and Dössel, 2008)

Special designed wetting additives have two functional sides as explained before. One is particle-affinic groups (polar) and second one is binder-compatible chains (less polar). Such additives can; not only stabilize the pigment dispersion by

steric hindrance, but also behave as wetting additives. In other words, such additive can be used as dispersing and surface wetting of the particles.

The stability performance of the aqueous dispersions is pH dependent since pH changes the surface charges of particles. Fundamentally, isoelectric point (IEP) can be described as pH at which surface or particle has no charge. In other words, surface charge is zero. Above IEP, the surface charge is negative and below IEP, its charge is positive. The stability of aqueous dispersions can be maintained at IEP ±1 pH. The IEP value can differ from particle to particle: For example, IEP is 4.8 for kaolin clay, 9 for calcite, 4-8 for titanium dioxide and 2.2 for silicon dioxide (Jones et al, 2017)

For non-aqueous or solvent borne systems, IEP point can also be used to analyze surface properties of particles. If IEP point is acidic, wetting and dispersing additives should be basic (Fairhurst, 2013).

2.4.3. Control of Stability / Dispersibility Performance of Nano SiO2 Particles, Synthesized by Sol-Gel Method Using Hansen Solubility Parameters (HSP)

Solubility parameter approach has been widely used for predicting and understanding polymer solubility. Hansen Solubility Parameters (HSP) are based on the total liquid evaporation energy and are evaluated in three parts: In these individual parts dispersion atomic, molecular dipole, and hydrogen bonding forces can be seen. Required energy for evaporating the liquid and breaking all the cohesive bonds is called as total cohesive energy, E. Therefore, the total cohesive energy can also be thought as energy of vaporization. It should also be noted that individual interaction between solvent molecules result these cohesive energies. Therefore the theory of HSP approach is very simple and it can be used in different kind of applications.

Materials having similar HSP can be thought as self-affinity. However, the same assumption cannot be considered for Hildebrand solubility parameter. For example, according to total solubility parameters, ethanol and nitromethane have be identically similar. Their total solubility parameters are 26.1 and 25.1 MPa ½,

respectively. Nevertheless their affinities are quite different. Although ethanol is soluble in water, nitromethane is not. There many similar examples. Unfortunately, Hildebrand could never help to predict such kind of examples. By using HSP concept, necessary prediction related to example can be easily carried out. (Hansen, 2002)

Significant form of energies related to HSP can be summarized as follow:

Dispersion forces (atomic) are related to van der Waals interactions between the atoms of the two molecules.

Polar forces (molecular) are related to dipole-dipole moment interaction. Polar interaction can be seen in almost all kind of molecules.

Hydrogen bond forces (molecular) are typical of polar forces related to hydrogen to fluorine, oxygen and nitrogen elements. In contrast, such forces are thought as some kind of electron exchange. That is the main reason of why CO2 shows strong hydrogen bonding forces even it does not have hydrogen molecule. (Abbott and Hansen, 2008)

The total cohesion energy, E, can be calculated using molar volume (V) of solvent and total Hansen solubility parameter (δ), consisting of disperse (δd), polar (δp) and hydrogen (δh) components:

$$E = E_D + E_P + E_H \tag{2.2}$$

$$E/V = E_D/V + E_P/V + E_H/V \tag{2.3}$$

$$\delta^2 = \delta_D^2 + \delta_P^2 + \delta_H^2 \tag{2.4}$$

The solubility parameter δd, δp, and δh can be located in 3-dimensional Cartesian coordinate system as illustrated in Figure 2.11.

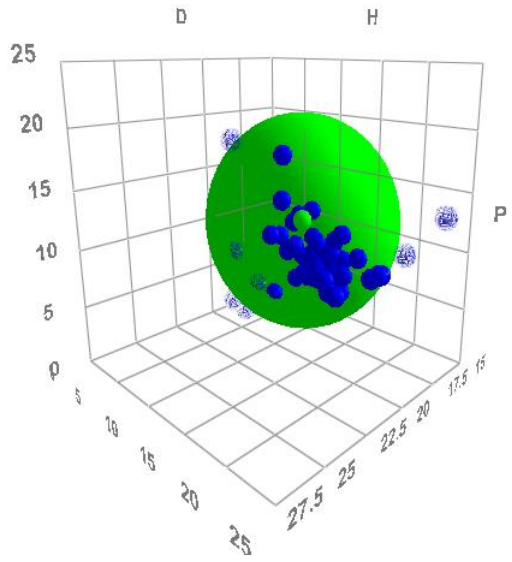

Figure 2.11 HSP solubility axes and solubility sphere (Abbott and Hansen, 2008)

In the literature, there are many different methods to evaluate solvents Due to complexity of solvent-polymer interactions, the most suitable solvent-polymer interaction method must be selected. Usage of HSP can allow to select possible solvent combinations for organic coatings. Hansen's theory of solubility parameters is a valuable semi-quantitative method of solvent selection and reformulation in the coatings industry.

Flocculation (cohesion) tendencies of pigments, fillers and extenders can be evaluated by observing their dispersion or sedimentation properties in different solvents. According to surface characteristics of the particles, some particles can adsorb some part of solvents and be suspended, so the sedimentation of the particles retards. In the suspension or sedimentation behavior, differences between densities of solvent and particle and viscosity of solvent are critical.

"Relative sedimentation rate" (RST) can give an idea about dispersion of particle in given solvent. RST can be determined by following equation. (Hansen, 2002)

$$RST = t_s(\rho_p - \rho_s)/\mu \qquad (2.5)$$

In the equation, t_s is sedimentation time, ρp and ρs are densities of particle and solvent, respectively, and μ is the viscosity of solvent. This can be used for either micro or nanoscale particles.

2.4.4. Determination of Isoelectric Point (IEP) of Nanoscale Particles by Using Zeta Potential Measurement

Zeta potential measurement is used to determine the stability of dispersions and it can be affected by the surface chemistry of the solid particles. The surface chemistry of particles can be modified by changing the pH, surfactant, salt concentration and special surface treatments. To choose appropriate wetting additive chemicals, isoelectric points of solid particles (IEP) are a guide. IEP is basically the pH at which zeta potential of suspension or solution is zero.

Zeta potential can be defined as potential difference between the dispersed solution medium and the layer of fluid attached to the surface of the dispersed particle as shown in Figure 2.12.

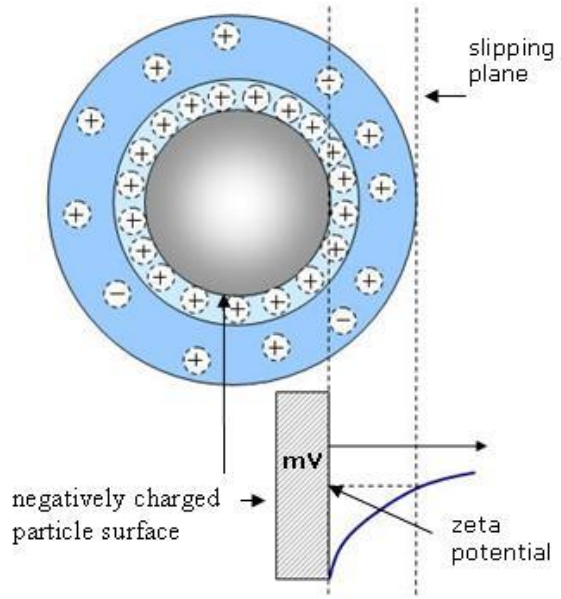

Figure 2.12 Schematic representation of zeta potential of a negatively charged particle (Bodycomb, J., & Scientific, 2014)

The charge or zeta potential of particles and molecules can be determined by measuring their movement as a result the velocity due to electrophoresis. Zeta potential can be calculated by theories established using proper equipment.

In colloidal chemistry principles, electrostatically stabilized dispersion systems can be obtained when their zeta potential is less than -30 mV and greater than +30mV. Dispersions having zeta potential between -30mV and +30mV lose their stability. IEP point is related to pH of this unstable region. If the unstable region can correctly be determined correctly, in order to prevent agglomeration, suitable wetting and dispersing additives can be used.

In Figure 2.13, it is seen that pH of sample A (blue) is 4 at IEP. Therefore, wetting additives at basic characteristics can be chosen to prevent flocculation and to provide stability of particulate dispersions.

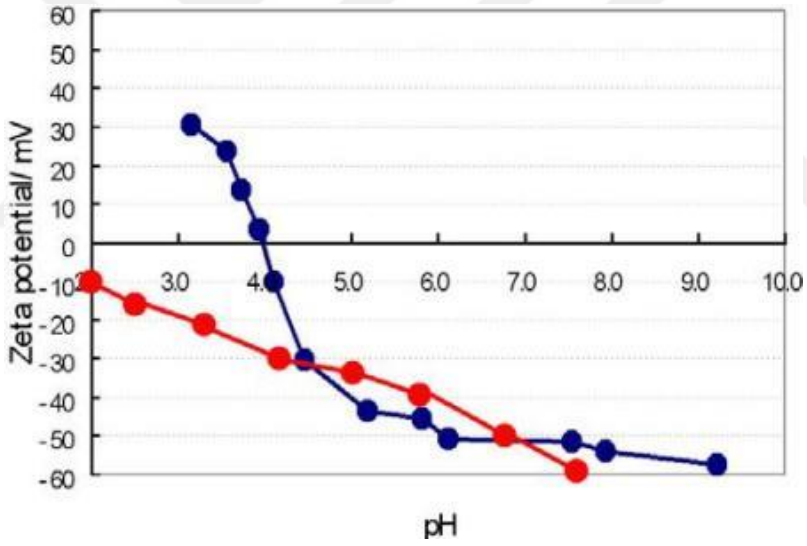

Figure 2.13 Isoelectric point determination of sample A (blue) and sample B (red) (Bodycomb and Scientific, 2014)

2.5. Determination of Particle Size of Nano SiO_2 Particles synthesized by Sol-gel Method

Dynamic light scattering (DLS) and Scanning Electron Microscopy (SEM) techniques are used to determine particle size distribution of nano sized silica particles.

2.5.1. DLS Technique

Dynamic Light Scattering (DLS) is the best reliable technique to measure the size of colloids, nanoparticles and molecules. In this particle size measurement technique, there is no need to mix the sample for making suitable for analysis. In addition, actual size of particles which are obtained from “sol-gel” processes even if they are in nanoscale can directly be measured.

The principle of dynamic light scattering depends on the Brownian motion of the particles which can be measured if only viscosity and temperature of the sample are known. Viscosity information should be provided according to temperature measurement. It is known that Brownian motions vary depending particle size, temperature, viscosity and diffusion coefficient of sample medium.

In DLS technique, “Z-average” or mean size are measured and compared. It should be noted that “Z-average” is hydrodynamic diameter therefore it is only used for the dispersions or, molecules in the solutions. In order to obtain reliable measurement in DLS, polydispersity index (PdI) and intercept values have carefully to be evaluated. PdI should be less than 0.7 and Intercept, more than 0.6, favorably 0.9 (Malvern, 2011).

2.5.2. Scanning Electron Microscope (SEM) Technique

Scanning Electron Microscopes (SEM) scan a sample with a focused electron beam and deliver images with information about the samples’ topography and composition. Dimensions of nanoscale particles can easily be measured visually using SEM images given in Figure 2.14.

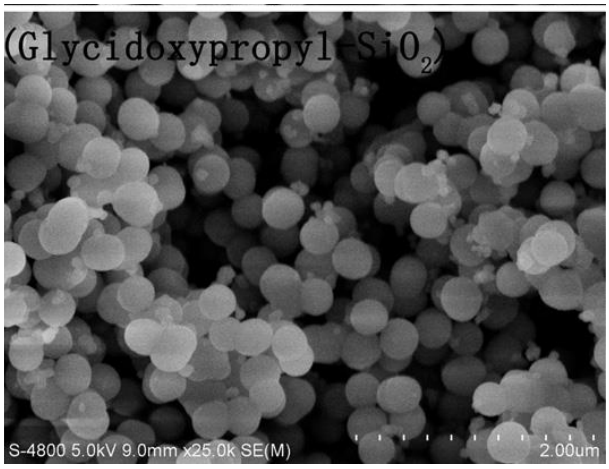

Figure 2.14 FE-SEM pattern of surface treated SiO2 (Perruzzo et al, 2016)

2.6. FTIR Spectrum of Nano SiO_2 Particles Synthesized by Sol-gel Method

Analysis of Fourier-transform infrared (FTIR) spectra of pure and surface treated silicon dioxide particles are given in Figure 2.15. It is seen that all spectra show a strong broad peak at 1100cm-1 corresponding to “Si-O-Si” groups. 469 cm-1 belongs to bending modes of “Si-O-Si” groups. The peak at 3420 cm-1 and 794 cm-1 are related to “Si-OH” and “Si-O” bonds, respectively.

Regarding to surface treated silicon dioxide particles, the peaks at 2853 cm-1 ,2923 cm-1 and 1410 cm-1 are related to “–CH= “, “=CH2” and “Si-CH=CH2” respectively. Surface treatment efficiency can be analyzed from 1410 cm-1 for vinyl type of surface treatment (Lin et al, 2012).

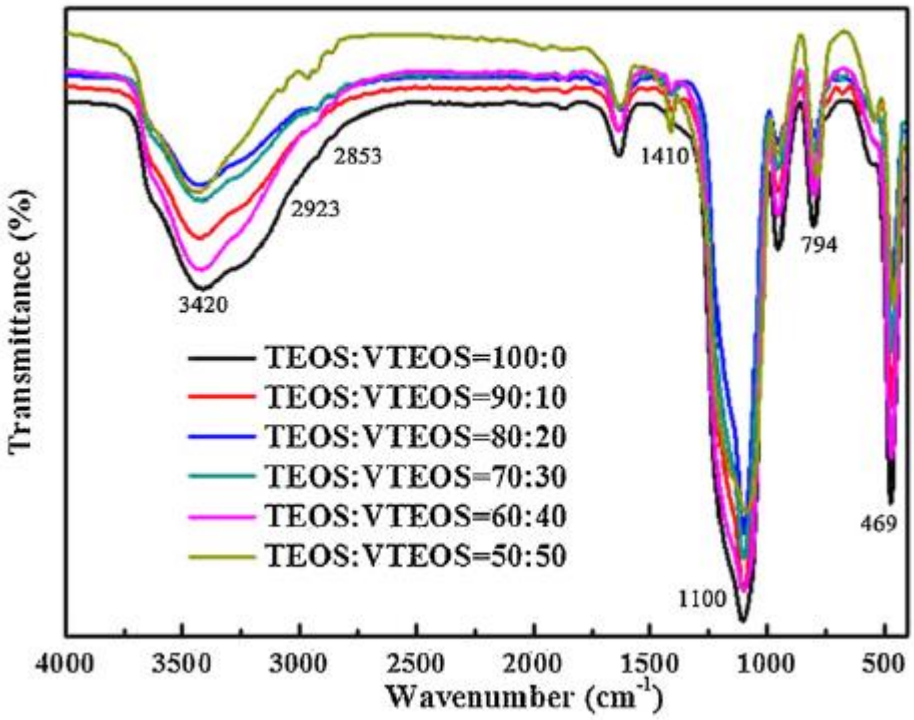

Figure 2.15 FTIR spectrum of pure and vinyl treated silica particles (Lin et al, 2012)

2.7. Thermal Gravimetric Analysis (TGA) of Nano SiO_2 Particles Synthesized by Sol-Gel Method

TGA analysis also gives idea of surface treatment efficiency of inorganic particles. The temperature dependent weight differences of pure and surface treated inorganic particles is basically used.

Weight loss up to 120°C can be considered as due to moisture and possible absorbed solvent. After 120°C, organic surface treatment agents evaporate then burn up to 800°C. TGA curves in terms of percentage of weight loss depending on surface treatment agent used given in Figure 2.16 indicate that the percentage of the weight loss increases with increasing amount of surface treatment agent.

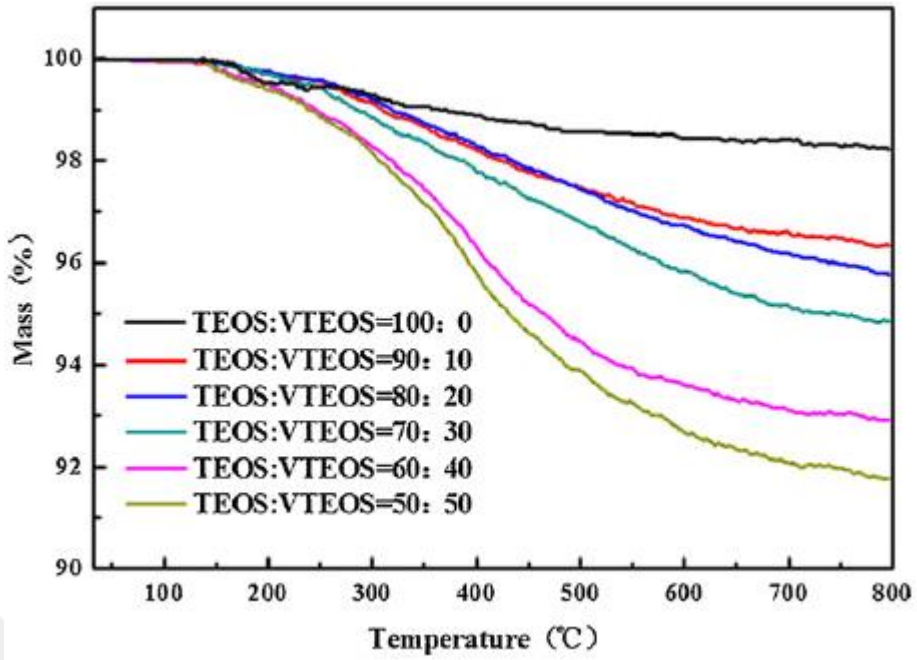

Figure 2.16 . TGA curves of pure and vinyl treated silica particles (Lin et al, 2012)

2.8. Enhancement Evaluations of Properties of Automotive Clear Coat

2.8.1. Rheology

Rheology science generally is basically related flow and deformation Strain and stress terms can be used to understand physical properties of liquids and solids. When substance is under an external force, strain is observed in both solid and liquid materials.

The flow properties in other terms rheology of coatings are critical for proper application and appearance of films. For example, in spray application of an organic coatings (paints), the rheological flow properties control the sedimentation of pigment during storage, how much paint is sprayed and transferred to the surface, dry film thickness, leveling of the applied film, and anti-sagging performance of the film. So, rheology measurements are important organic coatings in the automotive industry.

Shear flow can be defined and modeled as seen in Figure 2.17 In Figure 2.17, the lower plate is fixed whereas the upper plate is movable. The thickness between the parallel plates is assumed to be "*x*". The force "*F*" is applied parallel to movable plate having area "*A*" with velocity "*v*". In the model there is no slip at the plate-fluid interfaces and the fluid is inertia free. The upper plate moving with v velocity results in starting a movement of fluid layer adjacent to the plate this flow is also transferred to other adjacent fluid layer. In the model the velocity of the bottom plate is close to zero because the bottom plate is stationary. Therefore, the velocity gradient between two successive layers of fluid (dv/dx) is constant. This ratio is known as shear rate ($\dot{\gamma}$) whose unit is s^{-1}.

$$\dot{\gamma} = \frac{dv}{dx} = \frac{v}{x}; \frac{cm\ s^{-1}}{cm} = s^{-1} \tag{2.6}$$

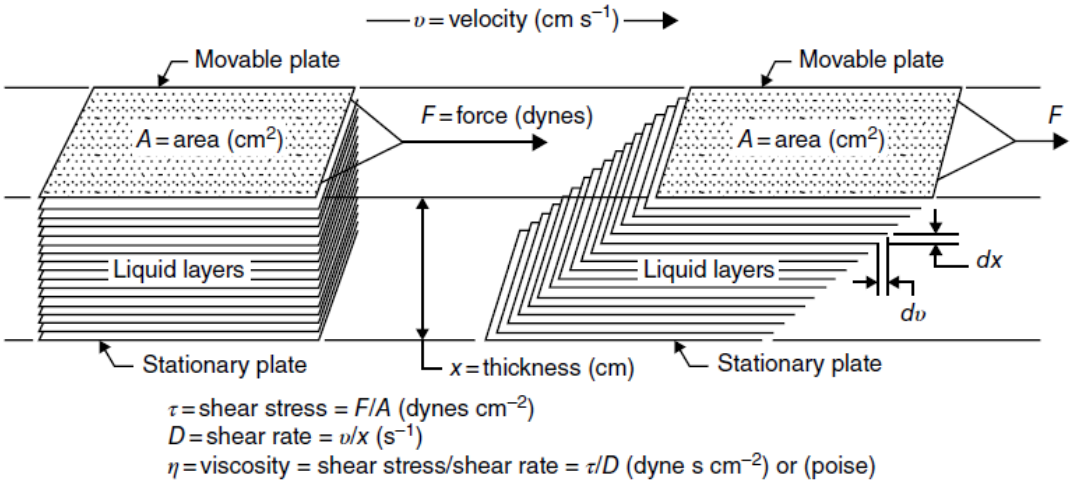

Figure 2.17 Model of shear flow of an ideal liquid and definition of viscosity (Jones et al, 2017)

With acting force "*F*" on the top plate having area "*A*", shear stress (τ) can be determined. Its unit is "Pa". The overall resistance of liquid to flow is called as viscosity which is ratio of shear stress to shear rate. Unit of viscosity is "Pa.s" It should also be noted that viscosity of liquid changes with temperature.

$$\tau = \frac{\mathrm{F}}{\mathrm{A}}; \quad \text{units: m kg s}^2\text{m}^{-2} = \text{Nm}^{-2} = \text{Pa} \tag{2.7}$$

$$\eta = \frac{\tau}{\dot{\gamma}}\ ; \frac{Pa}{s^{-1}} = Pa.s \tag{2.8}$$

For giving some guidance for shear rate present in coating industry, values given in Figure 2.18 can be taken into account. For example although spraying process takes place at the highest shear rates (10000 s^{-1}) resulting in low viscosity, settling process becomes efficient at the lowest shear rates (< 0.01 s^{-1}), so high viscosity.

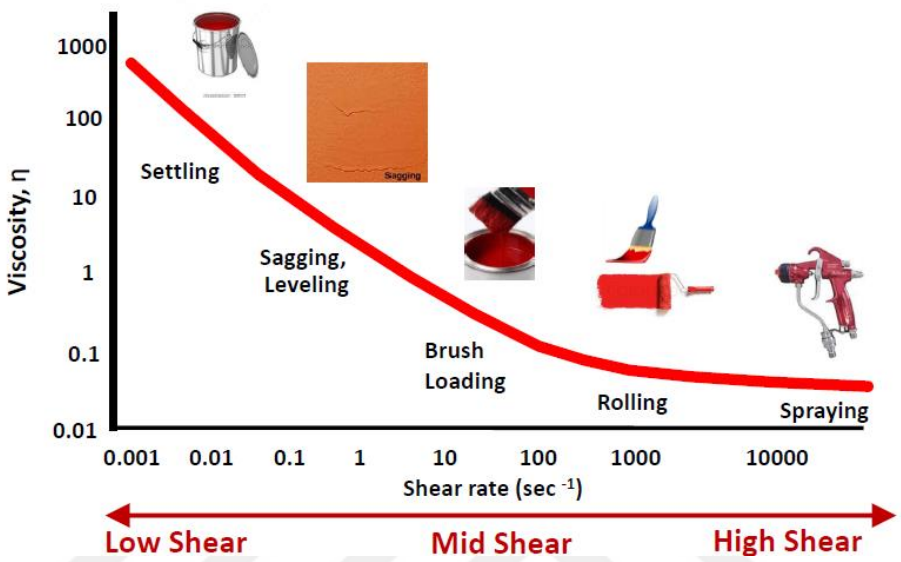

Figure 2.18 Schematic representation of typical values of shear rates and corresponding viscosities (Paar, 2015)

Newtonian liquids can be defined when the ratio of shear stress to shear rate is constant (Figure 2.19 (a)). In the figure viscosity is basically slope of the line. Therefore, for Newtonian fluids, viscosity becomes independent of shear rate. Water, olive oil, ethanol etc. can be given as example to Newtonian fluids.

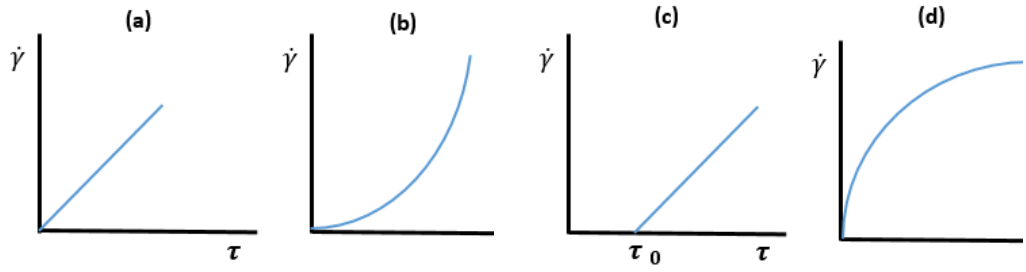

Figure 2.19 Schematic representation of shear rate "$\dot{\gamma}$" vs shear stress "τ" relations of (a) Newtonian (b) Shear-thinning (c) Bingham plastic and (d) Shear thickening liquids

Many liquids show Non-Newtonian behavior (Figures 2.19 (b)-(d)). In this case the ratio of shear stress to shear rate is not constant. Non-Newtonian fluids of which rheological behavior is given in Figure 2.19 (b) and (d) are considered as "*shear-thinning*" and "*shear-thickening*" fluids, respectively. Viscosity decreases with increasing shear rate in *shear-thinning* liquids whereas the viscosity increases with increasing shear rate in *shear thickening* ones.

In *shear-thinning* liquids (Figure 2.19(b)) when stress applied to liquids, their molecules line up parallel to flow direction and the stress (as a result viscosity) decreases due to a decrease in resistance to flow. Such kind of fluids can be diluted or semi –diluted solutions or dispersions, inks, orange juice and organic coating or paints.

Organic coatings are exposed to high shear rate depending application technique. However, the most common application technique in automotive coating industry is spray. To spray a (spray) gun similar to that illustrated in Figure 2.20 is generally used at high shear rates as mentioned in Figure 2.18. Estimated range of shear rates in spray applications is between 1000 to 10000 s^{-1}. Accordingly, at such high shear rates, rheology of organic coatings should indicate shear thinning behavior.

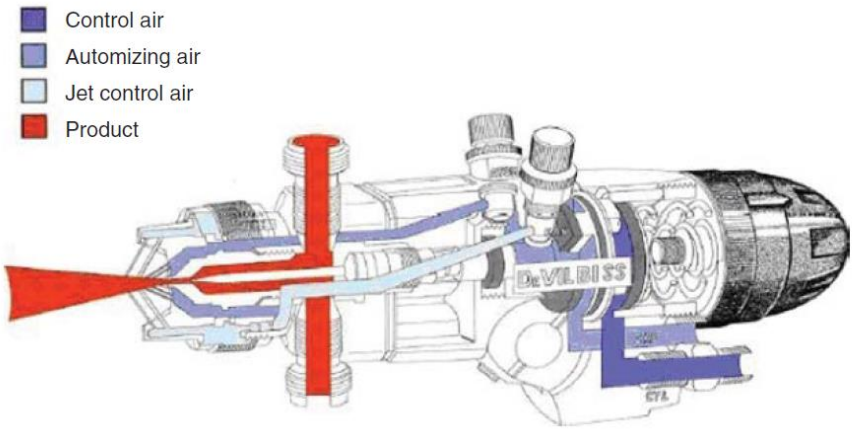

Figure 2.20 Schematic diagram of a pneumatic spray gun (Streitberger and Dössel, 2008)

In organic coating formulations, orientation of dispersion is random at rest but they are shear oriented under the stress and parallel to flow. Other ingredient of

organic coatings is polymers. They are entangled at rest but shear oriented-stretching under the stress and parallel to flow. Regarding emulsion droplets, they are resized under the stress. Their shapes become elliptical from spherical. In addition if there are possible aggregates, they are separated under the stress and broken into smaller particles. (Figure 2.21)

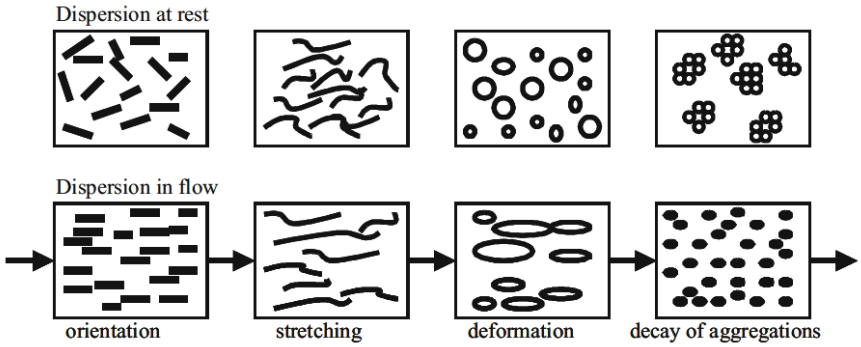

Figure 2.21 Flow characteristics of dispersion at rest and in flow. (Paar, 2015; Malkin and Isayev, 2017)

There are such liquids require some amount of shear stress to flow. Such fluids are called as “Bingham Plastic”. This minimum required shear stress is called the “yield stess”. (Figure 2.19-c)

In “shear-thickening” liquids when stress applied to liquids, their molecules don not line up parallel to direction of flow and the stress as a result viscosity increases due to increase in resistance to flow. (Figure 2.19-d). Such kind of fluids can be also called as “dilatant” fluids. Examples for “shear thickening” liquids are pigment and resin dispersions if the concentration of dispersed phase is sufficiently high enough so pigment particles approach their close packed states randomly. If required amount of stress is applied to make the dispersion to flow, only some microscopic voids are created within close packed dispersion therefore its viscosity increases. (Figure 2.22) Shear thickening is commonly a result of non-spherical particles, high concentration, rough particle surfaces and high shear rates (Malkin and Isayev,, 2017)

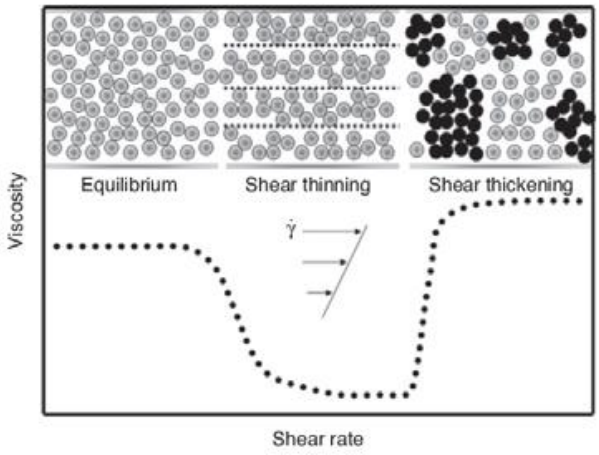

Figure 2.22 Schematic viscosity- shear rate diagram of close packed "shear thickening" liquid (Malkin and Isayev, 2017)

As it is known that some fluids can have time dependent of viscosity change, as it is illustrated in Figure 2.23. Viscosity of fluid tends to decrease at high shear rate and as soon as after shear rate stops, viscosity of fluid tends to increase or reach its initial state of viscosity. Such kind of time dependent viscosity behavior can be called as "thixotropic flow"

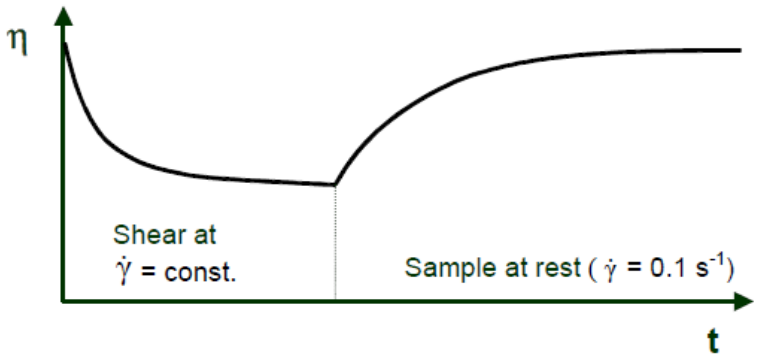

Figure 2.23 Viscosity –time curve of thixotropic fluids (Jones et al, 2017)

Thixotropic fluids are shear thinning fluids. In addition, their viscosity is dependent on time, pressure, shear rate/shear stress and time of shear (shear history). It can be stated that all thixotropic fluids are shear thinning fluids, but all shear thinning systems may not be thixotropic. (Malkin and Isayev 2017)

In order to understand “thixotropic” characteristic of fluid, shear stress vs shear rate graph can be analyzed. The area between two curves (“hysteresis area”) give information about the time-dependent flow behavior. When mentioned area between the curve increases, the material can be assumed as more thixotropic (Figure 2.24)

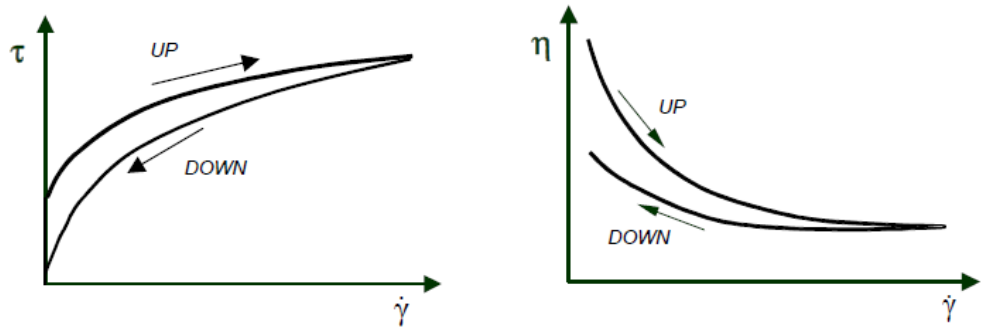

Figure 2.24 Flow and viscosity curves of “shear-thinning” and “thixotropic” material (Jones et al, 2017)

“Thixotropic” behavior is a necessary for all kind of paint systems because only by using this time dependent flow property, sedimentation /settling of paint can be retarded. Application characteristics (leveling appearances etc.) can be optimized. After the paint application, sagging and dripping tendency can be minimized. Thixotropic behavior is usually generated by reversible formation of a weak structure within paint. These weak interactions are broken upon shear rate and regained after given a sufficient time. This process of viscosity decrease and increase can be repeated as often as desired.

In order to make correct “thixotropic” behavior comparison, It should be noted that thixotropic behavior depends on time. Although “hysteresis area” do not give any information of shear rate history, viscosity-time curve (Figure 2.23) can give enough information to analyze “thixotropic” behavior of fluids. In addition such time dependent viscosity curve can give information about leveling, sagging performance after shear rate corresponding application technique.

On the other hands “*rheopetric*” fluids show opposite properties of “*thixotropic*” fluids. Viscosity of “*rheopetric*” fluid tends to increase at high shear rate and as soon as after shear rate stops, viscosity of fluid tends to gain or reach

again its initial state of viscosity. (Figure 2.25) Although "*thixotropic*" behavior of fluids is common, true "rheopetric" behavior is very rare.

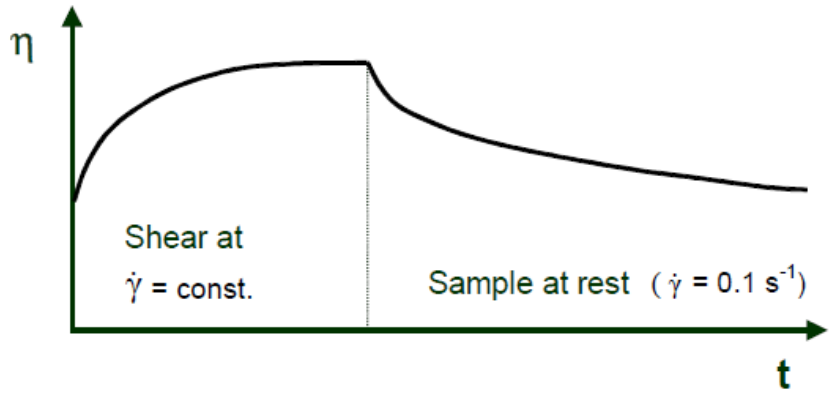

Figure 2.25 Viscosity –time curve of a "rheopectic" fluid (Jones et al, 2017)

2.8.2. Viscoelastic behavior of fluids

Viscoelastic behavior can be characterized for both solid and liquid phases. In this case, definition of strain can be given as in Figure 2.26. It can be represented by a cube having an edge length h. The bottom face in Figure 2.26 is stationary. Force "F" acts on the top face of the volume element and it is displaced by the amount s.

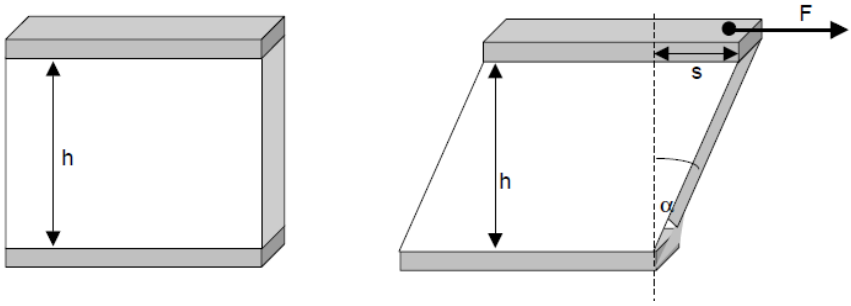

Figure 2.26 Schematic representation of strain for viscoelastic properties. (Malkin and Isayev 2017)

Strain is a dimensionless parameter. In order to provide enough strain to material angle 45° is used. This corresponds to 1 or 100%.strain. It can be noted that strain is the integral of shear rate with respect to time. (Wen and Dusek, 2017)

In purely elastic structures, the ratio of shear stress τ to strain γ is constant. This material-specific parameter can also describe the stiffness of the material and is known as the "*shear modulus*" G.

$$Shear\ modulus\ G = \frac{Shear\ stress\ \tau}{Strain\ \gamma} = \frac{Pa}{1} = Pa \quad (2.9)$$

Rheometers are not only used for viscosity measurement but also used to determine the viscous and viscoelastic material properties depending on shear stress applied

The dynamic response of viscoelastic materials to oscillatory stresses or strains is also important. Oscillatory motions are so common in the industry. There are many example related to operations and applications whose rheological information can be obtained from dynamic oscillatory measurements. By using oscillatory stress or strain and determining corresponding response, both elastic and viscous characteristics of materials can be easily analyzed. Solid like (elastic) materials store energy which can be only converted from mechanical to potential energy. This process can be easily recoverable. Liquid like materials do not store energy under the stress. They can only waste it as heat when they flow. (Wen and Dusek, 2017)

Viscoelastic materials exhibits both elastic (G') and viscous (G'') behavior. In order to differentiate them sinusoidal stress is applied whether or not a phase shift is observed. Obtained stress response under the sinusoidal stress can be seen in Figure 2.27. When sinusoidal stress is applied to an ideal elastic material, it produces strain proportional at same wave characteristic. At this case phase shift angle is 0°. However for ideal viscous materials, shift angle is 90°. In other words, regarding ideal viscous material deformation occurs out of phase when stress is applied.

Phase angle- tanδ: Phase angle tanδ is associated with the degree of viscoelasticity of the sample. A low value in tanδ or δ indicates more solid like viscoelasticity. The phase angle δ can be used to differentiate viscoelastic characteristics of fluids. If δ is between 45° to 0°, solid like structure occurs. If δ is

between 90° and 45°, liquid like structure occurs. If δ is equal to 0° or 90°, the structure is ideal solid or ideal viscous respectively (Wen and Dusek, 2017)

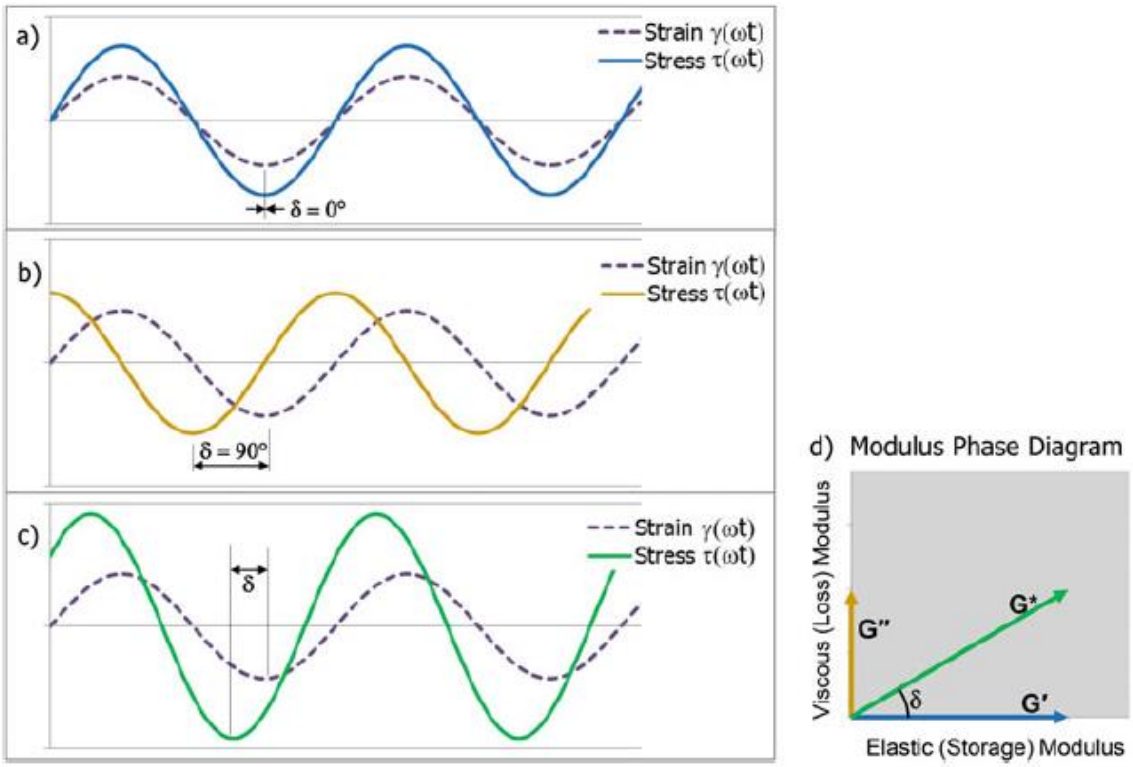

Figure 2.27 Stress response to an applied sinusoidal strain (a) ideal elastic solid (b) ideal viscous liquid (c) viscoelastic material (d) modulus phase diagram (Wen and Dusek, 2017)

2.8.3. Viscoelastic behavior of solids

Organic coatings in their service life encounter different mechanical stresses whereas their desired functionalities are wanted to remain unchanged. In practice, it is not possible. There will be regression on the performance upon mechanical stress but it has to remain at acceptable level. In automotive industry, coatings should withstand to being hit by a piece of flying gravel and any film rupture is not accepted. They have to be scratch resistant properties to maintain their appearances and glosses. They have to resist climate changes, high humidity, temperature, vibrations from moving parts of automobile. Many different examples can be given. As a result, coating formulation for automotive or other industries such kind of stress comes from outside has to be taken in account.

In order to analyze mechanical properties of organic coating, dynamic mechanical analysis (DMA) can be used for wide range of materials such as viscoelastic polymeric solid materials. DMA has two unique properties with respect to other mechanical testing devices. Firstly, DMA does not only focus on the elastic component but also the inelastic or viscous components. For example, for impact resistance performance, dry film of coating should have same part of viscous component. Secondly, universal tensile test devices work outside the linear viscoelastic (LVE) range. DMA works in LVE range. Therefore by using DMA more sensitive result can be obtained.

Tensile Test: DMA can perform tensile test depending on its traveler range, force limit and of course mechanical properties of sample. For example too rigid and too tough samples cannot be analyzed by DMA due mentioned reasons. Classic stress-strain curve obtained from traditional tensile tests in DMA can be seen in Figure 2.28. For tensile test in DMA, free film of organic coatings can be used due its sensitive clamps. Free film of organic coating is vertically mounted to DMA to make the tension analysis. All mechanical terms can be analyzed from resulted curve of DMA. For toughness measurement non-linear regression has to be performed to find the area under the curve (Roylance, 2001).

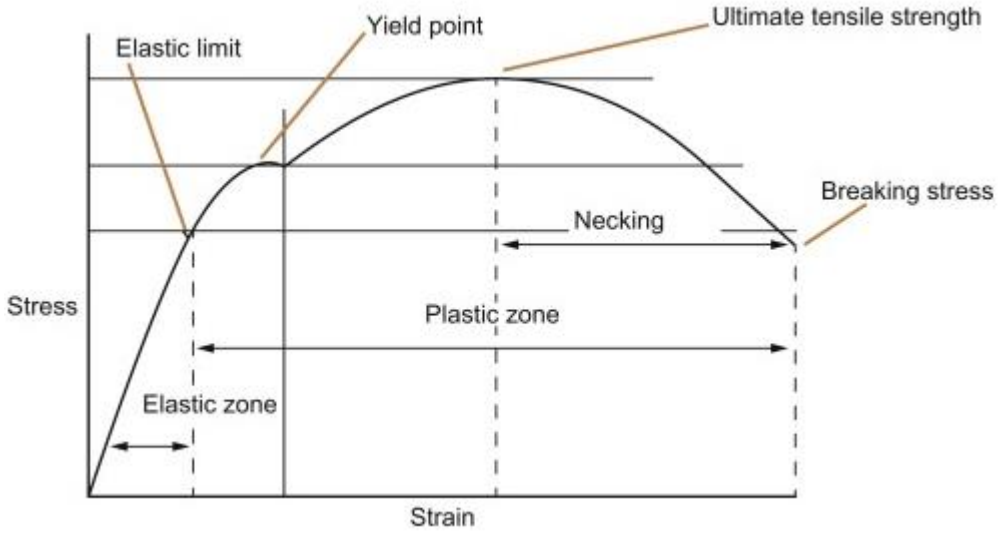

Figure 2.28 Schematic stress strain curve obtained from traditional tensile tests (Singh and Verma, 2017)

Dynamic Mechanical Test: Similar principles which mentioned in viscoelastic part of fluids are also valid for solid structure (Figure 2.29). Although, at this case organic coating has already completed its film formation reaction, again it can show same part of elastic and viscous properties. Results of measurements of elastic (*E'*) and viscous (*E''*) parts are summarized as a function of temperature as shown in Figure 2.30.

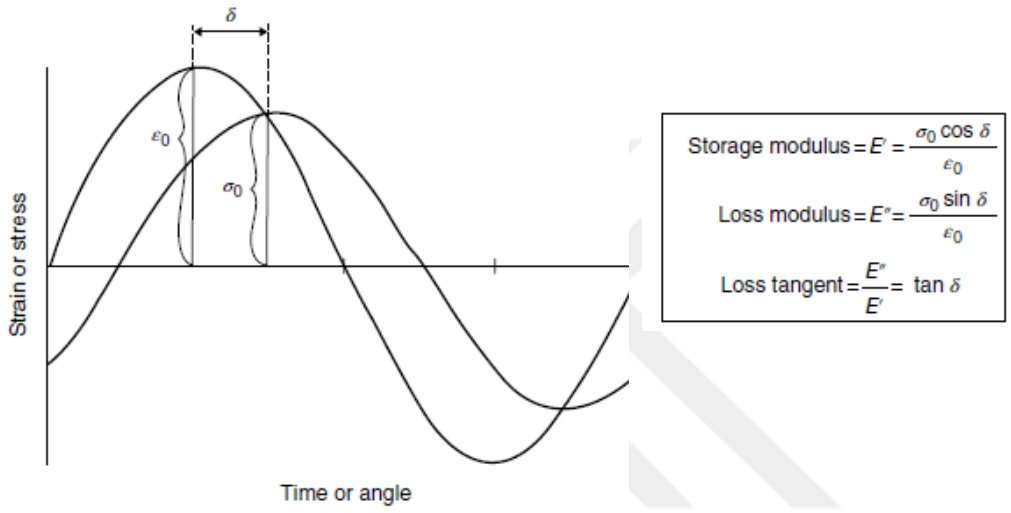

Figure 2.29 Dynamic sinusoidal strain input and stress response for viscoelastic material in DMA (Jones et al, 2017)

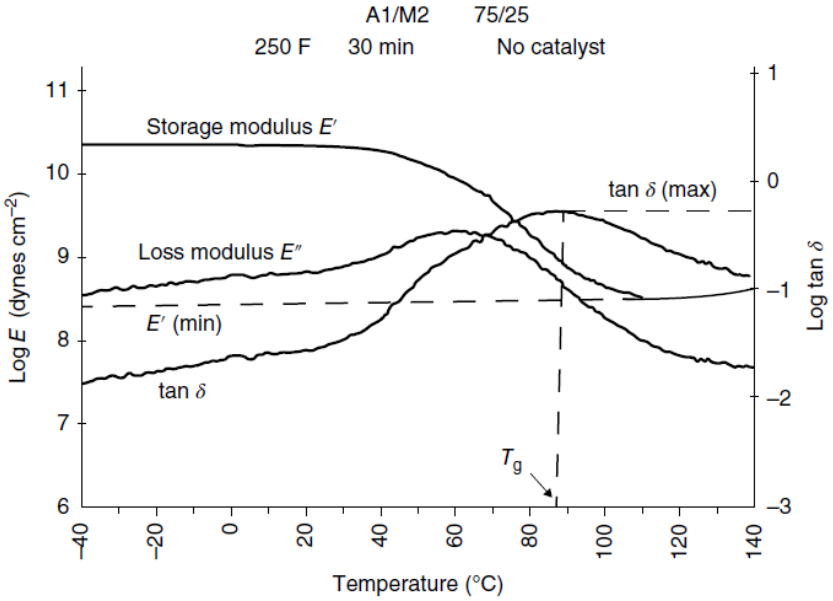

Figure 2.30 Elastic modulus (*E'*) and glass transition temperature (T_g) of polyether-melamine automotive clearcoat (Jones et al, 2017)

Glass Transition Temperature and Crosslink Density Calculation: Historically reason of technology, some years ago, *E'* could not be measured in the glassy state. Nowadays, instruments are sensitive enough to measure elastic modulus and the measurement repetition is high. Glass transition temperature can be obtained from peak of tanδ, peak of viscous modulus or according to onset method. However generally T_g is obtained from peak of tanδ.

Result of minimum elastic modulus is required to estimate crosslink density. Cross link density is closely related to many coating properties. Its estimation can give valuable information to the formulator for selection of film formation chemistry. It should be noted that crosslink of pigmented coating can be affected after glass transition temperature. Therefore, measurement should be performed without pigments free. Another point to pay attention, after glass transition temperature, elastic modulus has to reach almost its plateau region. If such elastic modulus plateau could not be obtained, crosslink density calculation is not performed. Crosslink density (M_c) can be calculated by using the following equations. (Jones et al, 2017; Li et al, 2016)

$$M_c = \frac{3RT\rho}{E'_{min}} \quad [\frac{g}{mol}] \tag{2.10}$$

$$M_c = \frac{3RT\rho}{E'_{Tg+50°C}} \; [\frac{g}{mol}] \tag{2.11}$$

where $R = 8{,}314 \frac{MPacm^3}{K.mol}$, T, temperature at E'_{min} or $E'_{Tg+50°C}$ and ρ, dry film density of organic coating.

2.8.4. Cure monitoring

In order to monitor curing performance of organic coatings, dielectric analysis (DEA) which is a thermal analysis technique to determine cure state can be used. Electrical properties such as permittivity and resistivity are measured by DEA to track the cure state of the coating. Permittivity is related to energy storage (similar to elastic modulus). Resistivity is related to energy loss (similar to viscous modulus). Dielectric analysis can also be performed at different frequencies. As it is expected, curing process is also related to viscosity increase because as soon as after curing of organic coating starts, viscosity of system increases due to solvent evaporation and crosslink density increase. Viscosity increase in curing of organic coating can be measured up to its vitrification point by suitable rheometer. However, curing of vitrified coatings continues. Hence, at this point ion viscosity obtained from DEA can be used. It can be monitored up to the end of cure. Ion viscosity is also proportional to rotational viscosity (Figure 2.31) (Lee, 2014).

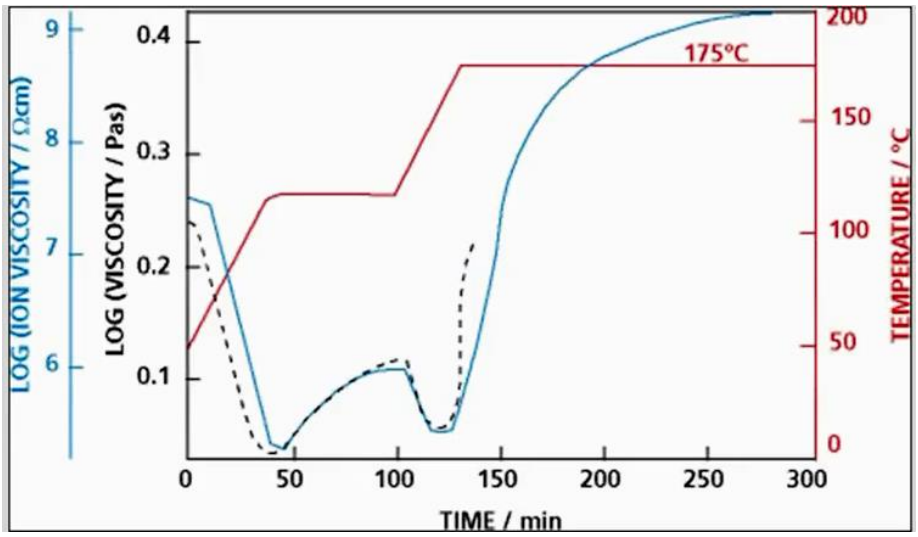

Figure 2.31 Rotational and ion viscosities during the cure. (Lee, 2014)

2.8.5. Water uptake

Water uptake performance properties are related to hydrophilic or hydrophobic properties of the paint system. Especially for anti-corrosion protective coatings, water uptake issue is critically thought. It is very useful to predict lifetime of coating. If water uptake rate of coating system is low as at acceptable level, tendency to blistering or adhesion failure of coating system can be suppressed (Yuan et al, 2015).

According to EIS models, coating system can be modeled by electric circuits. The term of impedance is related to resistance against to flow in design circuit and also frequency. "Randles" cell given in Figure 2.32 is basic EIS circuit model for coating systems. C_{DL} is coating capacitance, R_U is solution resistance and R_p is pore resistance.

Water uptake is calculated by "*Brasher-Kingsbury*" relation given in Eq.(2.12)

$$\phi\ (\%) = \frac{\log\left(\frac{C_t}{C_0}\right)}{\log\left(\varepsilon_w\right)} \times 100 \qquad (2.12)$$

where C_t and C_0 are capacitance of coating at time t and initial time, respectively. ε_w is dielectric constant of water. Φ(%) is volume percentage of water in the coating (Castela et al and Simoes, 2003)

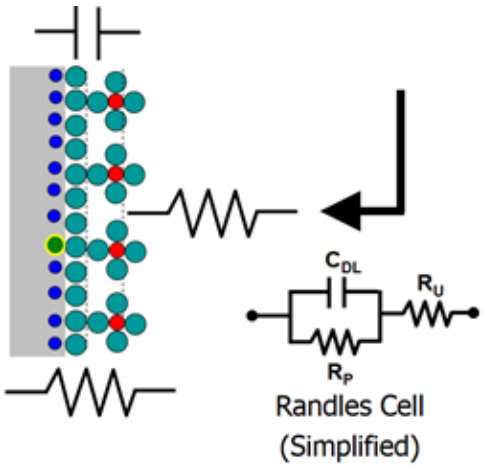

Figure 2.32 "Randles" circuit model in electrochemistry (Instruments, 2007)

EIS can be used to measure capacitive behavior of the coating system. At higher frequencies, total impedance has to be diminished low enough to measure the capacitance of coating system only.

2.8.6. Static and dynamic surface tension

Surface tension is one of the most critical points in the organic coating systems. Static and dynamic surface tensions are similar at the equilibrium state.

Static surface tension can be defined as required work to increase size of the surface of the liquid Surface tension can be considered as combination of cohesive and adhesive forces. Cohesive forces due to interaction between same types of molecules occur via hydrogen bonds. They are only short range and strong. Adhesive forces only occur between different type of molecules due to considerably weak interactions, that are van der Waals (vDW) and hydrogen bonds. Wetting only occurs when adhesive forces are stronger than cohesive forces.

As seen in Figure 2.33, there is a net force downward in Phase-1 and it is known as total surface tension. Surface tension of fluids is ~~are~~ measured by

Wilhelmy plate, Du Noüy ring or Pendant drop methods. In automotive coating industry Du Noüy ring method is generally used to measure the static surface tension.

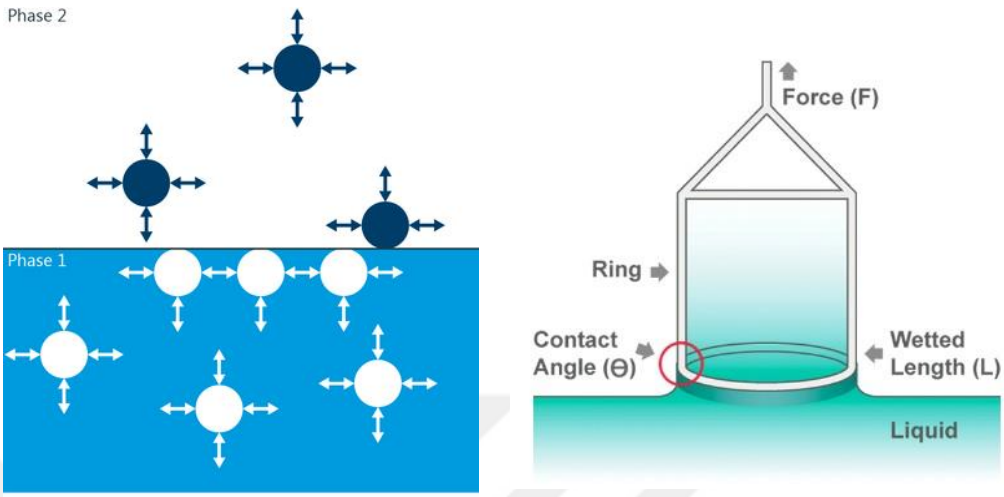

Figure 2.33 Schematic surface tension definition (Phase 1: fluid, Phase 2: air) and Du Noüy ring method to measure surface tension (Krüss, 2018) , (BiolinScientific,2018)

Static surface tension (SST) affects the performance of wetting (leveling) and adhesion of coating on solid surfaces. It also affects the droplet size of coating in spray application. Paints at high viscosity could not be sprayed in small droplet. Dispersion stability of pigments of fillers is also related to surface tension.

Dynamic surface tension (DST) is time dependent measurement. Surface equilibrium is changed with bubble (surface) creation inside the fluid. (Figure 2.34) This can simulate the surface tension state as soon as after spray application. DST can give information about surface tension change under shear rate. DST can be used for water-borne and solvent-borne systems

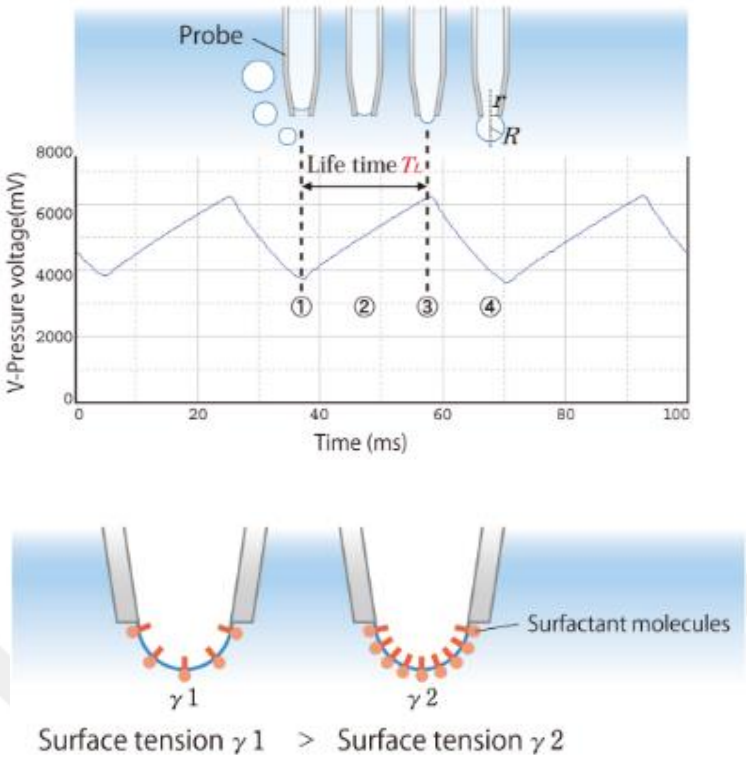

Figure 2.34 Schematic DST bubble and new surface creation inside the fluid (BiolinScientific, 2018)

2.8.7. Surface free energy

Principle of surface free energy is very similar to surface tension. However, in this case cohesive forces are more dominant and strong compared to adhesive forces. Surface free energy is calculated by using contact angle measurement of fluid whose surface tension is known. Contact angle measurement is illustrated in Figure 2.35. Surface free energy can be calculated according to "Young's equations". σ_{sl} is surface tension of liquid drop whose contact angle is measured. σ_s (σ_{sg}) is surface free energy of substrate or solid body. Surface tension between solid to liquid (σ_{sl}) is unknown It can be calculated special model stated Table 2.2.

Principle of surface free energy is very similar to surface tension. However, in this case cohesive forces are more dominant and strong compared to adhesive forces. Surface free energy is calculated by using contact angle measurement of fluid whose surface tension is known. Contact angle measurement is illustrated in

Figure 2.35. Surface free energy can be calculated according to "Young's equations". σ_{sl} is interfacial tension at liquid droplet-solid interface whose contact angle is measured. σ_s (σ_{sg}) is interfacial tension at solid substrate–gas interface, that can be calculated using Eq.(2.13) . Interfacial tension at solid-liquid interface (σ_{sl}) is unknown and can be calculated special models stated in Table 2.1.

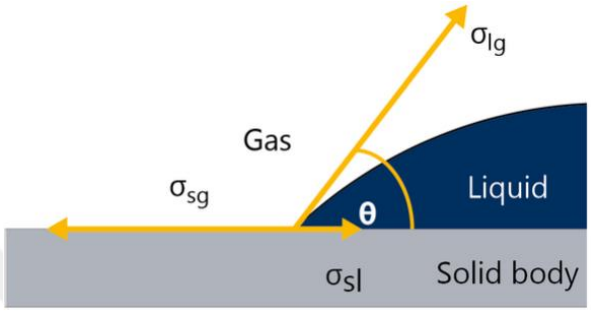

Figure 2.35 Schematic representation of contact angle and surface free energy calculation (Krüss,2018)

$$\sigma_s = \sigma_{sl} + \sigma_l cos\theta \qquad (2.13)$$

Table 2.1 A summary of special model equations to calculate-interfacial tension at solid-liquid interface (σ_{sl}) (Krüss,2018)

Model according to author(s)	**Interaction components of the SFT**	**Interfacial Tension (Solid to Liquid) σ_{sl} or σ_{ls}**
Fowkes	Disperse part and non-disperse part	$\sigma_{ls} = \sigma_l + \sigma_s - 2(\sqrt{\sigma_l^D.\sigma_s^D} + \sqrt{\sigma_l^{nD}.\sigma_s^{nD}})$ (2.14)
Owens-Wendt-Rabale & Kaelble	Disperse and polar part	$\sigma_{ls} = \sigma_l + \sigma_s - 2(\sqrt{\sigma_l^D.\sigma_s^D} + \sqrt{\sigma_l^P.\sigma_s^P})$ (2.15)
Wu	Disperse and polar part	$\sigma_{ls} = \sigma_l + \sigma_s - 4(\frac{\sigma_l^D.\sigma_s^D}{\sigma_l^D+\sigma_s^D} + \frac{\sigma_l^P.\sigma_s^P}{\sigma_l^P+\sigma_s^P})$ (2.16)
Oss, Good (acid-base)	Lewis acid part and Lewis base part	$\sigma_{ls} = \sigma_l + \sigma_s - 2(\sqrt{\sigma_l^D.\sigma_s^D} + \sqrt{\sigma_l^-.\sigma_s^+} + \sqrt{\sigma_s^-.\sigma_l^+})$ (2.17)
Extended Fowkes	Disperse and polar part and hydrogen part	$\sigma_{ls} = \sigma_l + \sigma_s - 2(\sqrt{\sigma_l^D.\sigma_s^D} + \sqrt{\sigma_l^P.\sigma_s^P} + \sqrt{\sigma_l^H.\sigma_s^H})$ (2.18)
Neumann Equantion of State	No division into components	$\sigma_{ls} = \sigma_l + \sigma_s - 2(\sqrt{\sigma_l.\sigma_s}.e^{-\beta(\sigma_l-\sigma_s)^2}$ (2.19)

2.8.8. Polar and disperse parts of the surface tension

The polar and disperse components of the surface tension of liquid can be determined by contact angle measurements on a non-polar solid surface. In this case, if the interfacial/ surface tension at solid-liquid interface is known, disperse and polar components can be calculated as shown the example given in Table 2.2;

Table 2.2 Determination of polar and disperse parts of surface tension of H_2O (Krüss,2018)

Data	**Equations**
Substrate: PTFE $\sigma_s = 20\ \mathrm{mN/m}$ **Liquid:** H_2O at 22°C $\sigma_l = 72.8\ \mathrm{mN/m}$ **Contact angle:** $\theta = 116^o$	$\sigma_{sl} = \sigma_s + \sigma_l - 2\sqrt{\sigma_s.\sigma_l^d}$ (2.20) $\sigma_l^d = \frac{1}{4\sigma_s}(\sigma_s + \sigma_l - \sigma_{sl})^2$ (2.21) $\sigma_{sl} = \sigma_s - \sigma_l \cos\theta$ (2.22) $\sigma_l^d = \frac{{\sigma_l}^2}{4\sigma_s}(1 + \cos\theta)^2$ (2.23)
Calculations	
Disperse component $\sigma_l^d = 20.9\ \mathrm{mN/m}$	Polar component $\sigma_l^p = 51.9\ \mathrm{mN/m}$

2.8.9. Hardness

Pencil hardness: Hardness of organic coating can be determined by using special pencils whose hardness levels are known as illustrated in Figure 2.36. Depending on hardness of organic coatings, from type 6B (the softest) to type 9H (the hardest) pencils can be used.

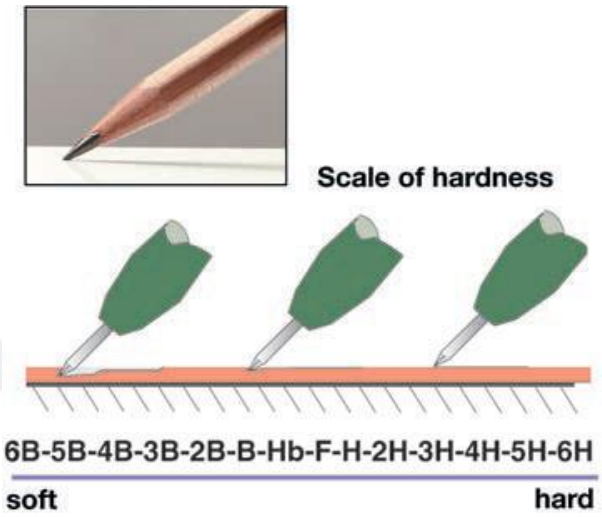

Figure 2.36 Pencil hardness. (Streitberger and Dössel, 2008)

Damping hardness (Persoz): The special designed pendulum illustrated in Figure 2.37 is placed on the coating. Then it is moved 12° away from the position of rest. After releasing the pendulum, the oscillations are recorded by a counter and stops at angle 4°.

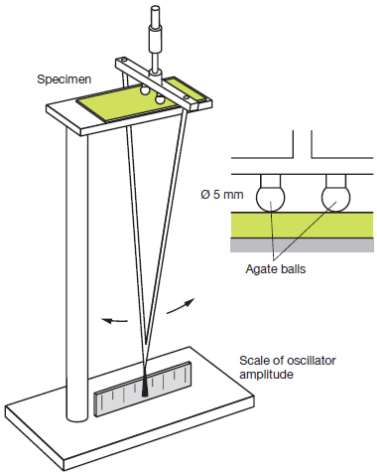

Figure 2.37 Damping pendulum hardness test equipment (Streitberger and Dössel, 2008)

2.8.10. Impact and stone chip resistance

Impact resistance test equipment (Figure 2.38): It is very simple but useful. The purpose is to determine the elasticity when falling body hits the coating. Then state of cracking and adhesion failures are checked.

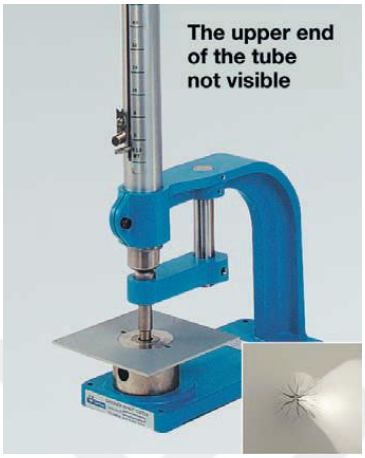

Figure 2.38 Impact test device (Streitberger and Dössel, 2008)

Stone chip resistance testing equipment (Figure 2.39): Regarding stone chip resistance control, special designed equipment is used. According to standards, chip type is chosen. Generally, gravel, steel or sand are used.

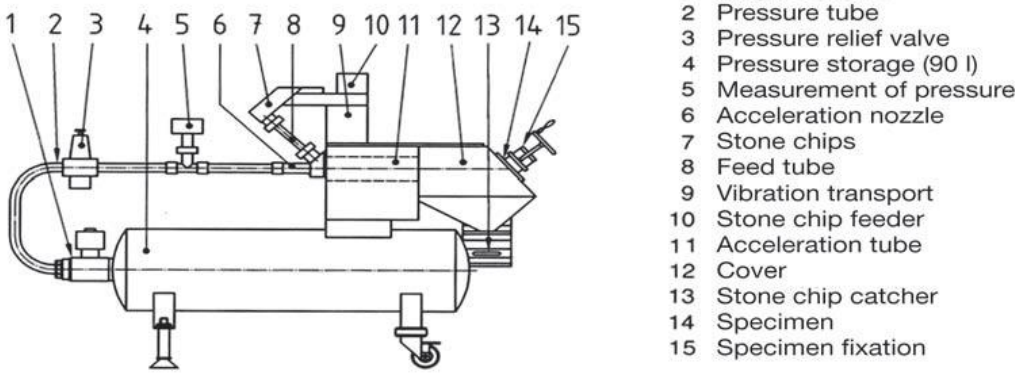

Figure 2.39 Stone chip resistance testing equipment (Streitberger and Dössel, 2008)

2.8.11.Elasticity control (cupping test)

Elasticity control test (cupping) equipment (Figure 2.41) is used to measure elongation in 2-dimensional and related elasticity of coating. In this test, piston having diameter 20mm punches coated panel at velocity 0.2 mm/s until first crack appear.

Elasticity control (cupping) test equipment (Figure 2.40) is used to measure elongation in 2-dimensional and related elasticity of coating. In this test, piston having diameter 20mm punches is coated panel at velocity 0.2 mm/s until first crack appear.

Figure 2.40 "Cupping" test device (Streitberger and Dössel, 2008)

2.8.12. Scratch simulation

The dry scratch resistance of a coating can be characterized by using special designed equipment. Crock meters with special scratch paper can be used to analyze the scratch resistance of organic coating. After that gloss retention at 20° of coating is measured.

In addition to crock meter, there are also special scratch resistance measurement devices such as diamond scratch, nail scratch tester etc.

Figure 2.41 Crockmeter- dry scratch test equipment (Streitberger and Dössel, 2008)

3. EXPERIMENTAL

Experimental work consists of four main parts as described below;

1- "Sol-Gel" SiO_2 Nano Particle Synthesis
2- Surface Treatment of "Sol-Gel" SiO_2 Nano Particles
3- Characterization of "Sol-Gel" SiO_2 Nano Particles
4- Characterization of Automotive Hybrid Clear Coat

3.1. "Sol-Gel" SiO_2 Nano Particle Synthesis

3.1.1. Materials

Solvents, precursors, catalysts used in synthesis of SiO_2 nanoscale particles by-"sol-gel" technique are tabulated in Table 3.1.

Table 3.1. Material used in "sol-gel" SiO2 nano particle synthesis.

Category	Description	Structure	Brand	Purity	M_w, g/mol
Precursor	TEOS (Tetraethylorthosilicate)	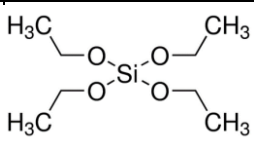	Merck	98%	208.33
Catalyst	Hydrochloric acid fuming (37% in water)	HCI	Merck	98%	36.46
	Ammonia solution (25% in water)	NH4OH	Merck	98%	35.04
Solvent*	Methanol	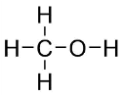	Merck	99%	32.04

*Solvent was decided after relative sedimentation rate evaulations (Section 3.1.3)

3.1.2. Experimental setup

In synthesis of SiO_2 nano particles by "Sol-gel" method jacketed glass reactors were used. Parameters effective such as reaction time, amount of TEOS, amount of catalyst, type of catalyst, reaction temperature and mixing rate were examined in particle synthesis. Sol was agitated by a magnetic stirrer at 500 rpm and 1000rpm. Reaction temperature in the mixing reactor was adjusted to a constant temperature with water bath. Reaction temperature was changed from 10°C to 80°C. In addition, volume of the reaction medium was held constant in all experiments under reflux using condenser which was cooled by tap water as illustrated in Figure 3.1. In this figure, water bath was connected in series to reactors. Reaction temperature was followed with help of digital screen of thermocouple. Set temperature of water bath and actual reaction temperature were checked in each experiment.

Figure 3.1 Jacketed glass reactors with magnetic stirrer.

After design of experiment was completed, in order to see effect of high shear, set-up stated in Figure 3.2 was used. In this setup, mixing of sols were done between 1000-3000 rpm with cowles dispersion impeller.

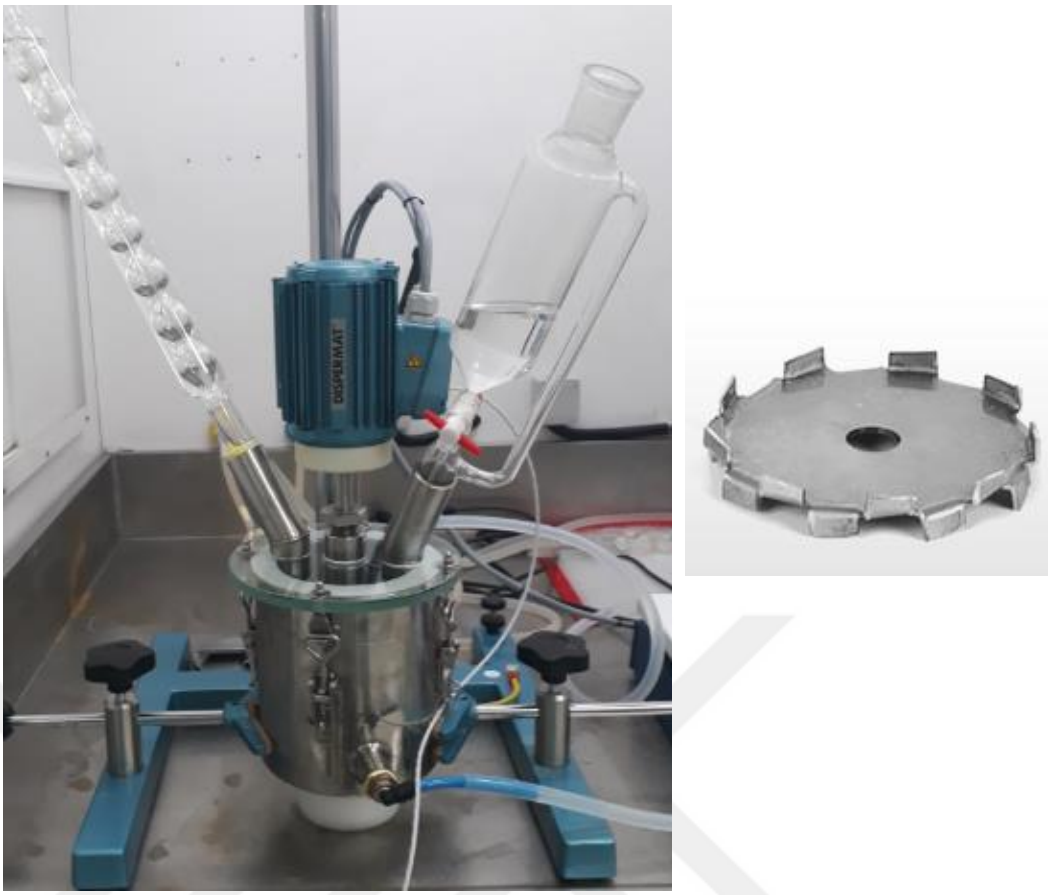

Figure 3.2 High shear mixing tank and Cowles dispersion impeller

3.1.3. Solvent selection

Solvent type for design of experiment was selected according to Hansen Solubility Parameters (HSP). By using relative sedimentation rate assumption, dispersibility parameters of Nano silica were determined. HSP solvent selection experiments were carried out according to solvents tabulated in Table 3.2.

Sedimentation time and mass of nanoscale powder silica particle were observed by sedimentation mode of force tensiometer. For this purpose special designed sedimentation check pan was used. (Figure 3.3)

2% (by weight) of nano-sized silica particles was added to solvent under the high shear mixing using cowles type disperser at 1000 rpm. After 15 minutes mixing, sedimentation control was started.

Table 3.2 Hansen solubility parameters for solvent selection experiment

Solvent	Solvent Notations	dD†	dP†	dH†	ρ [g/ml]	μ[s]*
Ethanol	S1	15.8	8.8	19.4	0.79	10.12
Methanol	S2	14.7	12.3	22.3	0.79	9.70
Deionized water	S3	15.5	16	42.3	1.00	10.55
2-Propanol	S4	15.8	6.1	16.4	0.79	10.85
Isobutyl Alcohol	S5	155	5.7	15.9	0.80	11.07
Ethyl Acetate	S6	15.8	5.3	7.2	0.90	10.00
Dimethyl Succinate	S7	16.1	7.7	8.8	1.09	10.71
Ethylene Glycol Butyl Ether Acetate	S8	15.3	7.5	6.8	0.94	10.30
Propylene Glycol Monomethyl Ether Acetate	S9	15.6	5.6	9.8	0.97	10.25
Propylene Glycol Monomethyl Ether	S10	15.6	0.3	11.6	0.89	10.45
Acetone	S11	15.5	10.4	7	0.79	9.50
Methyl Ethyl Ketone (MEK)	S12	16	9	5.1	0.81	9.72
Methyl Isoamyl Ketone	S13	16	5.7	4.1	0.81	9.71
N-Methyl-2-Pyrrolidone	S14	18	12.3	7.2	1.03	10.22
Cyclohexanone	S15	17.8	8.4	5.1	0.94	10.42
Solvesso 100	S16	17.6	0.8	2	0.87	10.10
Xylene	S17	17.6	1	3.1	0.86	9.87
Toluene	S18	18	1.4	2	0.87	9.10
Solvesso 150	S19	17.8	0.6	1.4	0.88	10.11
WhiteSprit	S20	14	0.1	0.1	0.77	10.11
n-Butyl Acetate	S22	15.8	3.7	6.3	0.88	9.90

*DC4 viscosity at 23°C

†dD: disperse component dP: polar component dH: hydrogen component of HSP

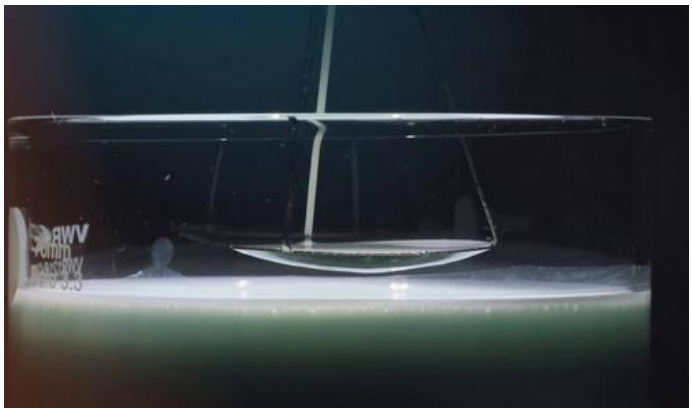

Figure 3.3 Sedimentation pan of force tensiometer. (BiolinScientific, 2018)

3.1.4. Design of experiment

Regarding experimental design "Minitab 17" has been used. In the design of experiment (DOE), six independent variables/factors (reaction time, amount of TEOS, amount of catalyst, type of catalyst, reaction temperature and mixing rate) have tried to be optimized. In the DOE, factors have 2 levels which are described in Table 3.3. Amount of methanol (250ml) and dosing rates of reagents were held as constant in 2-level factorial DOE.

Table 3.3 Experimental independent variables/factors and their levels in DOE

Variables / Factors	**Levels**
Reaction Time	1hr – 3hr
Amount of TEOS	20ml – 40ml
Amount of Catalyst	5ml – 10ml
Type of Catalyst	NH4OH 25%– HCI 25%
Reaction Temperature	40ºC - 60ºC
Mixing Rate	500rpm – 1000rpm

In order to create factorial design, "Minitab 17" shows the available design options as described in Figure 3.4. If full factorial design is desired to perform, for six factors 64 experiments have to be performed. However, in partial factorial design resolution of VI, only 32 experiments are enough to judge and to understand effect of factors to responses. In resolution VI, only 1 to 5, 2 to 4, 3 to 3-way interactions are confound therefore resolution VI gives reliable DOE. That is the reason of resolution VI of factor six which is in green region as illustrated in Figure 3.4. In addition, two center points are selected for the DOE.

Available Factorial Designs (with Resolution)

	Factors													
Run	2	3	4	5	6	7	8	9	10	11	12	13	14	15
4	Full	III												
8		Full	IV	III	III	III								
16			Full	V	IV	IV	IV	III	III	III	III	III	III	III
32				Full	VI	IV	IV	IV	IV	IV	IV	IV	IV	IV
64					Full	VII	V	IV	IV	IV	IV	IV	IV	IV
128						Full	VIII	VI	V	V	IV	IV	IV	IV

Figure 3.4 Available factorial design in the "Minitab 17"

Experiments for the synthesis of nano SiO_2 particles by "Sol-Gel" method have been designed as described in Table 3.4. 2_{VI}^{6-1} is the symbolic description of chosen DOE.

Table 3.4 2_{VI}^{6-1}DOE to optimize the "Sol-Gel" method.

Amount of MeOH [ml]	Amount of TEOS [ml]	Amount of Catalyst [ml]	Reaction Temperature [ºC]	Mixing Rate [rpm]	Type of Catalyst
250	40	10	40	1000	NH4OH
250	20	10	40	500	HCI
250	20	10	60	500	HCI
250	20	5	40	500	NH4OH
250	20	5	40	1000	NH4OH
250	40	10	40	500	HCI
250	20	10	40	500	NH4OH
250	30	7.5	50	750	HCI
250	40	10	60	1000	HCI
250	20	5	60	500	NH4OH
250	20	10	40	1000	NH4OH
250	40	5	60	1000	HCI
250	40	10	60	1000	NH4OH
250	40	5	60	500	HCI
250	20	10	60	500	NH4OH
250	40	10	40	1000	HCI
250	40	5	60	500	NH4OH
250	20	10	60	1000	HCI
250	20	5	60	500	HCI
250	40	10	40	500	NH4OH
250	30	7.5	50	750	NH4OH
250	40	5	40	500	HCI
250	40	5	40	1000	NH4OH
250	40	10	60	500	NH4OH
250	40	10	60	500	HCI
250	40	5	40	500	NH4OH
250	40	5	40	1000	HCI
250	40	5	60	1000	NH4OH
250	20	5	40	500	HCI
250	20	10	60	1000	NH4OH
250	20	5	40	1000	HCI
250	20	10	40	1000	HCI
250	20	5	60	1000	NH4OH
250	20	5	60	1000	HCI

In the optimization of the experiment, determination of response is so critical. Aim of the experimental design is to see effect of independent variables to non-volatile percentages, particle size, and zeta potential of nanoscale SiO2 particles. In addition, in order to increase sol to gel efficiency molar ratio of H_2O and TEOS was tried to be optimized.

3.1.5. Particle size measurement

According to DEO conditions given in Table 3.4, experiments were conducted. As result of the conditions "sol-gel" SiO_2 particles were synthetized. Their particle size was measured by Dynamic light Scattering Method (DLS). And obtained z-average [nm], PdI and Intercept results were compared.

In DLS size measurement operating procedure, measurement angle and sample temperature were arranged to 173° (backscatter) and 25°C, respectively. SiO_2 refractive indice was taken as 1.45 and absorption one, as 0.01. Glass cuvette was used for all measurements. In addition, before stating the measurement, 2 minutes time were given to let the sample to reach its equilibrium state.

In order to see the reproducibility of results, all experiments were repeated three times.

3.1.6. Measurement of Zeta potential

Zeta potential measurements were conducted in DLS equipment. In order to obtain correct results, glass dip cell apparatus (Figure 3.5) of DLS equipment was used due solvent content of "sol-gel" experiments.

In the zeta potential measurement operating procedure, "F(Ka)" was selected according to "Smoluchowski". Other parameters were identical to states mentioned in DLS section.

3.2. Surface Treatment of SiO_2 Nano Particles Synthesized by "Sol-Gel" Method

3.2.1. Materials

Types of silane and of wetting agents used in surface treatment of SiO_2 nano particles synthesized by "Sol-Gel" method are tabulated in Table 3.5 and Table 3.6, respectively

Table 3.5 Silanes used in surface treatment of SiO_2 nano particles synthesized by "Sol-Gel" method

Silane Agent	**Description**	**Structure**
A	Triethoxyvinylsilane, 98%	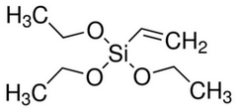
B	3-(Trimethoxysilyl) propyl methacrylate, 98%	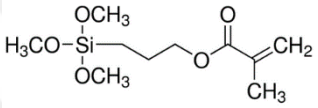
C	(3-Mercaptopropyl) trimethoxysilane , 95%	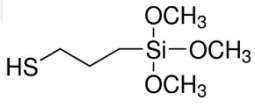
D	Triethoxy(octyl)silane ,97%	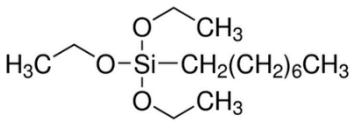
E	(3-Aminopropyl) triethoxysilane, 99%	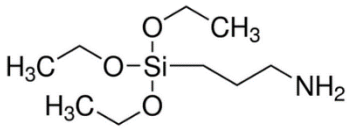

3.2.2. Determination of Iso-Electric Point (IEP)

0.5% (by weight) of nano-sized SiO_2 particles was mixed with deionized water at 1000rpm using Cowles type impeller. After 5 minutes mixing, pH and zeta potential were measured and IEP was obtained. pH of dispersion was adjusted by HCI solution. Deionized water specifications were 0.06µS, 71.2mN/m, and pH 6.8.

Table 3.6 Wetting and dispersing agents

Wetting/ Dispersing Agent	**Type**	**Polarity**	**Chemistry**
A	Basic	Medium to High	Polyurethane
B	Acidic	Medium to High	Phosphoric Acid Ester
C	Basic	Low to High	Polyurethane
D	Basic	Medium to High	Polyurethane
E	Basic	Low to High	Acrylate
F	Basic	Low to High	CPT based Acrylate
G	Neutral	Medium to High	Phosphoric Acid Ester
H	Basic	Medium to High	Polyurethane
I	Basic	Medium to High	HyperBranch Polyester

3.2.3. Evaluation of surface treatments

Surfaces of nano-sized SiO_2 particles were tried to be covered by one of surface treatment agents (silanes) given in Table 3.5, that have different functionalities. Then one of wetting/dispersing additives summarized in Table 3.6 which have different IEP dependence were added into the medium including the particles of which surfaces are to be treated.

Experiments were conducted at a ratio of surface treatment agent to silica particles as 1:1 by weight. The effect of ratio of amount of surface treatment agent to that of SiO_2 particles on surface properties of silica particles were also aimed to investigate. For this purposes, 0.1:1, 0.5:1, 1:1 and 2:1 ratios have been examined.

Surface treatment experiments were conducted at room temperature for 30min. And also, high shear Cowles type impeller was used.

3.3. Characterization of Nano-SiO_2 Particles Synthesized by "Sol-Gel" Method

Characterizations analyses were performed for dry nano-sized particles whether they are surface treated or not. The particles were dried at 120°C for 1h and washed with tetrahydrofuran (THF) using "Soxhlet" apparatus together with condenser and hot plate as shown in Figure 3.6. Hot plate was set to 250°C to evaporate THF from silica particles.

Even if nano-sized particles were dried, they can contain some part of unreacted substances. Therefore, washing procedure was let to continue 2 hours. After that washed particles were dried at 120°C for 1h.

Figure 3.5 Dip cell apparatus of DLS (Malvern, 2011)

Figure 3.6 "Soxhlet" apparatus, condenser and hot plate

3.3.1. SEM

Scanning electron microscope (SEM) images were taken in resolution scale of 100nm. Then, particle size of the particles synthesized by “sol-gel” method was compared with DLS results.

3.3.2. FTIR-ATR

Fourier Transform Infrared Spectrophotometer (FTIR) was used to analyse chemical structure of SiO_2 particles synthesized and surface treatment efficiency. Spectrums of SiO_2 particles in the absence and precence of surface treatment agent were compared. Measurements were conducted with KBr assisted pellets by Attenuated Total Relectance part (ATR) of FTIR.

3.3.3. TGA

Thermal Gravimetric Analyzer (TGA) was used to analyse the weight loss, related to the surface treatment efficiency: 10 mg of SiO_2 particle was weighed as sample. The sample was heated from 25°C to 800°C at a heating rate of 5’C/min under the oxygen atmosphere. The weight loss was recorded during the heating process and the weight loss after 120°C was considered to be corresponded to organic surface treatment agent.

3.4. Characterization of Automotive Hybrid Clear Coat

After surface treatment of SiO_2 nano particles was completed and analysed, their compatibilities were checked in automotive high solid (HS) type clear coat which is designed in two components. 1.75phr and 3.00phr (phr: per hundred resin) surface treated SiO_2 nano particles were incorporated into ready condition. So, these clearcoats known as “*Hybrid HS Clearcoat* ” are ready to spray.

In such coating systems, reactive sides are separated into two different parts as hydroxyls and isocyanates. One is only for acrylic polymer side and another one is only for isocyanate hardener side. As soon as after they mixed, film formation reaction starts even if in its solvent rich medium. After application of the clearcoat by using spray gun or applicator, solvent inside the clearcoat starts to evaporate. Time required for evaporation of all solvents inside the clearcoat can be decreased

using proper furnaces at 80°C for 30min, as a consequence, solvent free clearcoat films were obtained.

3.4.1. Rheology

Rheological behavior of "*Hybrid HS Clearcoat*", ready to be sprayed, was investigated using concentric cylindrical part of rheometer given in Figure 3.7. The rheological behavior of *Hybrid HS Clearcoat* was examined as follows:

- Shear thinning characteristic analysis: (Rotational test)
  - Viscosity change was analysed between $0.1s^{-1}$ and $1000s^{-1}$ shear rates
- Time dependent viscosity change i.e., thixotropic behaviour analysis.
  - Shear rate was adjusted to$1000s^{-1}$ then viscosity recovery was observed.
- Elastic and viscous modulus analysis (Oscillation test)
  - Modulus of samples at rest and after stress were compared
- Shear strain (amplitude) sweep
  - Frequency was kept as constant (1Hz) and strain was changed from 0.1% to 10%

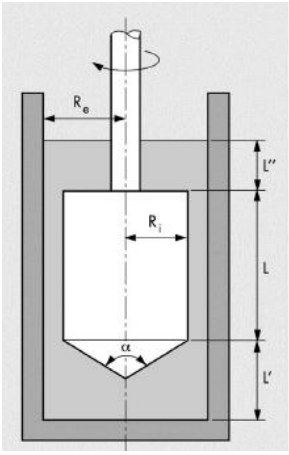

Figure 3.7 Schematic representation of concentric cylinder of rheometer (Paar,2015)

3.4.2. Dynamic mechanical analysis

Dynamic mechanical (DMA) and thermal analysis (TA) of "*Hybrid HS Clearcoat*" films were performed by film tension clamp given in Figure 3.8. These analyses of *Hybrid HS Clearcoat* films were performed as*:*

Free film dimension W: 5.3mm x L: 10mm x T: 40-50µm

- Strain ramp test (tensile test): (Temp: 25°C, equilibrium time: 1min, strain rate 500µm/min)
    - Young modulus, yield and fracture point was determined from stress-strain curve.
    - Toughness of elastic and plastic regions was calculated. Non-liner regression was needed to integrate the stress-strain curve.
- Frequency sweep oscillation test: (Temp: 25°C, equilibrium time: 1min, oscillation amplitude: 10µm (in LVE range), frequency range: 0.1 – 50Hz.)
    - Elastic and viscous characterises were compared upon frequency change at constant strain/amplitude.
- Temperature ramp test: (Temp: from 10°C to 120°C, heating rate: 5°C/min, oscillation amplitude: 10µm (in LVE range), frequency:1 Hz)
    - Glass transition temperatures were determined from tanδ max.
    - Cross link densities were calculated from elastic modulus of E'_{min} or $E'_{Tg+50°C}$

3.4.3. Cure monitoring

Film formation properties or kinetics of "Hybrid HS Clearcoat" were investigated by dielectric analysis (DEA). Applications on sensors (Figure 3.9) were made with 120µm manual applicator. After application of clearcoat on the sensor, 10 min flash off time was given due to appropriate wet film thickness on the sensor.

Film formation properties of "Hybrid HS Clearcoat" were analysed in the furnace which was set to 80°C with 10°C/min as up and down heating rates.

Figure 3.8 Film tension clamp of DMA (TA Instruments, 2018)

Figure 3.9 Sensors of DEA for cure monitoring (Lee, 2014)

3.4.4. Water uptake monitoring

Water uptake properties or kinetics of "*Hybrid HS Clearcoat*" were investigated using electro impedance spectrophotometer (EIS). In the EIS measurement unit, electrolyte solution contains 5% (by weight) salt; graphite as counter electrode and saturated calomel as reference electrode were used.

"*Hybrid HS Clearcoat*" was sprayed on bare metal to measure initial and final capacitances of the clearcoat. Firstly, open circuit potential, min voltage which is not to damage the bare metal was measured. Then, this measured voltage was set as DC voltage. AC voltage was selected 1 mV according to "Kramers Kronig" test. Single frequency EIS measurement was conducted at 10 kHz and time dependent capacitances were measured. Water uptake fraction was calculated by using Eq.(2.12) stated in Section 2.8.5.

3.4.5. Static and dynamic surface tension

Static and dynamic surface tension of ready to spray "Hybrid HS Clearcoat" were measured by using force and bubble pressure tensiometers. In dynamic surface tension measurement, deionized water (surface tension: 71.8-72.4 mN/m) was used to determine capillary diameter of tip which forms bubble 10mm inside the liquid sample.

Dynamic surface tension measurements were conducted on surface age basis from 10 to 10000 ms

3.4.6. Surface free energy

Contact angle measurement and surface free energy calculation of “Hybrid HS Clearcoat” were performed by using drop shape analyser.

Polar and disperse parts of clear coats were calculated by using contact angle of them on the PTFE surface.

Contact angle of water and diiodomethane were measured by drop shape analyser.

3.4.7. Scratch resistance and hardness control

Scratch resistance of “Hybrid HS Clearcoat” were test by using crock meter and nail scratch test equipment then gloss retentions were calculated.

3.4.8. Visual appearance controls

Visual appearance of “Hybrid HS Clearcoat” were controlled according to customer expectations

3.4.9. Mechanical controls

Stone-chip and impact resistance, elasticity (cupping) and adhesion performances of “Hybrid HS Clearcoat” were controlled according to customer expectations.

4. RESULT AND DISCUSSION

4.1. SiO_2 nano particle synthesized by "Sol-Gel" SiO_2 method

4.1.1. Solvent selection for "sol-gel" synthesis

All solvents given in Table 3.2 and 4.1 were used in the synthesis of silica particles by "sol-gel" method. According to results of mass sedimented after 15min in Figure 4.1, it is seen that S2-methanol is the best solvent to increase efficiency of sol to gel transition. Sedimentation tendencies of dried SiO_2 particles obtained from preliminary works of this thesis were checked in solvent selection studies.

Although S1-ethanol is seemed to be the second best solvent for sol to gel transition procedure, in practise, it has been determined that when concentration of synthesized "sol-gel" SiO_2 particles increases, the sol starts to become gel. Therefore, further evaluations were carried out with methanol.

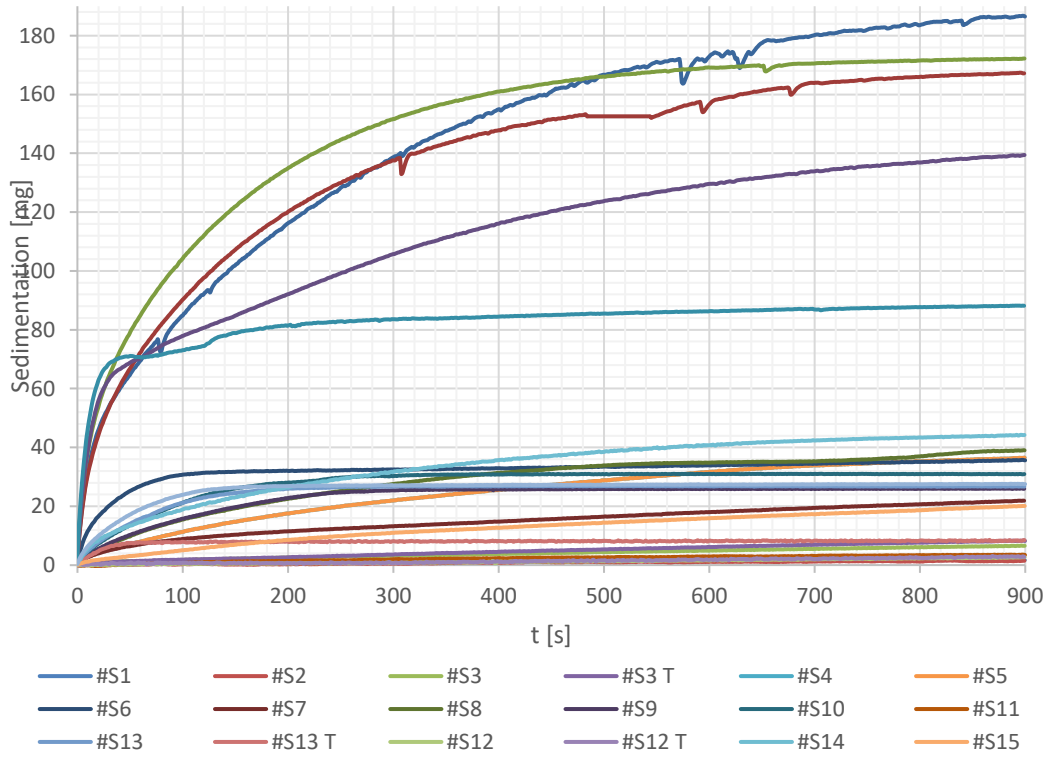

Figure 4.1 Sedimentation of SiO_2 particles synthesized by "sol-gel" method in different solvents (a)

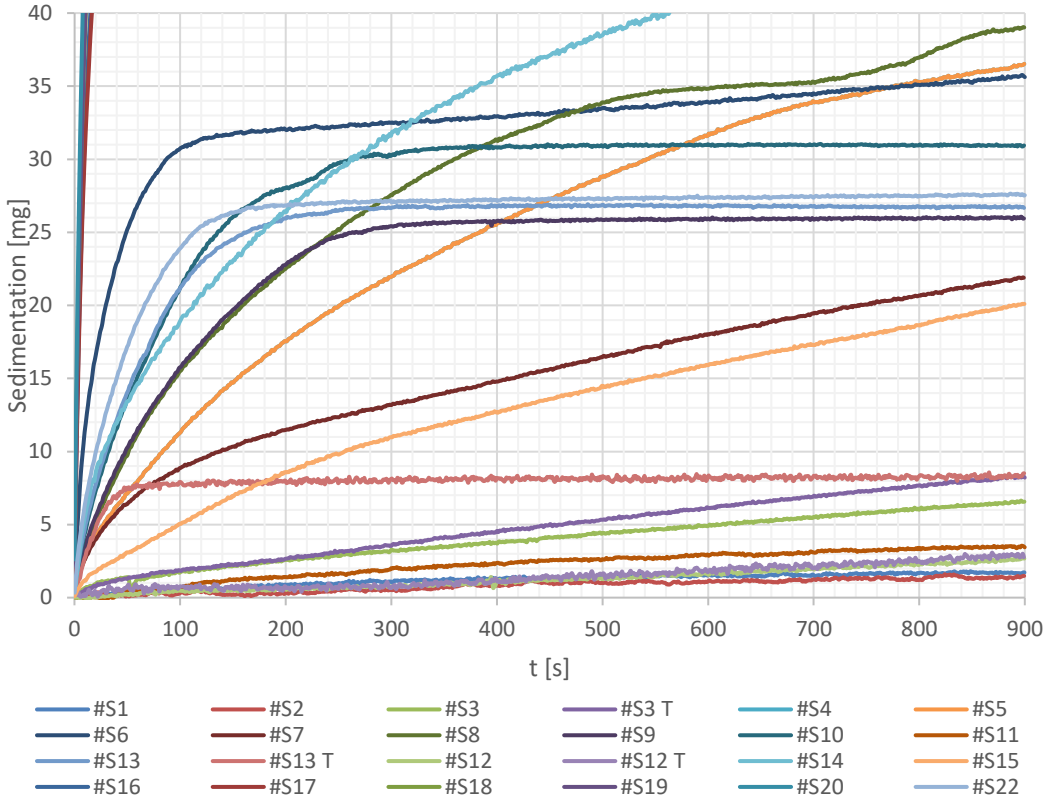

Figure 4.2 Sedimentation of SiO_2 particles synthesized by "sol-gel" method in different solvents (b)

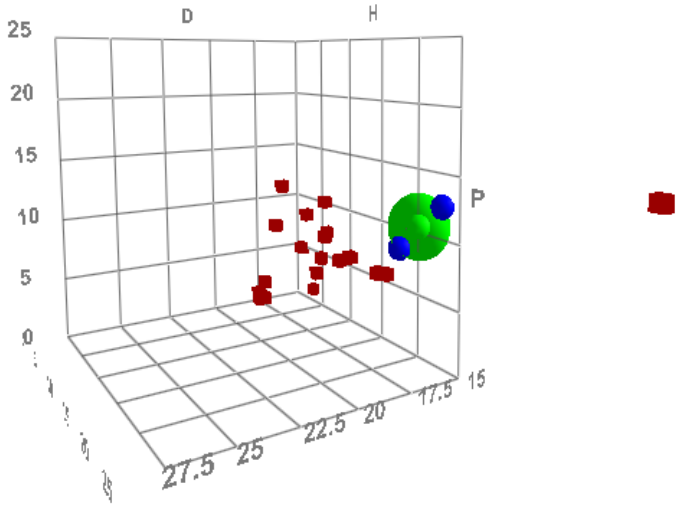

Figure 4.3 Hansen dispersibility parameters and corresponding sphere of SiO_2 particles.

Table 4.1 Sedimented mass of SiO_2 particles synthesized by "sol-gel" method in different solvents and Hansen Solubility Parameter (HSP) score

Solvent	**dD†**	**dP†**	**dH†**	**ρ [g/ml]**	**μ[s]***	**Sedimentation @900sn [mg]**	**HSP Score**
S1- Ethanol	15.8	8.8	19.4	0.79	10.12	1.72	0.90
S2- Methanol	14.7	12.3	22.3	0.79	9.70	1.49	1.00
S3- DIW	15.5	16	42.3	1.00	10.55	8.21	0.23
S4- 2-Propanol	15.8	6.1	16.4	0.79	10.85	41.25	0.04
S5- Isobutyl Alcohol	155	5.7	15.9	0.80	11.07	36.53	0.05
S6- Ethyl Acetate	15.8	5.3	7.2	0.90	10.00	35.62	0.05
S7- Dimethyl Succinate	16.1	7.7	8.8	1.09	10.71	21.89	0.10
S8- Ethylene Glycol Butyl Ether Acetate	15.3	7.5	6.8	0.94	10.30	39.02	0.05
S9- Propylene Glycol Monomethyl Ether Acetate	15.6	5.6	9.8	0.97	10.25	25.95	0.07
S10- Propylene Glycol Monomethyl Ether	15.6	0.3	11.6	0.89	10.45	30.94	0.06
S11- Acetone	15.5	10.4	7	0.79	9.50	3.45	0.42
S12- Methyl Ethyl Ketone (MEK)	16	9	5.1	0.81	9.72	2.77	0.54
S13- Methyl Isoamyl Ketone	16	5.7	4.1	0.81	9.71	8.51	0.18
S14- N-Methyl-2-Pyrrolidone	18	12.3	7.2	1.03	10.22	44.24	0.04
S15- Cyclohexanone	17.8	8.4	5.1	0.94	10.42	20.10	0.09
S16- Solvesso 100	17.6	0.8	2	0.87	10.10	186.50	0.01
S17- Xylene	17.6	1	3.1	0.86	9.87	167.19	0.01
S18- Toluene	18	1.4	2	0.87	9.10	172.21	0.01
S19- Solvesso 150	17.8	0.6	1.4	0.88	10.11	139.42	0.01
S20- WhiteSprit	14	0.1	0.1	0.77	10.11	88.16	0.02
S22- n-Butyl Acetate	15.8	3.7	6.3	0.88	9.90	27.54	0.06

*DC4 viscosity at 23°C
†dD: disperse component dP: polar component dH: hydrogen component of HSP

Hansen solubility parameter score was given according to Relative Sedimentation Rate (RST) calculation. Then, the dispersibility parameters of SiO_2 particles synthesized by "sol-gel" method were determined by HSP program. Dispersibility parameters of SiO_2 particles can be seen in Figure 4.3 as green sphere.

It can also be seen in Table 4.1 and Figure 4.1 that S3-water is found to be a bad solvent to synthesize SiO_2 particles by "sol gel" method, due to viscosity of water, primer particle size and surface characteristics of SiO_2 particles.

By using score values and HSP program, dispersibility parameters of nano sized SiO_2 particles were obtained as dD=15.33, dP=10.66 and dH=20.82.

4.1.2. Optimization of the variables

In the design of experiment, responses were non-volatile (NV) percentage [%], z-average [nm] and zeta potential. As it is seen in the Pareto charts given in Figures 4.4, 4.5 and 4.6, if one-way interactions are taken into account;

- NV% depends on amount of precursor-TEOS, catalyst type and reaction time
- Z-average and zeta potential depend on catalyst type

Regarding catalyst type, as it is expected homogeneous particle formation in smaller than 100 nm size could not be achieved with acidic catalyst (HCI_{aq}). The reason of this is why z-average values are almost in micrometre scale and zeta potential values are close to zero due to “sol-gel” network formation.

Another point is PdI and intercept values. PdI was lower than 0.7 and intercept value was close to 0.9 for basic catalyst. For acidic case both parameters were off spec. Therefore, by using acidic catalyst, nanoscale particles of which sizes are less than 100 nm could be synthesized.

Table 4.2 Results of responses of 2_{VI}^{6-1} DOE.

TEOS [ml]	Catalyst [ml]	Rxn Temp, [^{0}C]	Mixing Rate [rpm]	Type of Cat,	NV%	Z-Avg, [nm]	PDI	Zeta Pot. [mV]	MeOH/ TEOS	nH2O/ nTeOS
40	5	60	500	NH4OH	5.05	NA (Gel)	NA (Gel)	NA (Gel)	6.3	1.1
40	5	40	1000	NH4OH	4.77	NA (Gel)	NA (Gel)	NA (Gel)	6.3	1.1
40	5	40	500	NH4OH	4.72	NA (Gel)	NA (Gel)	NA (Gel)	6.3	1.1
40	5	60	1000	NH4OH	4.83	NA (Gel)	NA (Gel)	NA (Gel)	6.3	1.1
40	10	40	1000	NH4OH	5.9	15.92	0.293	-22.8	6.3	2.2
20	5	40	500	NH4OH	3.54	9.61	0.257	-15.8	12.5	2.2
20	5	40	1000	NH4OH	3.36	11.78	0.304	-29.4	12.5	2.2
20	5	60	500	NH4OH	3.41	25.26	0.422	-23.3	12.5	2.2
40	10	60	1000	NH4OH	5.94	23.04	0.375	-19.1	6.3	2.2
40	10	40	500	NH4OH	5.96	17.1	0.328	-16.5	6.3	2.2
30	7.5	50	750	NH4OH	4.74	16.12	0.281	-19.3	8.3	2.2
40	10	60	500	NH4OH	5.71	24.99	0.445	-25.2	6.3	2.2
20	5	60	1000	NH4OH	3.37	15.88	0.271	-21.9	12.5	2.2
20	10	40	500	NH4OH	3.01	12	0.267	-18.3	12.5	4.3
20	10	40	1000	NH4OH	3.36	14.26	0.334	-21.7	12.5	4.3
20	10	60	500	NH4OH	3.28	17.93	0.399	-24.8	12.5	4.3
20	10	60	1000	NH4OH	3.19	15.33	0.323	-23	12.5	4.3
40	5	60	1000	HCI	7.91	736.4	0.587	0.593	6.3	1.1
40	5	60	500	HCI	7.61	173.1	0.423	0.302	6.3	1.1
40	5	40	500	HCI	8.14	592.1	0.345	0.782	6.3	1.1
40	5	40	1000	HCI	7.46	2540	1	0.548	6.3	1.1
40	10	40	500	HCI	7.08	228.9	0.429	1.53	6.3	2.2
30	7.5	50	750	HCI	5.97	417.9	0.787	-0.24	8.3	2.2
40	10	60	1000	HCI	7.88	620	0.434	-2.73	6.3	2.2
40	10	40	1000	HCI	8.3	906.9	0.633	-2.84	6.3	2.2
20	5	60	500	HCI	4.76	901.2	0.588	-3.18	12.5	2.2
40	10	60	500	HCI	7.69	321.1	0.566	1.15	6.3	2.2
20	5	40	500	HCI	4.47	1591	0.813	1.2	12.5	2.2
20	5	40	1000	HCI	5.26	529.5	0.335	-0.866	12.5	2.2
20	5	60	1000	HCI	4.66	1013	0.667	0.561	12.5	2.2
20	10	40	500	HCI	5.26	300.3	0.529	-1.96	12.5	4.3
20	10	60	500	HCI	5.52	1665	1	-4.69	12.5	4.3
20	10	60	1000	HCI	5	2401	0.969	-3.97	12.5	4.3
20	10	40	1000	HCI	4.43	88.13	0.147	-0.797	12.5	4.3

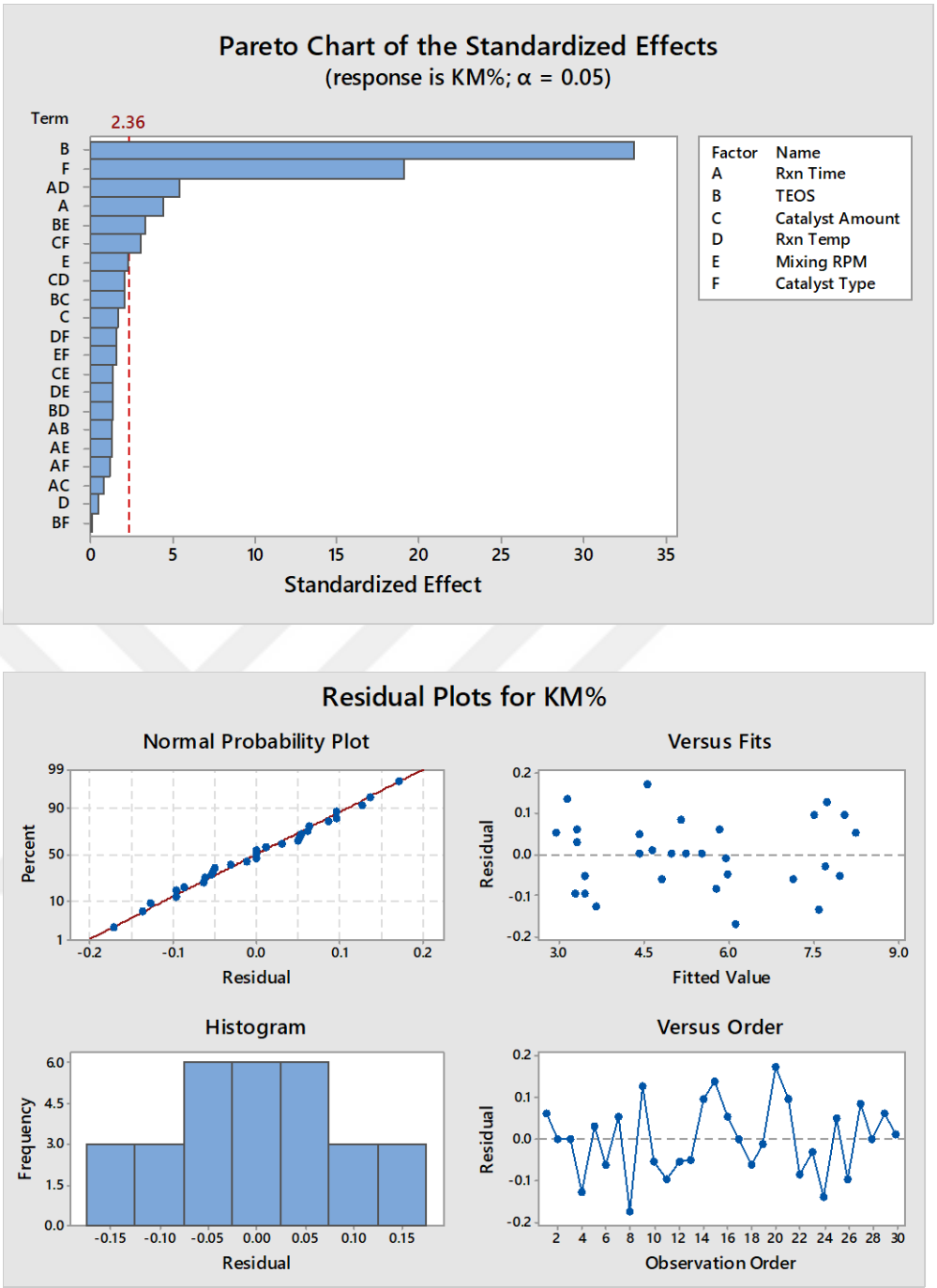

Figure 4.4 Pareto chart and residual plots for NV% response

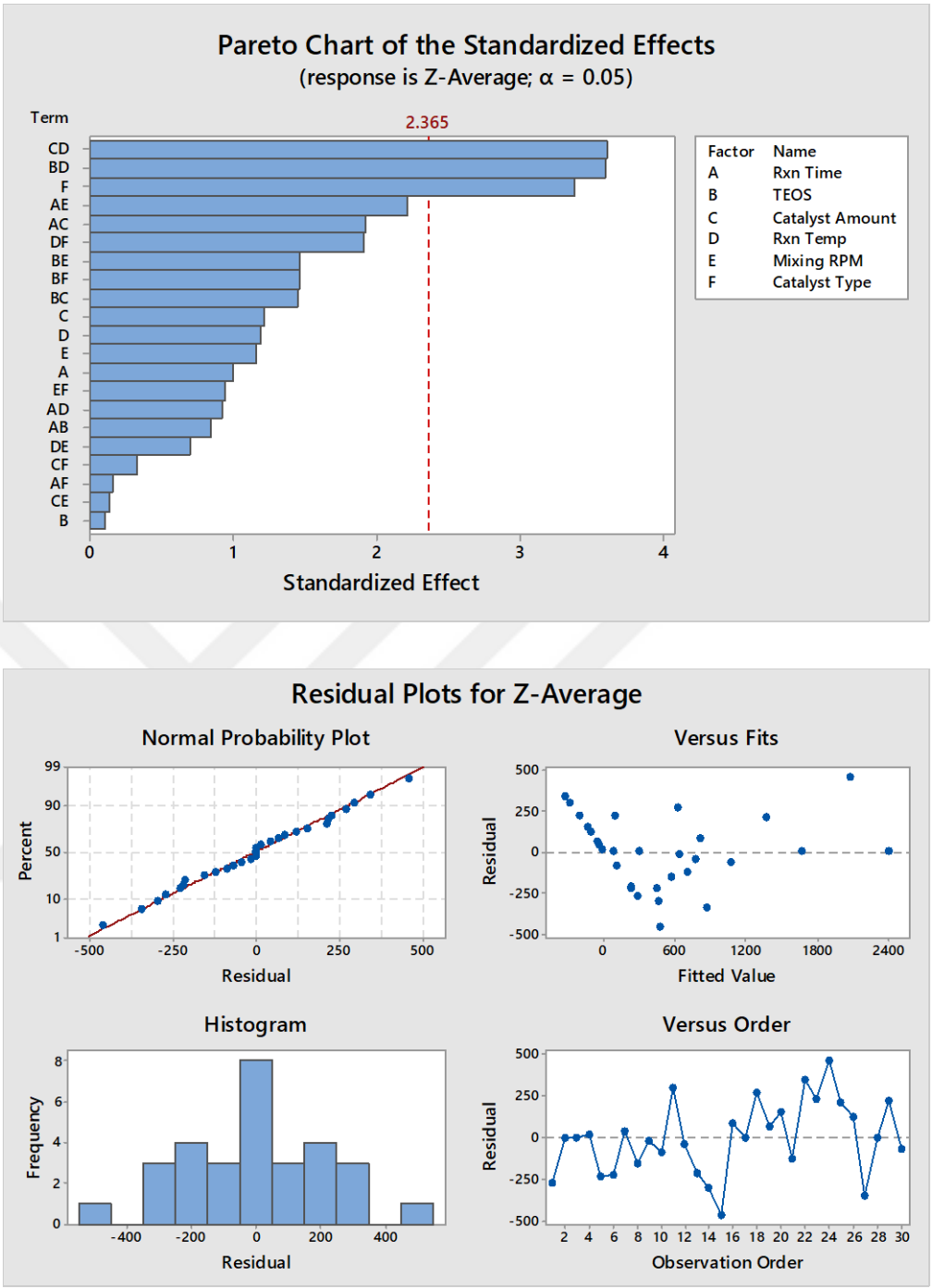

Figure 4.5 Pareto chart and residual plots for z-average [nm] response

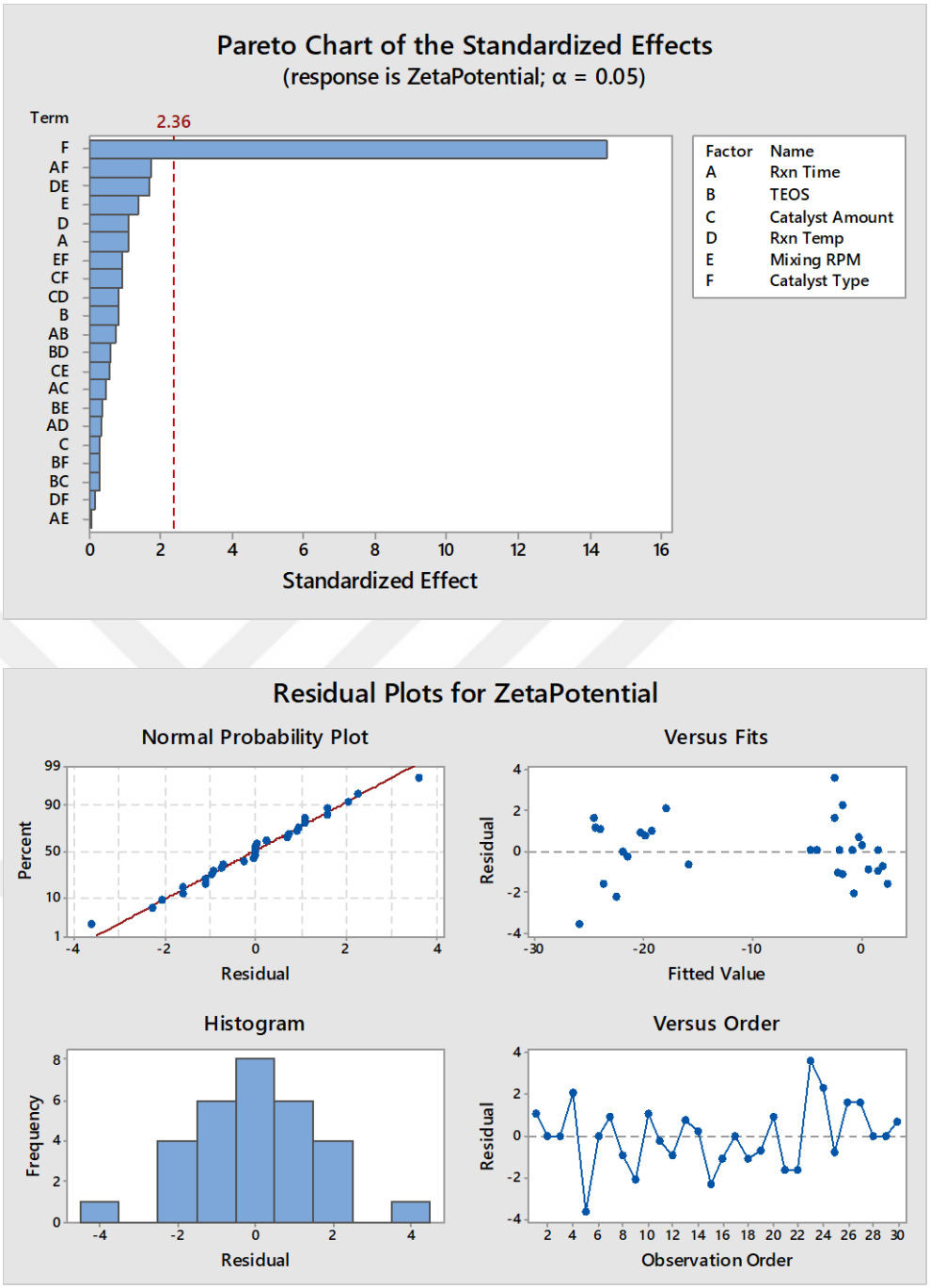

Figure 4.6 Pareto chart and residual plots for zeta potential [mV] response

Considering effect of one and two way variable interactions from the results of DOE on the responses, it was understood that particle size, non-volatile % and zeta potential can be optimized when amount of precursor and basic catalyst were able to be adjusted. Basic catalyst also contains 75% water. Therefore, the effect of molar ratio of H_2O to TEOS on ratio of sol to gel transformation was also

investigated. The ratios studied, H_2O: TEOS=2, 4, in the presence of NH_4OH were found to be acceptable according to z-average, NV% and zeta potential results.

In addition, it was seen that, all proposed experimental conditions in Table 4.2 are miscible according to condition given in Figure 2.5.

4.1.3. Enhancement in efficiency of Sol to gel transformation

In order to enhance efficiency of sol to gel transformation reaction i.e., to increase NV% and decrease the z-average value, the effects of molar ratio of H_2O to TEOS, volumetric ratio of MeOH to TEOS and amount of NH4OH were deeply investigated. Experimental details and the results obtained can be seen in Table 4.3. All ingredients of the experiment TS10 were in miscibility zone (Figure 2.5) and the results of TS10 were seemed to be acceptable according to its particle size and non-volatile %. Therefore TS10 was used for further investigation of the work.

Table 4.3 Results of experiments conducted to enhance efficiency of sol to gel transformation

	MeOH [ml]	TEOS [ml]	NH4OH [ml]	NV%	Z-Avg, [nm]	PDI	Zeta Pot. [mV]	MeOH/ TEOS (V/V)	nH2O/ nTeOS (mole/mole)
TS1	150	96	3	3.82	NA (gel)	NA	NA (gel)	1.6	0.3
TS2	150	48	3	4.63	NA (gel)	NA	NA (gel)	3.1	0.5
TS3	150	24	3	4.75	NA (gel)	NA	NA (gel)	6.3	1.1
TS4	150	12	3	3.24	37.67	0.770	-22.3	12.5	2.2
TS5	150	96	6	6.5	546	0.934	-23.7	1.6	0.5
TS6	150	48	6	8.38	141.8	0.431	-20.1	3.1	1.1
TS7	150	24	6	5.66	22.92	0.247	-24.9	6.3	2.2
TS8	150	12	6	3.19	14.35	0.305	-27.4	12.5	4.3
TS9	150	96	12	10.89	310.6	0.325	-22.7	1.6	1.1
TS10	150	48	12	9.54	67.24	0.199	-26.6	3.1	2.2
TS11	150	24	12	5.02	28.17	0.226	-28.1	6.3	4.3
TS12	150	12	12	2.89	47.73	0.336	-22.3	12.5	8.7
TS13	150	96	24	14.65	274	0.279	-25.9	1.6	2.2
TS14	150	48	24	8.61	245.1	0.089	-20.1	3.1	4.3
TS15	150	24	24	5.31	150.2	0.091	-19.9	6.3	8.7
TS16	150	12	24	3.03	255.6	0.116	-21.1	12.5	17.4

4.2. Surface Treatment of SiO_2 Nano Particles synthesized by "Sol-Gel" method

4.2.1. Determination of isoelectric point (IEP)

In determination of isoelectric point of TS10, deionized water, of which specifications are 0.06µS, 71.2mN/m and pH 6.8 was used. Deionized water at different pH values in the range of pH2 and pH12 was prepared using aqueous HCl and NaOH solutions. Definite amount of silica particles was added into the water having different pH values, mixed at 500 rpm for 2 h. And then mixing was stopped and waited for 24 hours. Mixtures of silica particles and water came to equilibrium and zeta potential was measured by using zeta-sizer. Zeta potential values were plotted as a function of pH as shown in Figure 4.7 and IEP of TS10 that is the intercept of dotted line with zero zeta potential line was found to be 1.34. Therefore, surface of TS10 has acidic characteristic.

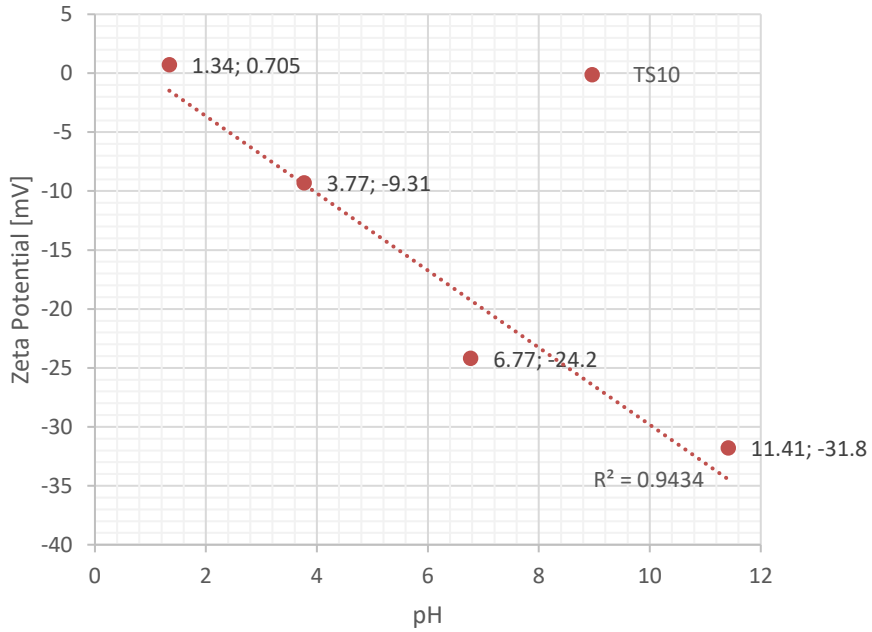

Figure 4.7 Determination of IEP of TS10

4.2.2. Surface treatment trials

Wetting and Dispersing Additives: Regarding performance evaluation of wetting and dispersing agents given in Table 3.6, wettability performance of powder of TS10 was checked with wettability probe (Figure 4.8) based on

Washburn equation (Eq.(2.1)). The results were given in Figure 4.8. Nevertheless, such kind of agents could not worked for TS10. Only Agent–H, basic polyurethane, is slightly (~6%) better than blank i.e methanol without wetting and dispersing agents. At this point, for wetting and dispersing agents further investigations were not be carried out because of the fact that unpromising TS10 wettability results.

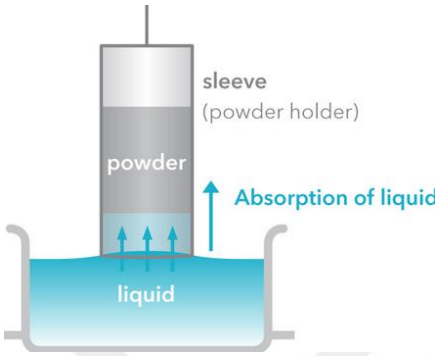

Figure 4.8 Schematic representation of powder wettability probe. (BiolinScientific, 2018)

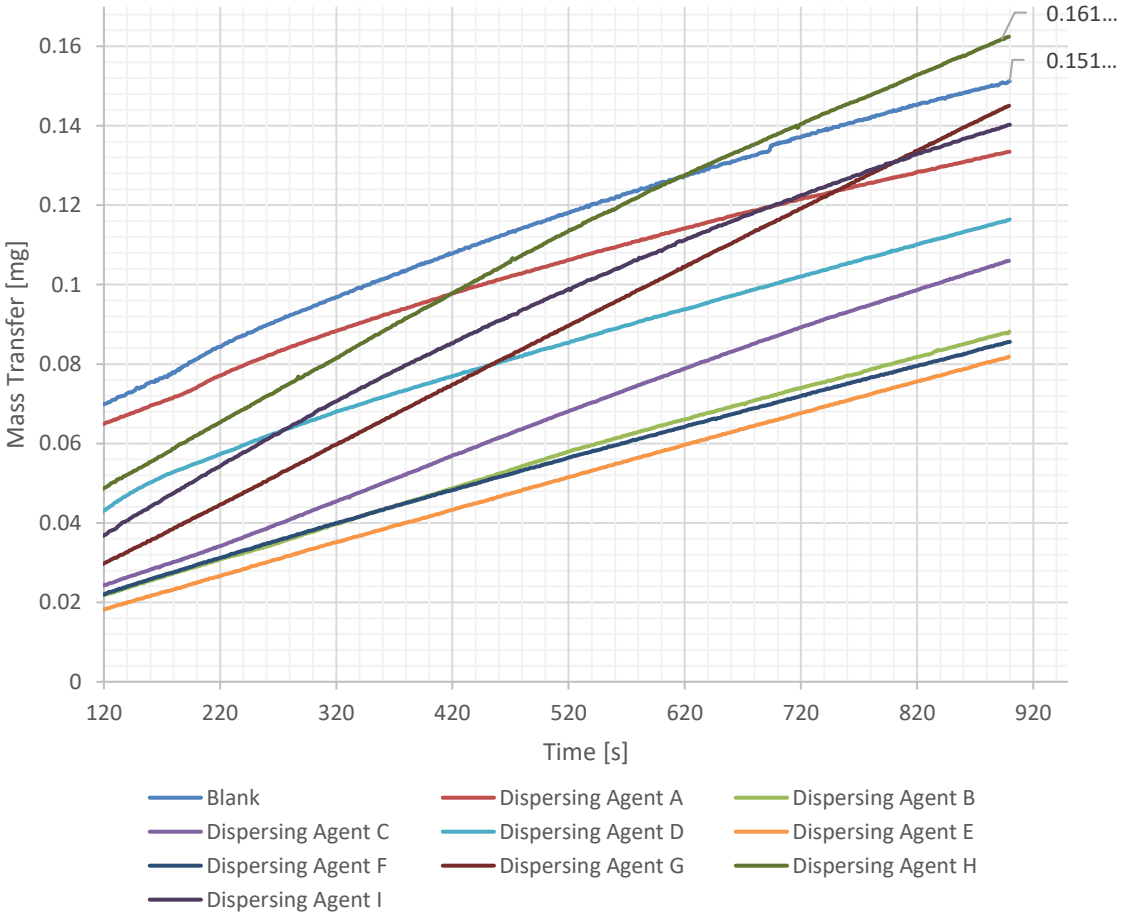

Figure 4.9 Wettability control of TS10 powder in methanol in the absence (blank) and presence of wetting and dispersion agents (the ratio of TS 10 to agent = 1:1 based on solid)

Silane surface treatment agents: SiO_2 nano particles in TS10 sol were treated in its own sol at ratios of silane:SiO_2; 0.1:1, 0.5:1, 1:1 and 2:1 by weight. Surface treatment of SiO2 particles was conducted at room temperature for 30min. And high shear Cowles type impeller was also used to mix the sol.

Physical state and stability of TS10 sol, containing surface treated SiO_2 particles were checked. Only silane agent –D treated SiO_2 particles could not stay stable in TS10 due to hydrophobic characteristic of -octyl chain side of silane agent-D. Others were able to stay stable in TS10.

1.75phr and 3.00phr silane surface treated TS10 were incorporated into the ready to spray HS clearcoat called as "*Hybrid HS Clearcoat*" to check the compatibility issue.

Regarding silane agent E treated TS10, it was seen that it is observed gel formation in the clearcoat as soon as after mixing with its hardener. It was the result of the amine functionality of silane agent E (basically due to fast reaction of amine and isocyanate in ready to use hybrid clearcoat)

Related to silane agent C treated TS10, although there was not any incompatibility issue in Hybrid HS clearcoat, pot life of hybrid HS clearcoat shortened from 3hr to 1hr. It was the result of the mercaptan functionality of silane agent C (basically due to reaction of mercaptan and isocyanate in the ready to use hybrid clearcoat). Although there were not any incompatibility and pot life issue in silane agent B treated TS10, preliminary scratch resistance evaluation was not so satisfying. In silane agent A treated TS10, overall preliminary assessments were found as promising. Hence hybrid clearcoat was performed by usage of silane agent A treated TS10.

4.3. Characterization of SiO_2 Nano Particles synthesized by "Sol-Gel" method

4.3.1. FTIR spectrums

FTIR spectra of SiO2 particles synthesized using TS10 sol and of the surface treated particles at different ratios of TS10: silane agent A was given in Figure 4.10. Peak at1100 cm^{-1} was an indication of characteristics of SiO_2 particle formed. The characteristic peak for surface treated particles by silane agent A was observed at

1410 cm^{-1}. It was also concluded that the surface treatment efficiency in the case of the ratio of TS10: silane agent A=1:0.5 is higher than those of other ratios (1:0.1, 1:1, and 1:2).

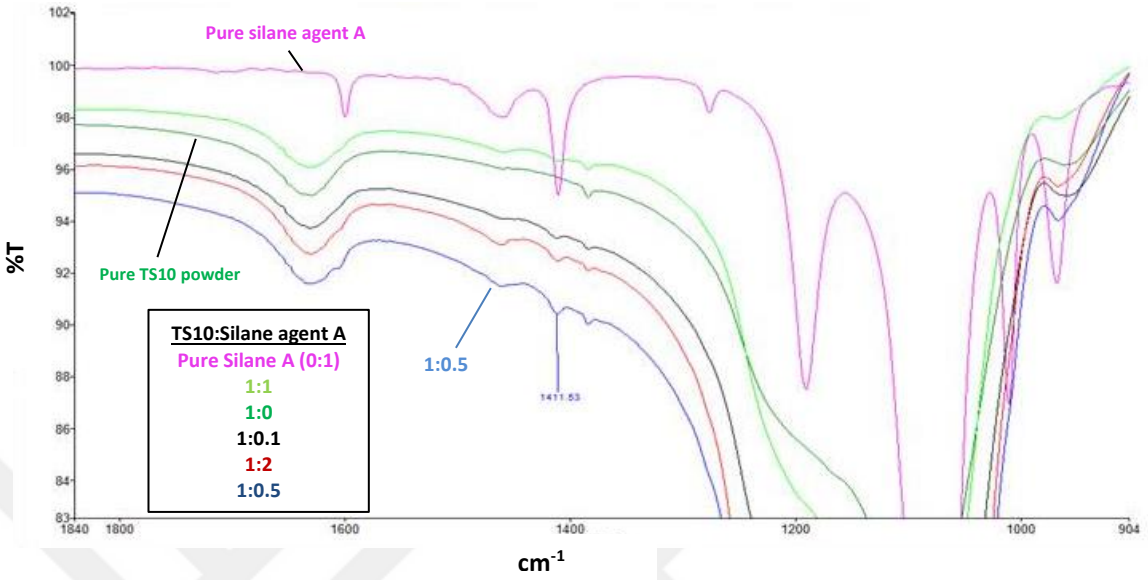

Figure 4.10 Partial FTIR spectrum of TS10 before and after surface treatment of silane agent A

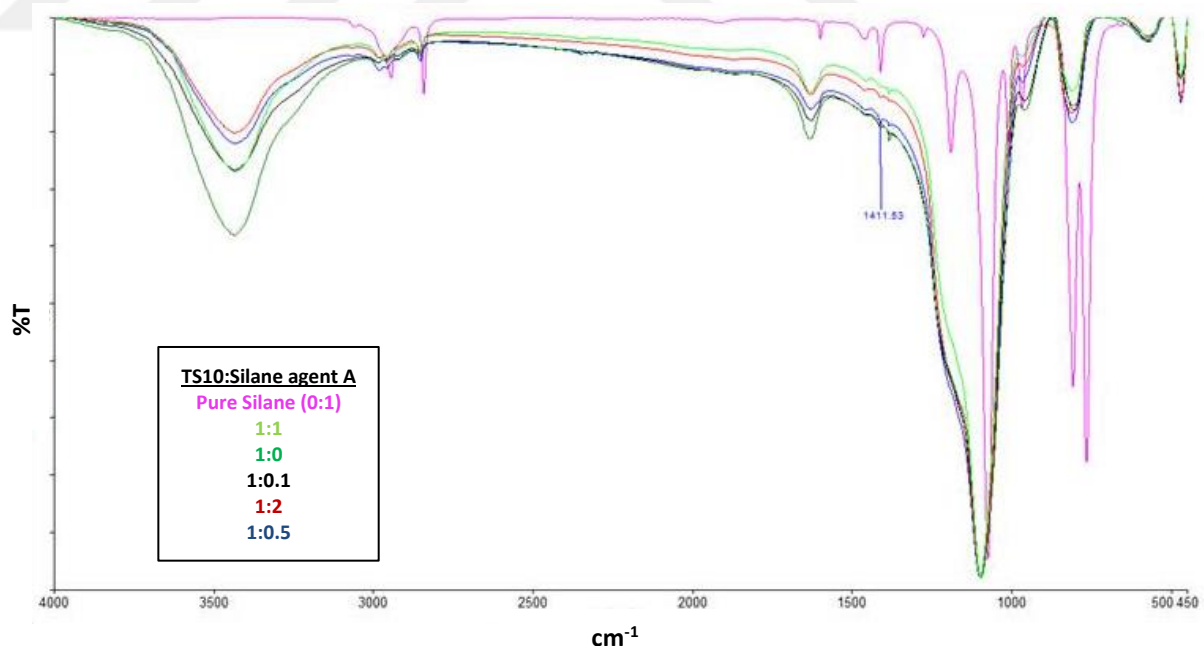

Figure 4.11 Full FTIR spectrum of TS10 before and after surface treatment of silane agent-A

4.3.2. TGA results

Results of thermal gravimetric analysis of silica particles in the absence and presence of silane agent A were given in Figure 4.12. It was observed that weight loss of the particles of which surfaces were treated at a ratio of TS10: Silane agent A =1: 0.5, is higher than those at 1:1 and 1:2 ratios after 700°C.

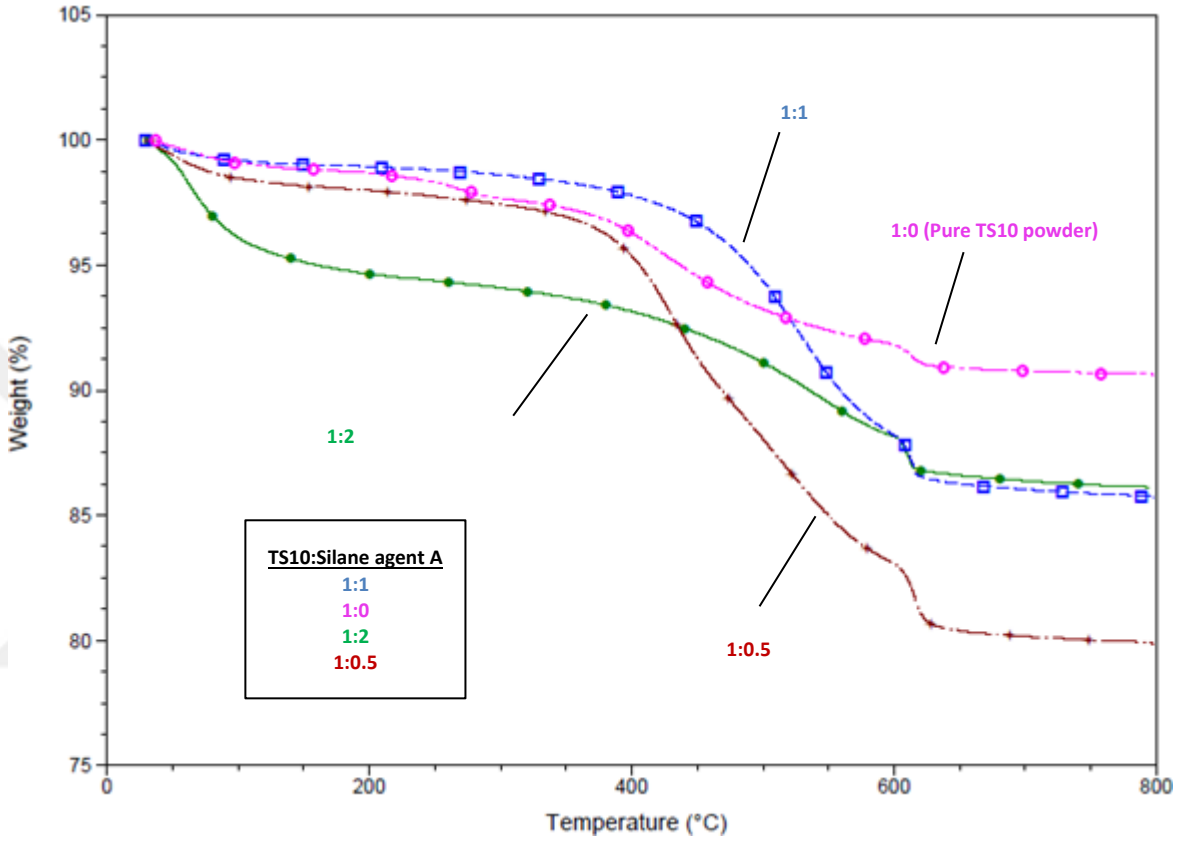

Figure 4.12 TGA curves of silica particles in the absence and presence of silane agent A

4.3.3. SEM images

Diameters of SiO_2 particles were measured and illustrated in Figure 4.13. As seen in the images, SiO_2 particles are in spherical shape and sizes of silica particles changed in the range of 22- 45 nm. The size distribution of TS10 obtained from DLS measurement given in Figure 4.14 indicated that the particle sizes change from 12 to 200 nm. However, the z-average of the particle size distribution was recorded as 67 nm. As a consequence, it can be said that both SEM and DLS analyses confirm the size of particles synthesized.

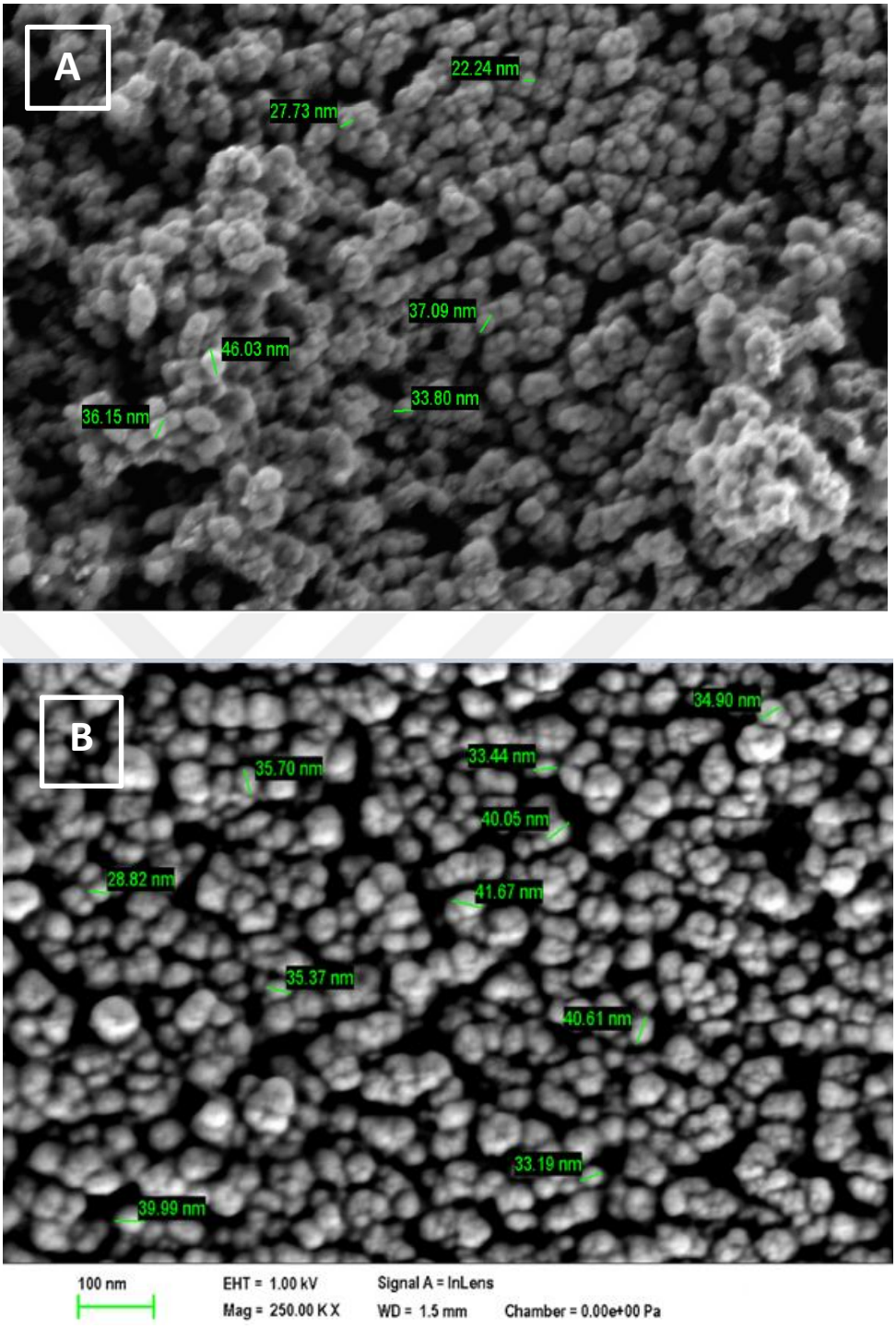

Figure 4.13 SEM images (A- 1:0.5 surface treated TS10, B- pure TS10)

		Size (d.nm):	% Intensity:	St Dev (d.nm):
Z-Average (d.nm): 67.24	Peak 1:	92.58	100.0	57.07
PdI: 0.239	Peak 2:	0.000	0.0	0.000
Intercept: 0.953	Peak 3:	0.000	0.0	0.000
Result quality : Good				

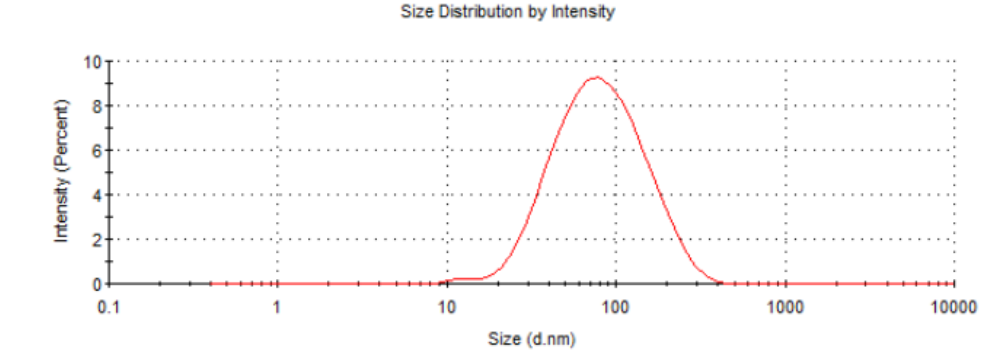

Figure 4.14 Particle size distribution of TS10 obtained from DLS measurement.

4.4. Characterization of Automotive Hybrid Clearcoat

4.4.1. Determination of system polarity of clearcoat system

System polarity of clearcoat can be compared as polar part of static surface tension. The polar and disperse components of the surface tension of clearcoat was determined by contact angle measurements on a non-polar PTFE surface. As it is seen from Table 4.4., system polarity in other words polar part of static surface tension is higher in HS clearcoat. Therefore, further evaluation was performed for HS clearcoat in terms of compatibility of SiO2 nano particles.

Table 4.4 Disperse and polar components of HS and MS clearcoat

	Static Surface Tension [mN/m]	Contact Angle [°] on PTFE	Disperse Part [mN/m]	Polar Part [mN/m]
HS[a] Clearcoat	24.85	56.65	17.62	7.23
MS[b] Clearcoat	24.45	46.84	20.14	4.31

[a] High Solid; [b] Medium Solid

Table 4.5 Calculation of disperse and polar components of HS clearcoat

<table>
<tr><th>Data</th><th>Equations</th></tr>
<tr><td rowspan="4">Substrate: PTFE
$\sigma_s = 21.04\ \mathrm{mN/m}$</td><td>$\sigma_{sl} = \sigma_s + \sigma_l - 2\sqrt{\sigma_s.\sigma_l^d}$
(2.20)</td></tr>
<tr><td>$\sigma_l^d = \frac{1}{4\sigma_s}(\sigma_s+\sigma_l - \sigma_{sl})^2$
(2.21)</td></tr>
<tr><td>$\sigma_{sl} = \sigma_s - \sigma_l\cos\theta$ (2.22)</td></tr>
<tr><td>$\sigma_l^d = \frac{{\sigma_l}^2}{4\sigma_s}(1+\cos\theta)^2$ (2.23)</td></tr>
<tr><td colspan="2">Calculations (HS Clearcoat)
$\sigma_l^d = \frac{{\sigma_l}^2}{4\sigma_s}(1+\cos\theta)^2 = \frac{(24.85)^2}{4*21.04}(1+\cos(56.65*0.0174532925)^2)$
$= 7.23\ \mathrm{mN/m}$
$\sigma_l^p = 24.85 - 7.23 = 17.62\ \mathrm{mN/m}$</td></tr>
<tr><td>Disperse component
$\sigma_l^d = 7.23\ \mathrm{mN/m}$</td><td>Polar component
$\sigma_l^p = 17.62\ \mathrm{mN/m}$</td></tr>
</table>

4.4.2. Rheology of hybrid clearcoat

Rheological behavior of HS clearcoat (HS CC) was investigated in the absence (HS CC TS10) and presence of silane agent A (TS10M). HS Hybrid clearcoat containing 1.75phr and 3 phr are noted as HS Hybrid CC 1.75phr TS10M,indicated with Grey color and HS Hybrid CC 3phr TS10M, indicated with Red color in Figure 4.14 respectively. When concentration of SiO_2 nano particles was increased from 1.75phr to 3phr in the hybrid clearcoat (HS CC), rheological properties changed. 3phr usage in HS clearcoat -TS10M increased the hysteresis area and changed thixotropic behavior i.e., increased viscosity recovery rate. In addition, the HS clearcoat became more elastic at low shear rate.

1.75phr usage in HS clearcoat- TS10M did not affect the rheological behavior of HS CC and its viscoelastic properties. According to rheological point of view, HS Hybrid CC 1.75phr TS10M was seemed more promising. (Figure 4.15)

In Figure 4.16, It was seen that elastic modulus (part) of HS Hybrid CC 3phr TS10M is higher than others. This means that concentration of nano particles in the clearcoat may affect the viscoelastic properties of clearcoat due to their secondary interactions

To analyse thixotropic behaviour of clearcoat, 3-time interval test is used. It consists of a low shear condition (reference interval), a high shear condition to simulate application equipment and a low shear condition (regeneration interval). In Figure 4.16, these intervals can be seen. At low shear interval, HS Hybrid CC 3phr TS10M has viscoelastic characteristic. However after high shear interval, It shows viscous characteristic whereas its viscosity recovery is fast. (Figure 4.17)

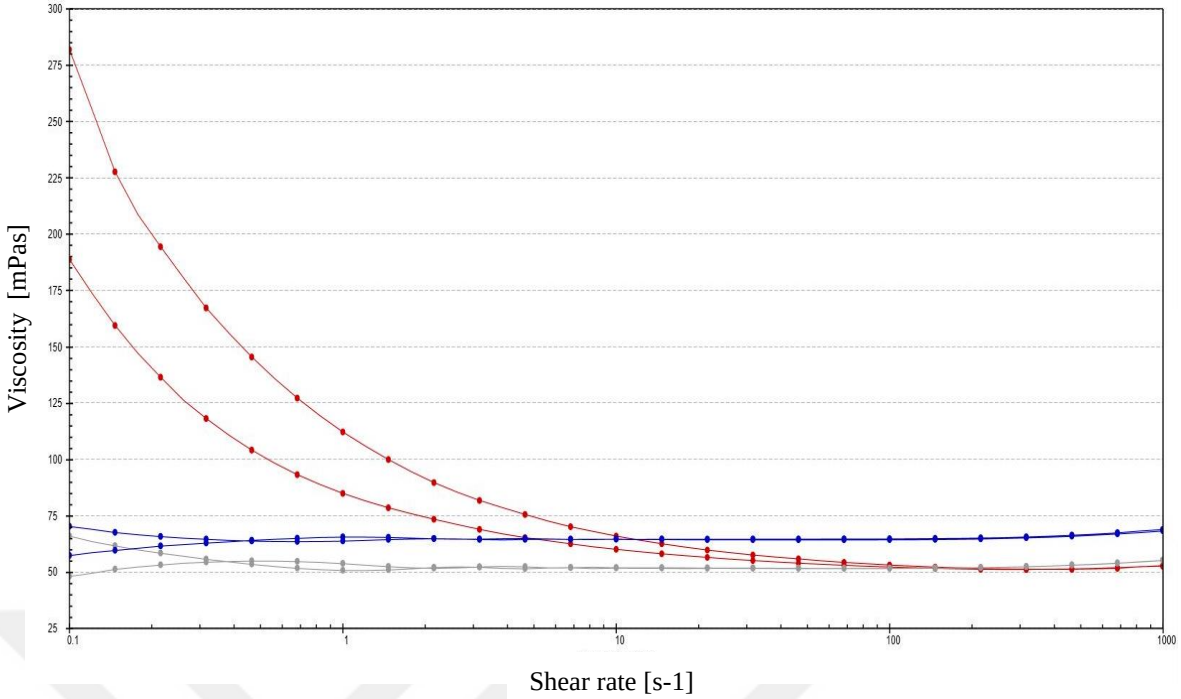

Figure 4.15 Viscosity vs shear rate relation (Blue: HS CC, Grey: HS Hybrid CC 1.75phr TS10M, Red: HS Hybrid CC 3phr TS10M)

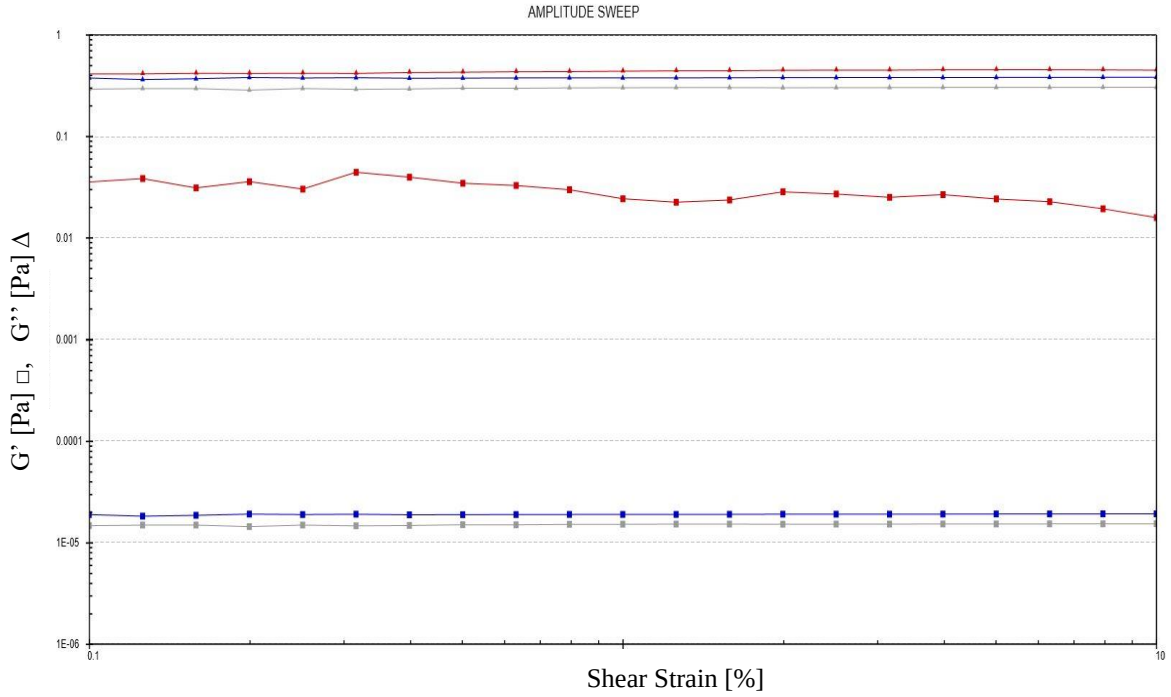

Figure 4.16 Amplitude sweep (Blue: HS CC, Grey: HS Hybrid CC 1.75phr TS10M, Red: HS Hybrid CC 3phr TS10M)

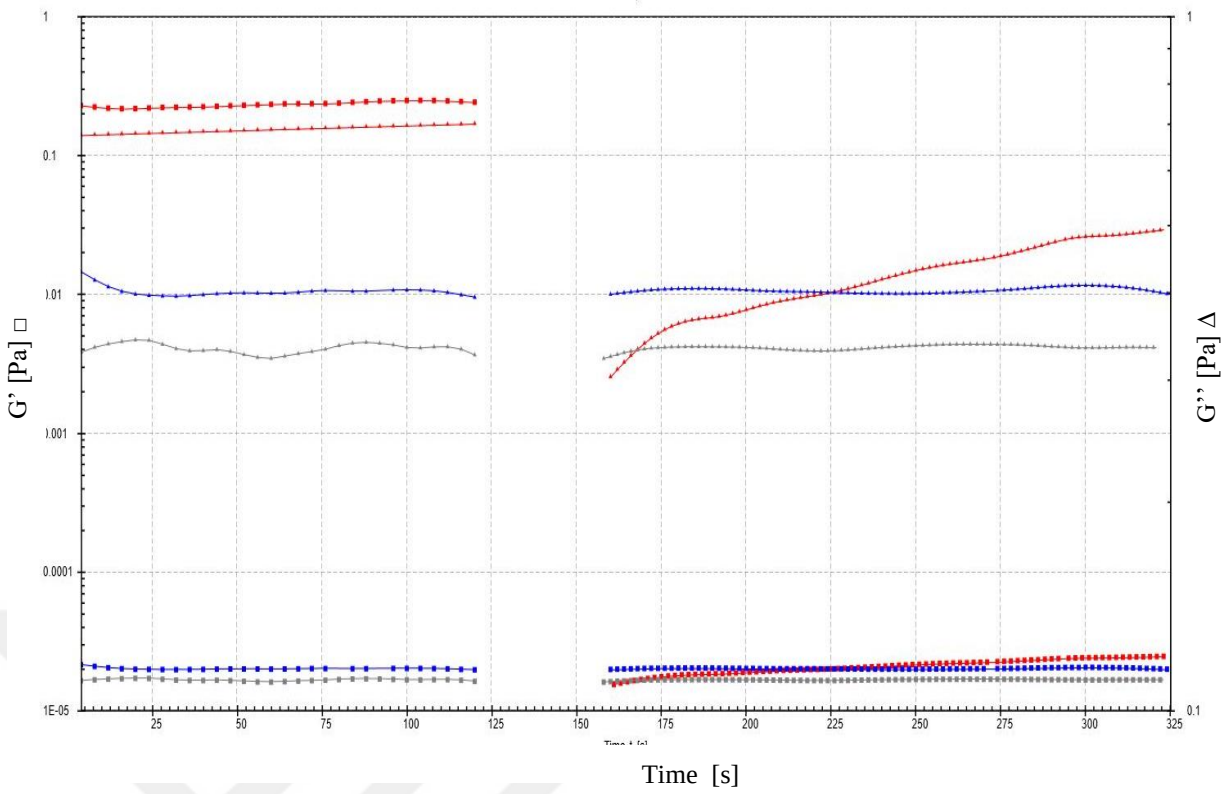

Figure 4.17 3 interval thixotropy test (Blue: HS CC, Grey: HS Hybrid CC 1.75phr TS10M, Red: HS Hybrid CC 3phr TS10M)

4.4.3. Dynamic mechanical thermal analysis of hybrid clearcoat

Dynamic mechanical thermal analysis comparisons were conducted for HS clearcoat i.e. reference, HS Hybrid clearcoat i.e. contains 1.75phr TS10M , HS Hybrid clear i.e. contains 3phr TS10M. (TS10M is silane agent A treated TS10.)

Dynamic mechanical thermal analysis of HS CC, HS Hybrid CC 1.75phr TS10M and HS Hybrid CC 3phr TS10M were made and compared. For these purposes strain ramp (tensile) (Figure 4.18-19-20), frequency sweep oscillation tests (Figure 4.21-22) and temperature sweep tests (Figure 4.23 to 4.27) were made and analysed.

Strain ramp test (tensile test) was performed to measure and determine elastic modulus, yield-ultimate strength, fracture point and toughness values of HS CC, HS Hybrid CC 1.75phr TS10M and HS Hybrid CC 3phr TS10M. In Table 4.6, overall results can be investigated and compared.

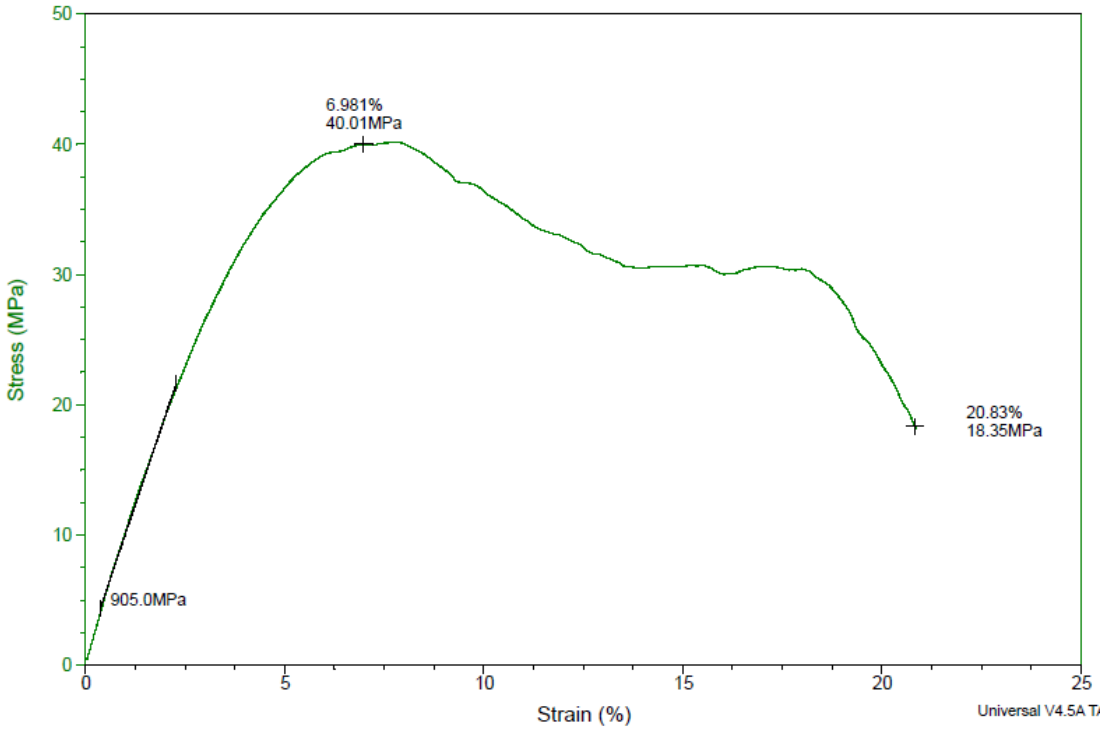

Figure 4.18 Strain ramp test (tensile test) result of HS clearcoat (reference)

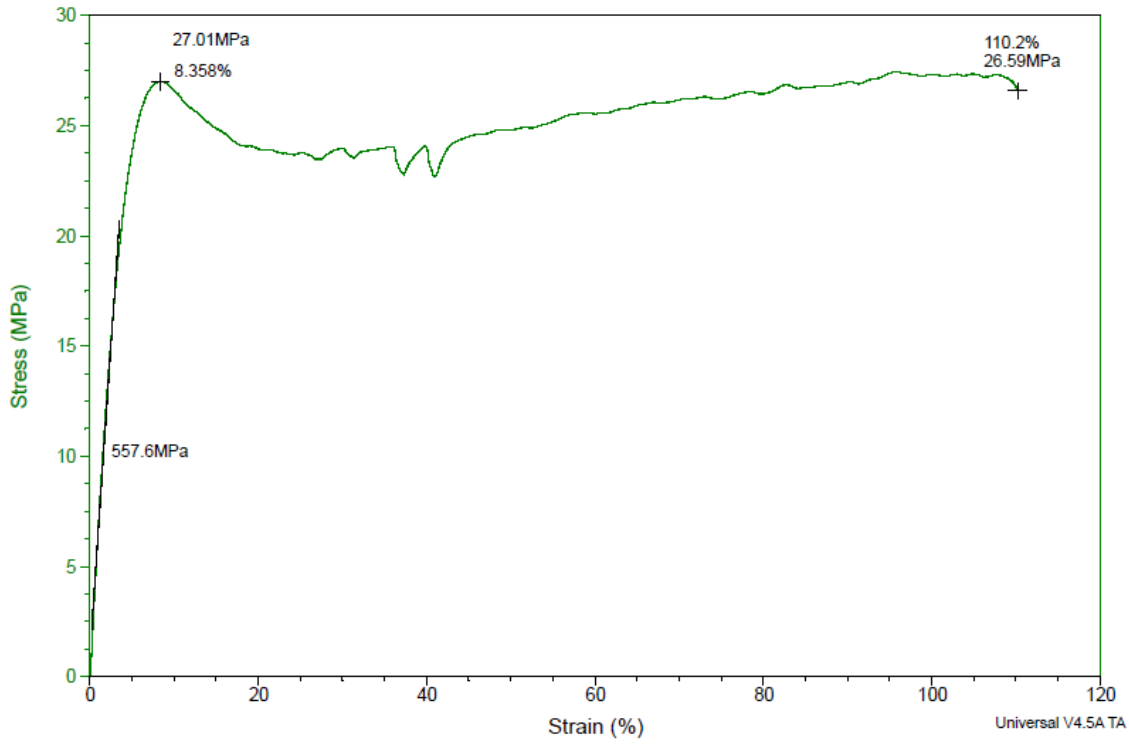

Figure 4.19 Strain ramp test (tensile test) result of HS Hybrid clearcoat i.e. contains 1.75phr TS10M

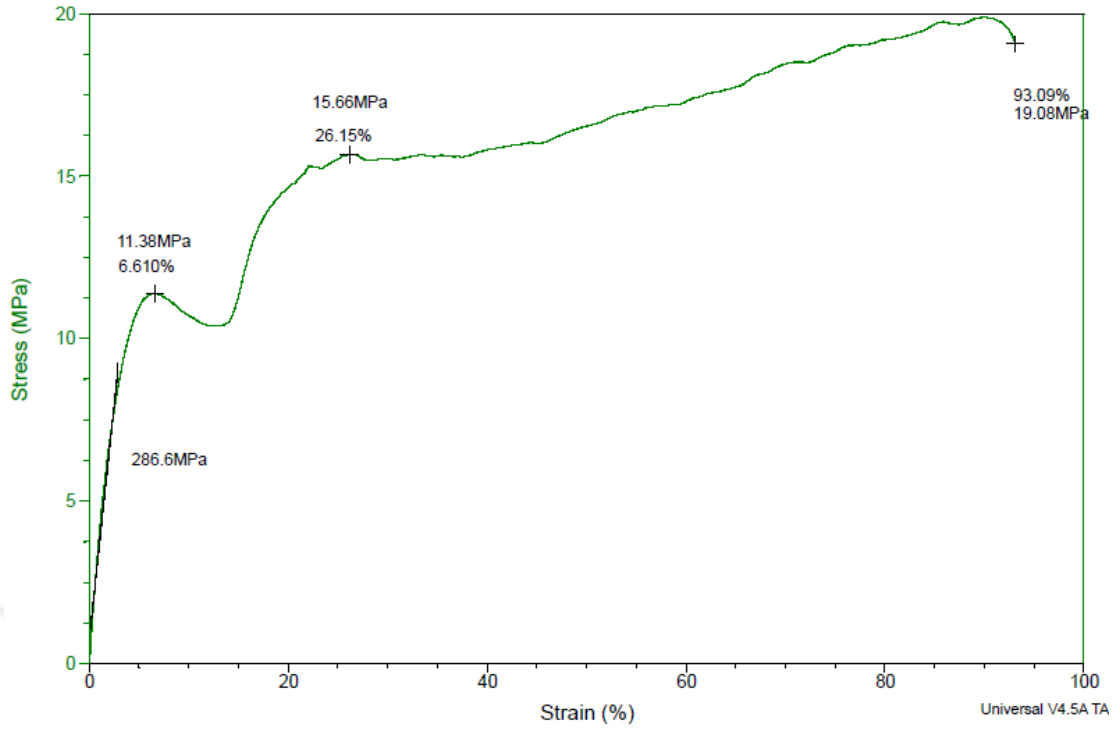

Figure 4.20 Strain ramp test (tensile test) result of HS Hybrid clearcoat i.e. contains 3phr TS10M

Frequency sweep oscillation test was performed to analyse the elastic and viscous modulus of HS CC, HS Hybrid CC 1.75phr TS10M and HS Hybrid CC 3phr TS10M. It was seen that concentration of nano particles in the clearcoat affects the storage modulus of clearcoat. It lowers the storage modulus and increase loss modulus.

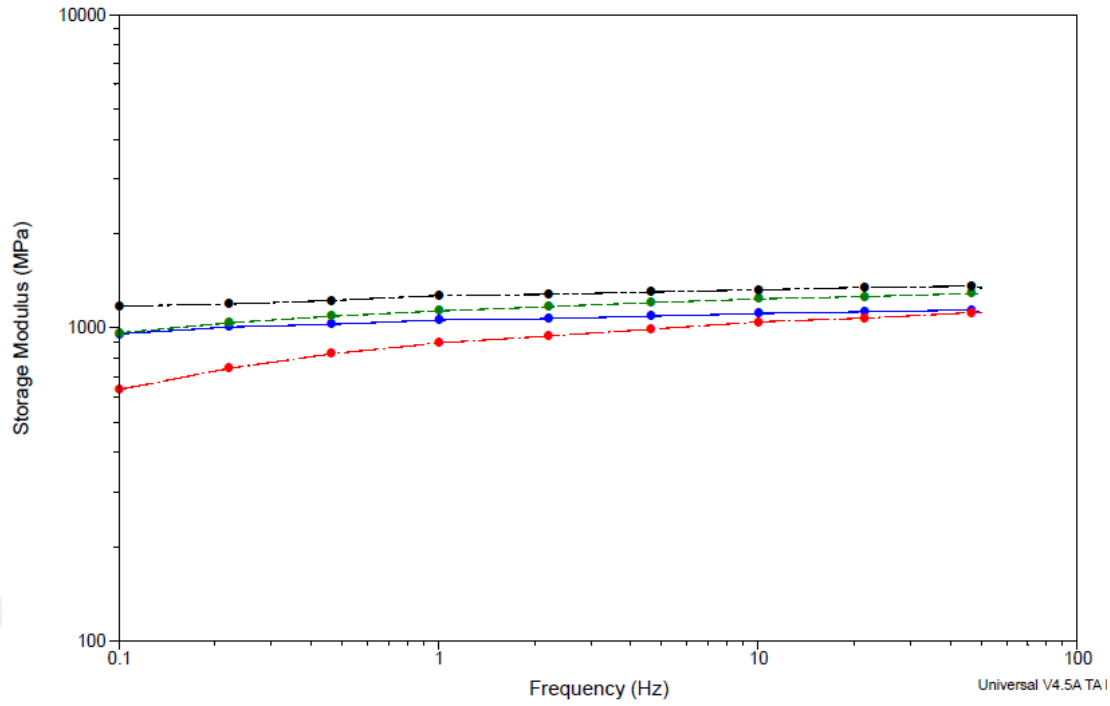

Figure 4.21 Frequency sweep oscillation –storage modulus of HS clearcoat (blue), HS Hybrid clearcoat i.e. contains 1,75phr TS10M (green) and 3phr TS10M (red)

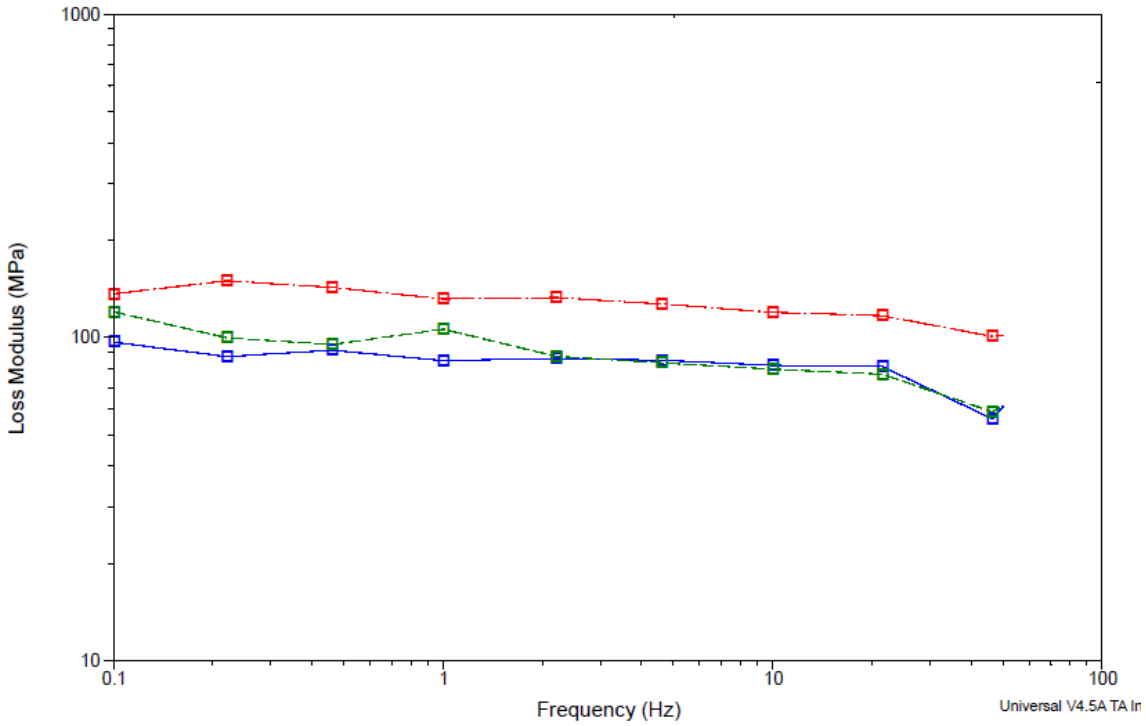

Figure 4.22 Frequency sweep oscillation –loss modulus of HS clearcoat (blue), HS Hybrid clearcoat i.e. contains 1,75phr TS10M (green) and 3phr TS10M (red)

Temperature ramp test: was performed to analyse crosslink density and glass transition temperate of HS CC, HS Hybrid CC 1.75phr TS10M and HS Hybrid CC 3phr TS10M. It was seen that concentration of nano particles in the clearcoat affects the glass transition temperature and crosslink density negatively due to polarity difference between SiO2 particles and polymeric network of clearcoat.

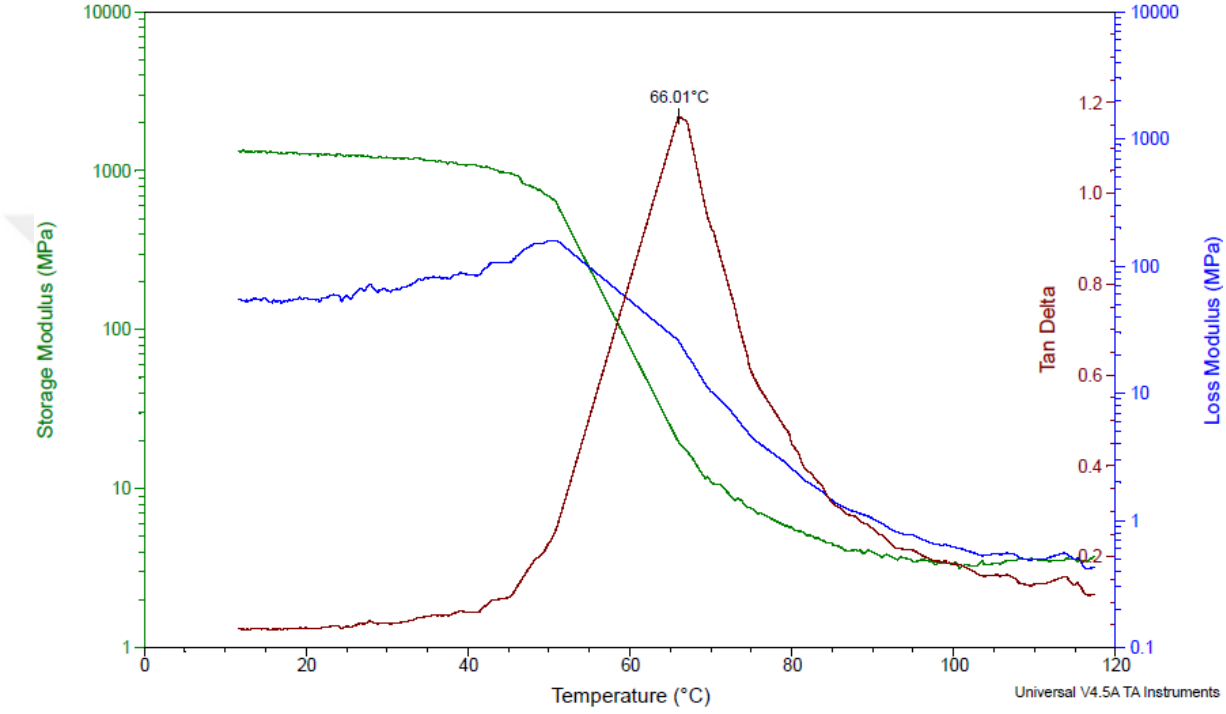

Figure 4.23 Results of temprature ramp tests and T_g of HS clearcoat (reference)

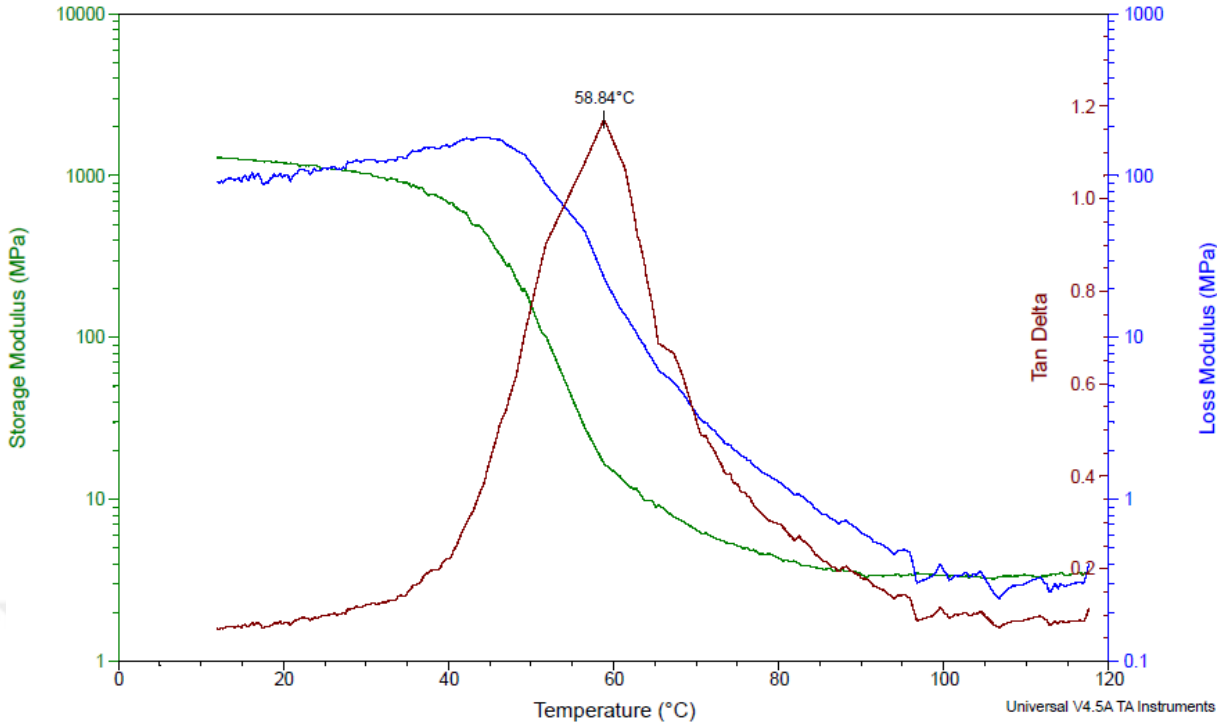

Figure 4.24 Results of temprature ramp tests and T_g of HS Hybrid clearcoat i.e. contains 1.75phr TS10M

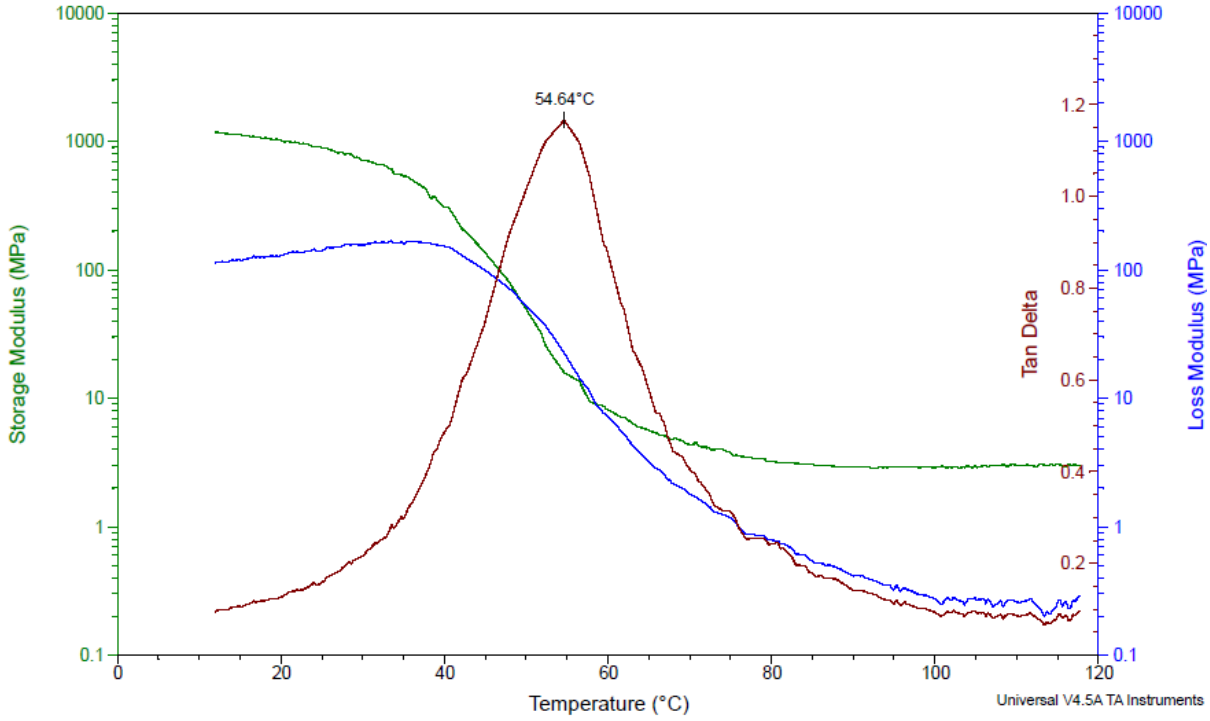

Figure 4.25 Results of temprature ramp tests and T_g of HS Hybrid clearcoat i.e. contains 3phr TS10M

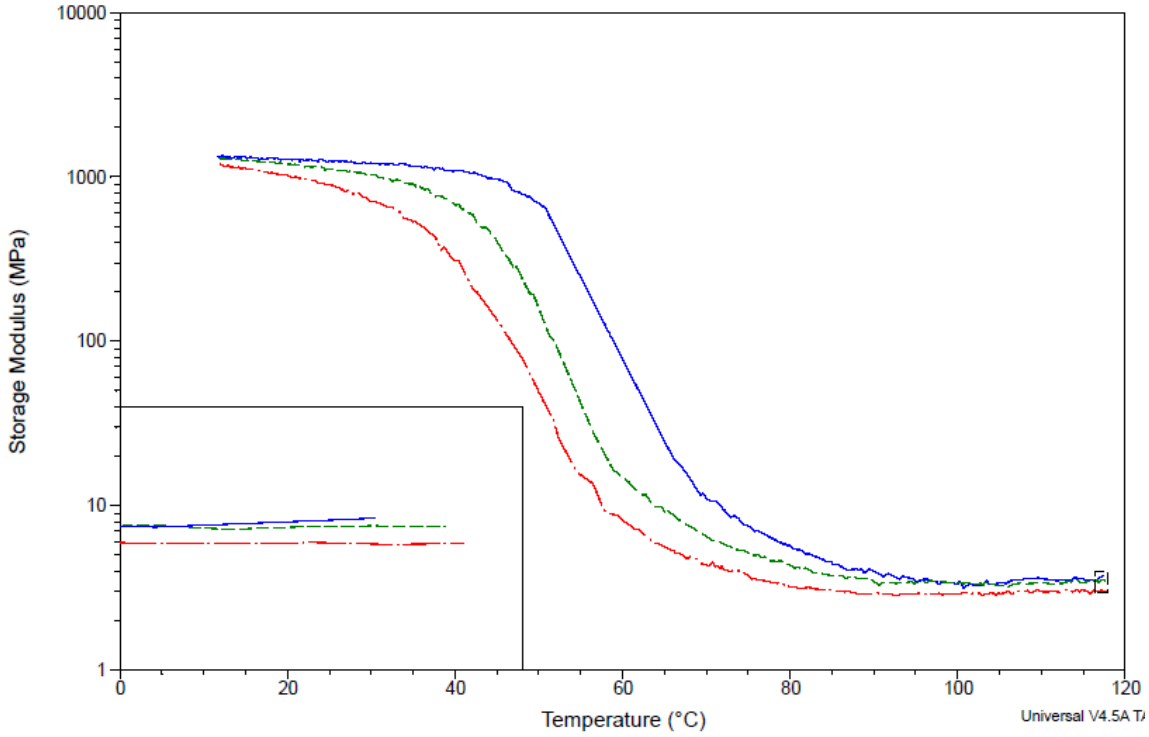

Figure 4.26 Results of temperature ramp test and storage modulus of HS clearcoat (blue), HS Hybrid clearcoat i.e. contains 1,75phr TS10M (green) and 3phr TS10M (red)

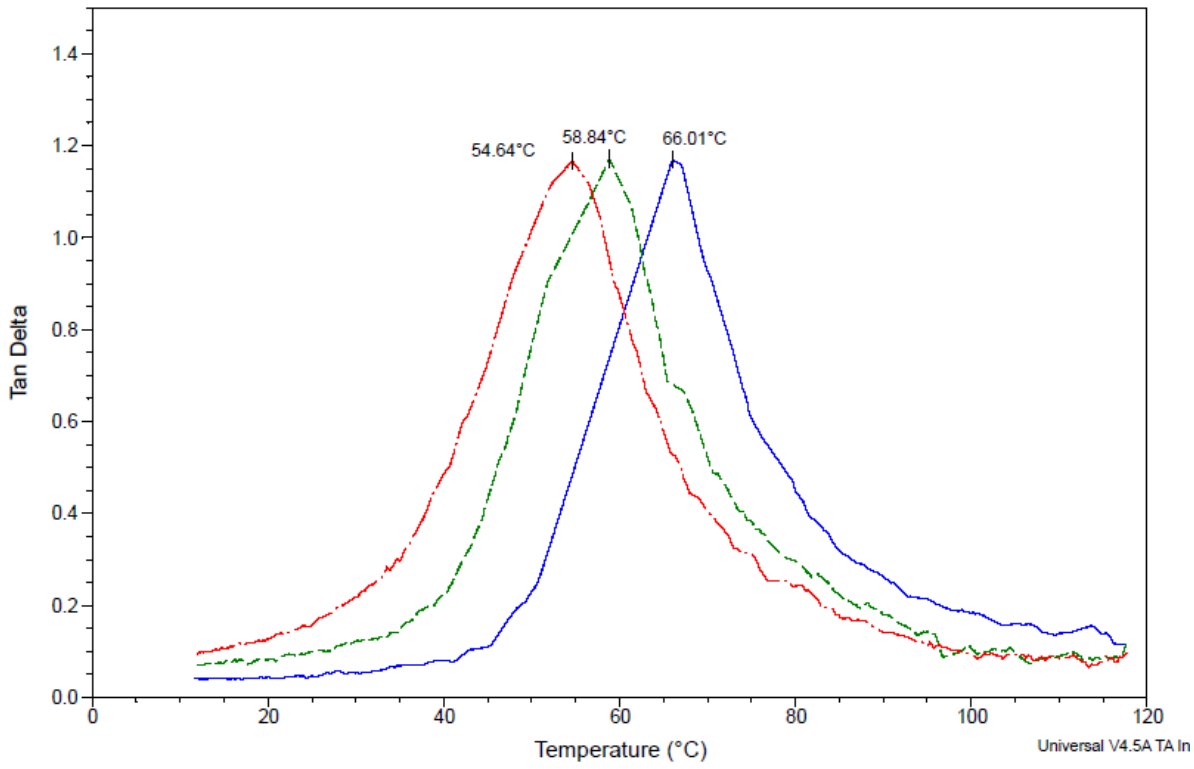

Figure 4.27 Results of temperature ramp test and Tg of HS clearcoat (blue), HS Hybrid clearcoat i.e. contains 1,75phr TS10M (green) and 3phr TS10M (red)

Overall assessment of dynamic mechanical and thermal analysis

As it can be seen in Table 4.6, when surface treated “sol-gel” SiO2 nano particle concentration of hybrid HS clearcoats was increased, mechanical and thermal response of hybrid coating changed considerably.

Regarding scratch resistance property of hybrid HS clear coat, crosslink density, toughness and stiffness are critical. Toughness, crosslink density and Tg have to be high enough and stiffness /elastic properties has to be optimized. Consequently, HS Hybrid CC 1.75phr TS10M can be appropriate due to its toughness and young modulus values.

Table 4.6 Results of dynamic mechanical and thermal analysis

HS CC	Tg [°C]	E' [MPa] @ Tg+50 [°C]	Mc [g/mol]	Young's Modulus [MPa]	Yield Strength [MPa]	Ultimate Strength [MPa]	Fracture Point [MPa]	Strain @ Fracture Point [%]	Toughness [MJ/m3]
Ref	66.01	3.55	2871	905	40.01	-	18.35	20.83	626.62
1.75 phr	58.84	3.38	2958	557.6	27.01	-	26.59	110.2	2763.65
3.00 phr	54.54	2.97	3330	286.6	11.38	15.66	19.08	93.09	1474.37

4.4.4. Film formation kinetics of hybrid clearcoat

As it can be seen in Figure 4.28, when concentration of surface treated SiO_2 nano particles in hybrid HS clearcoats was increased, curing rate i.e., temperature dependent ion viscosity change behavior was speeded up due to methanol concentration of TS10M. However, in some case such curing characteristics are desired especially such low bake and 2K systems. In addition, curing rate is related to final crosslink density of coating system.

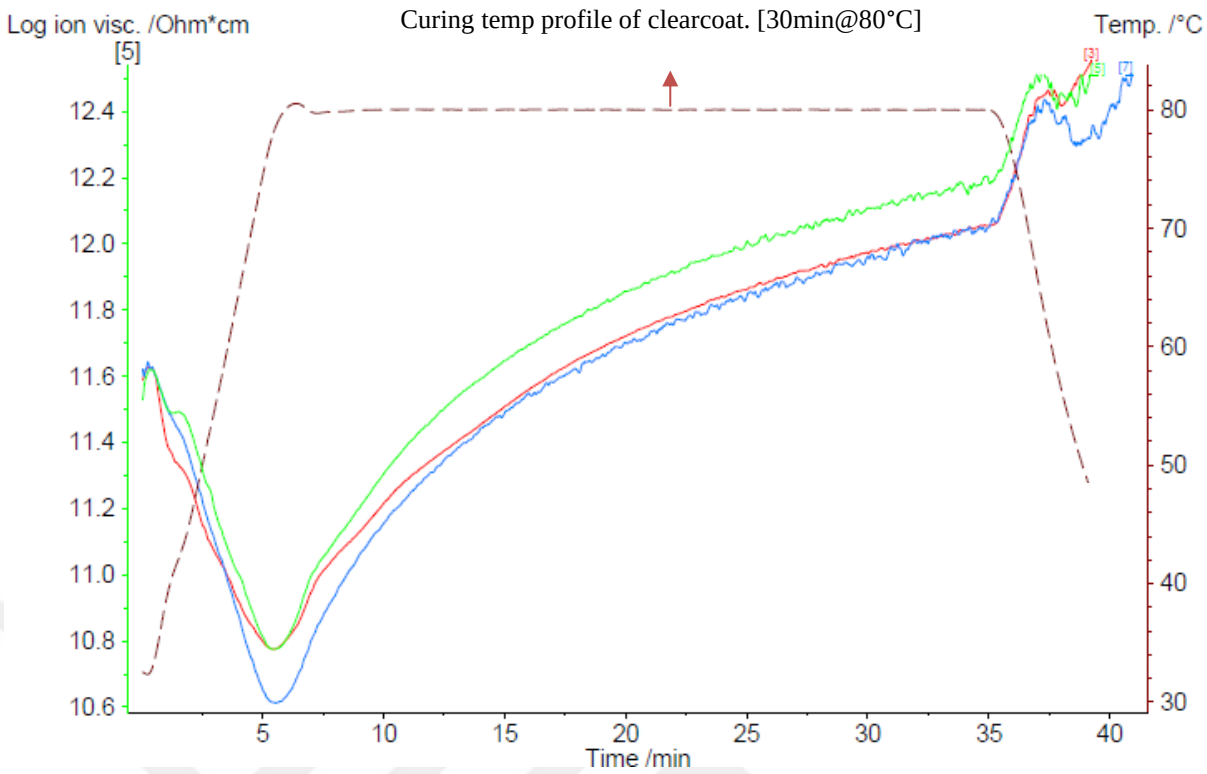

Figure 4.28 Film formation kinetics of HS clearcoat (blue), HS Hybrid clearcoat i.e. contains 1,75phr TS10M (green) and 3phr TS10M (red)

4.4.5. Static and dynamic surface tension of hybrid clearcoat

Results of static surface tension were given in Figure 4.29. It was determined that static surface tension of hybrid HS clearcoat containing surface treated SiO_2 nano particles was decreased. This may be occurred due to possible sedimentation of nano SiO_2 particles. So, the surface free energy of SiO_2 nano particles is higher than those of solvents.

Regarding dynamic surface tension results (Figure 4.30), at low surface age value, surface tension value of HS Hybrid CC 1.75phr TS10M could not be measured so high compared with those of HS CC (reference) and HS Hybrid CC 3phr TS10M . Due to this property HS Hybrid CC 1.75phr TS10M can be promising for further evaluations.

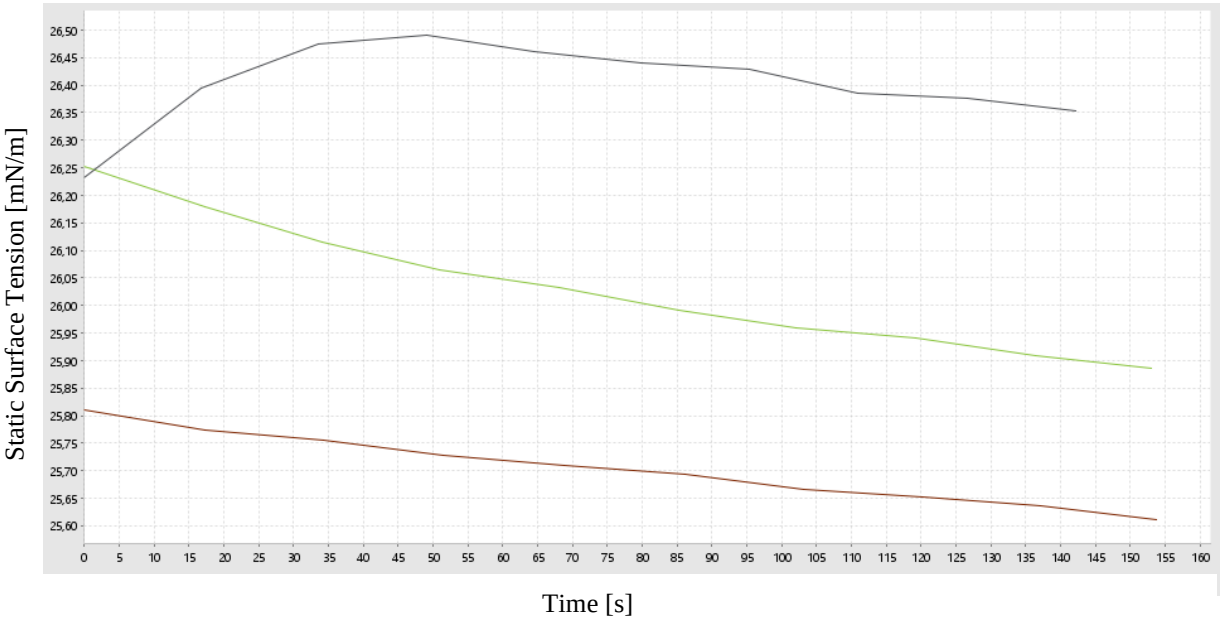

Figure 4.29 Static surface tension of HS CC (black), HS Hybrid CC 1.75phr TS10M (green) , HS Hybrid CC 3phr TS10M (red)**.**

Table 4.7 Average static surface tension of HS clearcoat, HS Hybrid clearcoat i.e. contains 1,75phr TS10M and 3phr TS10M

	<SST> [mN/m]
HS clear coat	25,703
Hybrid 1,75phr	26,033
Hybrid 3.00phr	26,404

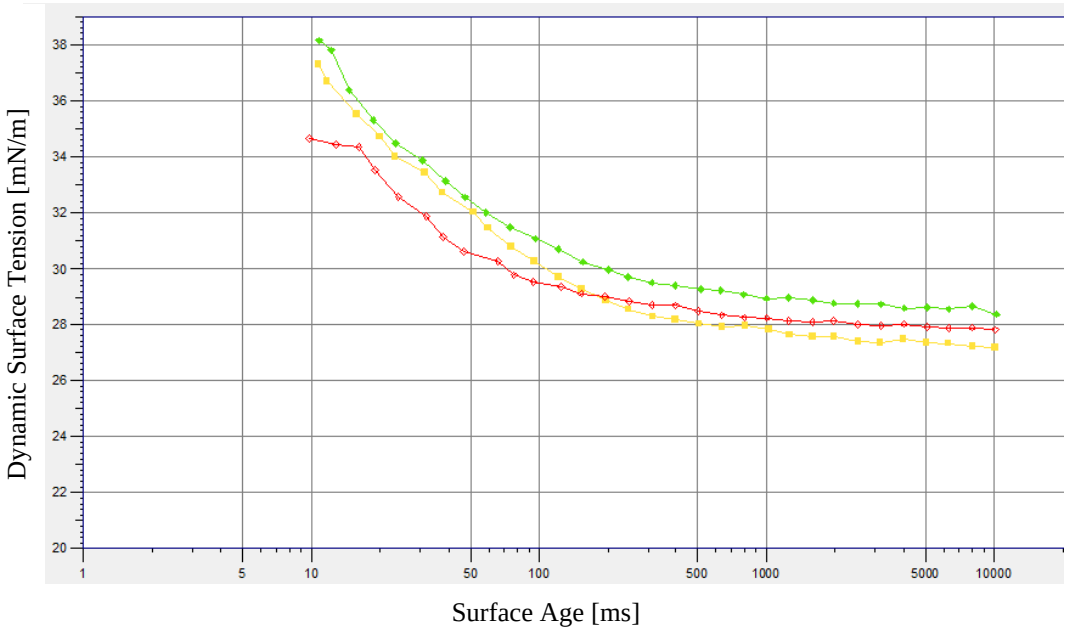

Figure 4.30 Dynamic surface tension of HS CC (green), HS Hybrid CC 1.75phr TS10M (red) and HS Hybrid CC 3phr TS10M (yellow)

4.4.6. Surface free energy of hybrid clearcoat

It was determined that surface free energy of surface treated "sol-gel" SiO2 nano particle containing hybrid HS clearcoats decreased and those polar components of surface tension also increased. It may be occurred due to surface treatment of nano SiO2 particles. It seems that surface treated "sol-gel" SiO2 nano particles were being transferred during their film formation mechanism. As it is known, SiO2 particles are polar due to their hydroxyl if they are located near to surface-air interface, contact angle of semi-polar liquid on the clear coat has to increase as stated in Table 4.8.

Table 4.8 Results of surface free energy and contact angle measurements of HS CC, HS Hybrid CC 1.75phr TS10M and HS Hybrid CC 3phr TS10M

	Surface Free Energy [mN/m]	Disperse Part of SFE [mN/m]	Polar Part of SFE [mN/m]	Contact Angle of Water [°]	Contact Angle of Diido methane [°]
HS CC	45.32	42.95	2.37	81.79	32.96
HS Hybrid CC 1.75phr TS10M	39.86	36.27	3.59	81.7	46.38
HS Hybrid CC 3phr TS10M	39.33	36.24	3.09	83.27	46.43

4.4.7. Water uptake of hybrid clearcoat

Water uptake performance of hybrid HS clearcoats containing surface treated SiO_2 nano particles were tried to calculate. When concentration of nano SiO_2 particles in the hybrid clearcoat increased, water uptake ratio also increased because of hydrophilic characteristic of SiO2 particles (Table 4.9)

In automotive coatings industry, hydrophilic clearcoats are not desired. Therefore, instead of HS Hybrid CC 3phr TS10M, HS Hybrid CC 1.75phr TS10M or less ones has to be proposed.

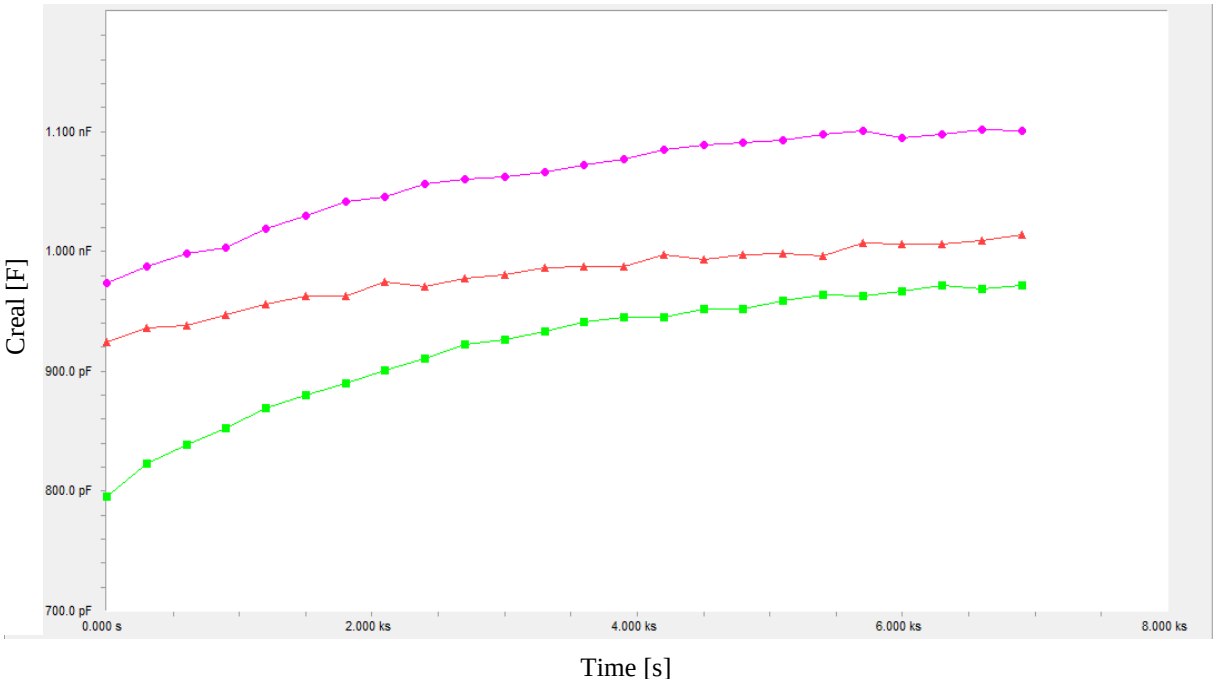

Figure 4.31 Capacitance increase within 2h of HS clearcoat (red), HS Hybrid CC 1.75phr TS10M (pink) and HS Hybrid CC 3phr TS10M (green)

Table 4.9 Water uptake ratio of hybrid HS clearcoat

	HS CC	HS Hybrid CC 1.75phr TS10M	HS Hybrid CC 3phr TS10M
WaterUptake % @ 2h	2.12	2.80	4.56

4.4.8. Scratch resistance and hardness of hybrid clearcoat

Results of scratch resistance experiments were summarized in Table 4.10. Regarding scratch resistance properties of hybrid clear coats, HS Hybrid CC 1.75phr TS10M was seemed to give better scratch resistance than HS Hybrid CC 3phr TS10M in terms of gloss retention.

Table 4.10 Results of scratch resistance experiments and evaluation of scratch resistance performance of hybrid HS clearcoats

	HS Clearcoat		HS Hybrid CC 1.75phr TS10M		HS Hybrid CC 3phr TS10M	
	Gloss @ 20°	Gloss Retention [%]	Gloss @ 20°	Gloss Retention [%]	Gloss @ 20°	Gloss Retention [%]
Initial	90.1	-	90.2	-	90.3	-
Nail Scratch Test (0.5kg)	81	90	86.8	96	84.3	94
Nail Scratch Test (1 kg)	68.7	76	84.5	94	79.3	88
Crockmeter Test	17.7	20	31.9	35	23.2	26

4.4.9. Control of visual appearance and mechanical performance of hybrid clearcoat

Related to visual appearance and mechanical performance controls of hybrid clear coats,

- “Sol-gel” SiO2 nano particles in the hybrid clearcoats were seemed to cause haze problem although there was not any color difference.
- OP, Lw and Sw values of hybrid clearcoats were not as good as reference. This might be occurred due to methanol content of TS10M
- Other mechanical performance test results verified the obtained DMA test results

Table 4.11 Evaluation of visual appearance and mechanical performance of hybrid clearcoats

	HS Clear coat	Hybrid Clearcoat 1,75phr	Hybrid Clearcoat 3phr
Dry film thickness	25.6	0.13	0.34
L	25.6	0.13	0.34
a	-0.18	-0.01	0.01
b	-0.71	-0.25	-0.29
dE	-	0.29	0.45
Initial Gloss 20°/60°/85°	90.1/93.1/97.3	90.2/93.3/88.1	90.3/92.4/97.7
DOI	93.1	94.3	93.6
OP	70.4	34.5	47.2
LW	3	19.3	10
SW	13.1	11.8	15.3
Haze on Glass	0.08	4.51	6.47
Reverse Impact Resistance	15	10	15
Diamond Scratch Resistance	1.5N	1.5N	2N
Pendulum Hardness [persoz]	108	100	83
Pencil Hardness	2B	HB	HB
Elasticity, Cupping (0,2mm/s)	6.6	5.5	6.5
Initial Adhesion	OK	OK	OK
Conical bending	OK	OK	OK
Adhesion after 40'C water immersion 1week	OK	OK	OK
Adhesion after moisture exposure test 10days	OK	OK	OK
Stone chip resistance 2bar 1cycle	1B	1C	1B
Stone chip resistance 2bar 2cycle	0B	2C	0B

5. CONCLUSION

In this thesis, silica nano particles were synthesized by sol-gel method. These particles were tried to use in automotive hybrid clearcoat formulations and promising results were obtained. Overall assessment of the thesis can be summarized as:

- In order to maximize the efficiency of nano particles synthesis, methanol was selected as main solvent by analysing mass of SiO_2 particles synthesized in 21 solvents including water. Therefore non-volatile percentage i.e. concentration of SiO_2 nano particles in the sol could be increased.
- By using Hansen Solubility Parameters program, dispersibility parameters of SiO_2 particles synthesized by "sol-gel" method ~~was~~ were determined as (d:15.33, p:10.66, h:20.82)
- Design of experiment (DOE) was used to optimize the variables that may affect the responses directly. Consequently, result oriented experiments could be carried out.
- From DOE it was seen that, NV% was dependent on amount of precursor-TEOS, catalyst type and reaction time. Z-average and zeta potential were dependent on catalyst type.
- To obtain mono-dispersed and almost spherical nano SiO_2 particles in less than 100nm size, aqueous 25% NH4OH solution was used.
- Molar ratio of nH2O/nTEOS was investigated within miscibility zone. Firstly, results of "1:1", "2:2" and "4:3" were checked. The ratio higher than 2 was found to be appropriate in terms of efficiency. However, when amount of water was increased, this may lead critical surface defect on the clearcoat. Optimum conditions can be reached.at nH2O/nTEOS = 2
- In order to increase SiO_2 concentration in the sol, precursor i.e. TEOS amount was increased within the miscibility zone. Owing to mentioned optimization, TS10, nano-sized SiO_2 particles, containing 9.54 NV%, 67.2nm z-average and -26.6mV zeta potential properties could be synthesized by "sol-gel" method. Surface of TS10 was tried to be covered or treated by wetting and surface treatment (silane) agents having different functionalities.

- Related to surface treatment, isoelectric point of TS10 was found as acidic (pH 1.3)
- Wetting and dispersing agents were firstly evaluated with TS10 powder wettability test. Nonetheless, only wetting and dispersing agent-H slightly increased the wetting performance (~6%). Further investigations related to wetting and dispersing agents could not be carried out because of the fact that unpromising TS10 wettability results.
- Different functional groups such as -vinyl, -methacyl, mercaptan, -octyl, -amino were used for the surface treatment of TS10.
- The best compatibility performance was obtained by Silane Agent-A whose functional group is –vinyl. Surface treatment was performed at different ratios of silane: SiO_2 such as 0.1:1, 0.5:1, 1:1, and 2:1.
- Silane Agent- A treated TS10 was named as TS10M and characterization of TS10M was performed by FTIR, TGA and SEM.
- FTIR spectrum according to peak at 1410 cm^{-1} showed that surface treatment efficiency at silane: SiO_2 ratio = 0.5:1 was higher than those of 1:1 and 2:1.
- TGA also verified the FTIR spectrum: The ratio 0.5:1 has higher overall weight loss at 800°C.
- SEM images provided information about shape and size of TS10 and TS10M particles
- Characterizations of HS clearcoats, HS clearcoat, HS Hybrid CC 1.75phr TS10M and HS Hybrid CC 3phr TS10M were carried out.
- Firstly polarities of MS and HS type automotive clearcoats were compared. HS was found to be more polar and it is concluded that HS is compatible with TS10M and more appropriate for further trials.
- When concentration of SiO_2 nano particles were increased from 1.75phr to 3phr in the hybrid clear coat, rheological properties changed. 3phr usage in TS10M increased the hysteresis area and changed thixotropic behavior i.e., increased viscosity recover rate. In addition, it made the HS clear coat more elastic at low shear rate. 1.75phr usage in TS10M in the HS clear coat did not affect the rheological and viscoelastic properties. According to

rheological point of view, 1.75 phr usage in TS10M was seemed to be more promising.

- Regarding DMTA analysis, it was seen that, when concentration of surface treated SiO_2 nano particles in hybrid HS clearcoats increases, mechanical and thermal responses of hybrid coating considerably changed.
- Considering scratch resistance property of hybrid HS clearcoats, their crosslink density, toughness and stiffness properties are critical. Toughness, crosslink density and T_g have to be high enough and stiffness /elastic properties has to be optimized. Consequently, 1.75 phr usage in TS10M was suitable due to its toughness and young modulus values.
- Regarding cure kinetics, when concentration of surface treated SiO_2 nano particles in hybrid HS clearcoats was increased, curing rate i.e., temperature dependent ion viscosity change behavior due to methanol concentration of TS10M, was speeded up.
- According to static surface tension control, it was determined that static surface tension of hybrid HS clearcoat containing surface treated SiO2 nano particles is decreased. This may be occurred due to possible sedimentation of nano SiO_2 particles. Because surface free energy of SiO_2 nano particles is higher than those of solvents.
- According to dynamic surface tension measurements, at low surface age value, surface tension of HS Hybrid CC 1.75phr TS10M could not be measured so high compared with HS clearcoat and HS Hybrid CC 3phr TS10M. HS Hybrid CC 1.75phr TS10M was decided to be appropriate for further evaluations due to this property.
- It was determined that surface free energy of hybrid HS clearcoats containing surface treated SiO_2 nano particle decreases and polar components of surface tension also increase. This might be occurred due to surface treatment of nano SiO_2 particles. It seems that surface treated SiO2 nano particles are transferred during their film formation mechanism.
- Water uptake performance of hybrid HS clearcoats containing surface treated SiO_2 nano particles were tried to calculate. When concentration of nano SiO_2 particles in the hybrid clearcoat increased, water uptake ratio also increased because of hydrophilic characteristics of SiO_2 particles.

- Regarding scratch resistance properties of hybrid clear coats, HS Hybrid CC 1.75phr TS10M was seemed to give better scratch resistance than that of HS Hybrid CC 3phr TS10M in terms of gloss retention.
- Control of visual appearance and mechanical performance of hybrid clear coats were performed. SiO2 nano particles in the hybrid clearcoats were caused haze problem although there was not any color difference. OP, Lw and Sw values of hybrid clearcoats were not as good as reference. This might be occurred due to methanol content of TS10M. Other mechanical performance test results confirmed the obtained DMTA test results.

6. FUTURE WORKS

- Different functionalities of silane surface treatment agents can be used to modify the SiO2 surface.
- Concentration of SiO2 nano scale particles in sol to gel process can be optimized and increased.
- Surface treatment can be analyzed by XPS and NMR technique
- Sample preparation for SEM can be performed with spin coater to increase resolution of image.
- Organic and inorganic polymer synthesis can be conducted.

REFERENCES

Abbott, S., & Hansen, C. M. 2008. Hansen solubility parameters in practice. Hansen-Solubility.

An Y., Chen M., Xue Q., 2007, Preparation and self-assembly of carboxylic acid functionalized silica, Journal of Colloid and Interface Science 311, 507–513.

Arkles, B. 2006. Silane coupling agents: connecting across boundaries v2. 0. Gelest. Inc., Morrisville, PA, 16.

Athawale V. D., Kulkarni M.A., 2011, Synthesis and performance evaluation of polyurethane/silica hybrid resins, Pigment & Resin Technology 40/1 49–57.

Bailey J. K. , Mecartney M. L., 1992, Formation of colloidal silica particles from alkoxides,
Colloids and Surfaces, vol. 63, no. 1-2, pp. 151–161.

BiolinScientific 2018, https://www.biolinscientific.com/

Boday D., Tolbert S., Keller M., 2014, Non-hydrolytic formation of silica and polysilsesquioxane particles from alkoxysilane monomers with formic acid in toluene/tetrahydrofuran solutions, Nanopart Res 16:2313.

Bogush G.H., Tracy M. A., Zukoski C. F., 1988, Preparation of monodisperse silica
particles: control of size and mass fraction. Journal of Non-Crystalline Solids, vol. 104,
no. 1, pp. 95–106,

Brochier Salon, M. C., & Belgacem, M. N. 2011. Hydrolysis-condensation kinetics of different silane coupling agents. *Phosphorus, Sulfur, and Silicon*, *186*(2), 240-254.

Castela, A. S., & Simoes, A. M. 2003. Assessment of water uptake in coil coatings by capacitance measurements. *Progress in Organic Coatings*, *46*(1), 55-61.

Collins A. M., 2012, Nanotechnology cookbook: practical, reliable and jargon-free experimental procedures. (1st ed.), Elsevier, Netherlands.

Fairhurst, D. 2013 **.** An overview of the zeta potential part 3: uses and applications. American Pharmaceutical Review.

Fernando R.H., Sung L.P., 2009, Nanotechnology applications in coatings. (1st ed.)American
Chemical Society. Washington, DC, USA.

Fouilloux S., Daillant J.,Thill A., 2012, Single step synthesis of 5–30 nm monodisperse silica nanoparticles: Important experimental parameters and modeling, Colloids and Surfaces A: Physicochem. Eng. Aspects 393, 122– 127

Green D. L., Lin J. S., Lam Y. F., Hu M. Z., Schaefer D. W., Harris M. T., 2003, Size,
volume fraction, and nucleation of Stöber silica nanoparticles. Journal of Colloid and
Interface Science, vol. 266, no. 2, pp. 346–358.

Guo J., Liu X., Cheng Y., 2008, Size-controllable synthesis of monodispersed colloidal silica nanoparticles via hydrolysis of elemental silicon, Journal of Colloid and Interface Science 326 138–142

Hansen, C. M. 2002. Hansen solubility parameters: a user's handbook. CRC press.

Hassan A.F, Abdelghny A.M., Elhadidy H., Youssef A.M., 2014, Synthesis and characterization of high surface area nanosilica from rice husk ash by surfactant-free sol–gel method, J Sol-Gel Sci Technol., 69:465–472.

Bodycomb, J., & Scientific, Horiba (2014). Introduction to Dynamic Light Scattering for Particle Size Determination. Horiba Scientific.

Innocenzi P., 2016, The sol to gel transition.(1st ed.) Springer International Publishing. Switzerland.

Instruments, G. 2007. Basics of electrochemical impedance spectroscopy. G. Instruments, Complex impedance in Corrosion, 1-30.

Jones, F. N., Nichols, M. E., & Pappas, S. P. 2017. *Organic coatings: science and technology*. John Wiley & Sons. USA

Jonschker G., 2014, Sol-gel technology in praxis .(1st ed.) European Coating. Germany

Kar K.K., Pandey J.K., Rana S., 2015, Handbook of polymer nanocomposite: Processing,
performance and application Springer-Verlag Berlin Heidelberg.

Kim, H. G. 2002, Dielectric cure monitoring for glass/polyester prepreg composites. Composite structures, 57(1-4), 91-99.

Krüss GmbH 2018, https://www.kruss-scientific.com/contact/

Lane J., Manzano M., Hay J., 2004 Synthesis of Organic-Inorganic Hybrid Particles by Sol-Gel Chemistry, Journal of Sol-Gel Science and Technology 31, 31–36

Lee, H. L. 2014. The handbook of dielectric analysis and cure monitoring. *Boston, MA, Lambient Technology LLC*, *156*.

Lee K, Sathyagal A. N., McCormick A. V., 1998, A closer look at an aggregation model of
the Stober process. Colloids and Surfaces A, vol. 144, no. 1–3, pp. 115–125.

Levy D., Zayat M., 2015, The sol-gel handbook; syntheisi characterization and applications., Wiley, Singapure

Liaw W., Chen K., 2007, Preparation and Properties of Poly(imide siloxane) Segmented Copolymer/Silica Hybrid Nanocomposites, Journal of Applied Polymer Science, Vol. 105, 809–820

Li, Y. F., Xiao, M. Z., Wu, Z., Peng, K., Han, C. M., Xiang, W., & Dai, J. Y. 2016, July. Effects of epoxy/hardener stoichiometry on structures and properties of a diethanolamine-cured epoxy encapsulant. IOP Publishing.

Liu G., Li L., Yang X., Dai Z. 2008, Preparation of silica/polymer hybrid microspheres and the corresponding hollow polymer microspheres with functional groups, Polym. Adv. Technol. , 19: 1922–1930

Lin, J., Chen, H., Ji, Y., & Zhang, Y. 2012, Functionally modified monodisperse core–shell silica nanoparticles: Silane coupling agent as capping and size tuning agent. Colloids and Surfaces A: Physicochemical and Engineering Aspects, 411, 111-121

Lu Y., McLellan J., Xia Y., 2004, Synthesis and Crystallization of Hybrid Spherical Colloids
Composed of Polystyrene Cores and Silica Shells, Langmuir, 20, 3464-3470.

Malvern, I. 2011 . Inform white paper dynamic light scattering. Malvern: Malvern Instruments Ltd, 1-6.

Malkin, A. Y., Isayev, A. I. 2017. Rheology: concepts, methods, and applications. Elsevier Canada

Mittal V., 2011, Advance polymer nanoparticles, synthesis and surface modifications. (1st
ed.), CRC Press Taylor & Francis Group.

Mishra A. K., 2017, Sol-gel based nanoceramic materials: preparation, properties and
Applications. (1st ed.) Springer International Publishing. Switzerland.

Moriguchi, K. 2013. Silane: chemistry, applications and performance. Nova Science Publishers, Incorporated.

Murray E., Born P., Weber A., 2014, Robust, ultrasmall organosilica nanoparticles without silica Shells, Nanopart Res., 16:2462.

Naka Y., Komori Y., Yoshitake H., 2010, One-pot synthesis of organo-functionalized monodisperse silica particles in W/O microemulsion and the effect of functional groups on addition into polystyrene Colloids and Surfaces A: Physicochem. Eng. Aspects 361,162–168.

Niederberger M., Pinna N., 2009, Metal oxide nanoparticles in organic solvents, synthesis,
formationi assembly and application. (1st ed.) , Engineering materials and processes,
Springer

Rahman I. A., Vejayakumaran P., Sipaut C. S., 2007, An optimized sol-gel synthesis of
stable primary equivalent silica particles. Colloids and Surfaces A, vol. 294, no. 1–3, pp.
102–110.

Roylance, D. 2001. Stress-strain curves. Massachusetts Institute of Technology study, Cambridge.

Paar, A. 2015. The modular compact rheometer series. Retrieved, 3, 16.

Peruzzo P., Anbinder P., Pardini F., 2016, On the strategies for incorporating nanosilica aqueous dispersion inthe synthesis of waterborne polyurethane/silica nanocomposites:Effects on morphology and properties, Materials Today Communications 6, 81–91.

Singh, J. P., & Verma, S. 2016. Woven Terry Fabrics: Manufacturing and Quality Management. Woodhead Publishing.

Sitthiracha M., Kilmartin P., Edmond N., 2015, Novel organic–inorganic hybrid materials based on epoxy-functionalized silanes, Sol-Gel Sci Technol., 76:542–551

Sprenger S. , 2016, The effects of silica nanoparticles in toughened epoxy resins and fiber-
reinforced composites.(1st ed.) Hanser Publications, Cincinnati, Ohio.

Streitberger, H., Dössel, K., 2008. Automotive paints and coatings .Wiley, Germany

TA Instrument, 2018, http://www.tainstruments.com/wp-content/uploads/dma.pdf

Voutou, B., Stefanaki, E. C., Giannakopoulos, K. 2008. Electron microscopy: The basics. Physics of advanced materials winter school, 1(11)

Vega-Baudrit J., Navarro-Banon V., Vazquez P., Martin-Martinez J.M., 2006, Addition of nanosilicas with different silanol content to thermoplastic

polyurethane adhesives, International Journal of Adhesion & Adhesives 26 378–387.

Wang H., Fang J., Cheng T., 2008, One-step coating of fluoro-containing silica nanoparticles for universal generation of surface superhydrophobicity, Chem. Commun., 877–879

Wen M. , Dusek K., 2017, Protective coatings-film formation ans properties, Springer, Switzerland

Yu Y., Chen W., 2003, Transparent organic–inorganic hybrid thin films prepared from acrylic polymer and aqueous monodispersed colloidal silica, Materials Chemistry and Physics 82 388–395.

Yuan, X., Yue, Z. F., Chen, X., Wen, S. F., Li, L., & Feng, T. 2015. EIS study of effective capacitance and water uptake behaviors of silicone-epoxy hybrid coatings on mild steel. *Progress in Organic Coatings*, *86*, 41-48.

Zeno W., Jones N., Pappas P., 2007, Organic coatings, John Wiley & Sons, USA

Zhang X-T, Sato O., Taguchi M., Einaga Y., Murakami T., Fujishima A., 2005, Self-

Cleaning Particle Coating with Antireflection Properties. Chem. Mater., 17 696–700

Zou H., Wu S., Shen J., 2008, Polymer/silica nanocomposites: preparation, characterization,

properties, and applications. America Chemical Society, 108, 3893-3957.

ACKNOWLEDGEMENT

I would like express my gratitude to my supervisor, Prof. Dr. Şerife Ş. HELVACI for her guidance and support throughout this MSc thesis.

I am very grateful to Selim YETİŞ, Director of Kansai Altan R&D Center and Özlem ÜNLÜ IŞIK, Manager of Kansai Altan Automotive Coating Laboratory Manager for their guidance and great patience and opportunities provided to me for this thesis

Finally, I would like thank my wife and my unborn son for their endless support and patience which help me to complete this thesis.

RESUME

NECATİ GÜDÜMCÜOĞLU
Phone: (506)9310156
e-mail:necatigo@gmail.com
Address: Soğukpınar Mah.
264 Sk. No:17 A/4 Kemalpaşa
İzmir/TURKEY

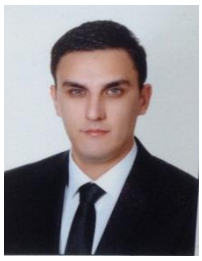

EDUCATION

2008 - 2012

TURKEY

B.S. – Double Major
Middle East Technical University / Ankara-

Department of Chemical Engineering
CGPA: 3.25 / 4.00

2007 – 2011

TURKEY

B.S. - Major
Middle East Technical University / Ankara-

Physics Department
CGPA: 3.46 / 4.00

2002 – 2006

/Izmir-TURKEY

High School:
HulusiUçaçelik Anatolian High School

Mathematics – Science Branch
CGPA: 4.72 / 5.00

WORK EXPERIENCE

May 2014-
TURKEY

Kansai Altan Boya Sanayi A.Ş. /Izmir-

R&D Department / R&D Engineer
OEM Car Repair, Plastic and Metal Paints

March 2013- May 2014

Saint-Gobain Weber / Izmir- TURKEY
R&D Department / R&D Engineer
External Thermal Insulation Composite Systems *(ETICS)*
Mineral Renders &Coatings
Tile Adhesives
Scientific and Technological Research Council of Turkey TUBITAK-TEYDEB Project

January 2012-June 2012 **Terralab Instruments A.Ş/Ankara-TURKEY**
R&D department / R&D Engineer
Total Organic Carbon (TOC) Analysis Laboratory Instrument

August 2010 (Intern) **TÜPRAŞ /Izmir-TURKEY**
Atmospheric distillation unit
Learned separation principles and calculated number of trays in column

July 2010 (Intern) **Shell&Turcas Petrol A.Ş. /Kocaeli-TURKEY**
Quality control laboratory
Performed various quality control measurements

Lubricants and grease manufacturing
Learned production processes and observed continuous stirred-tank reactor

LANGUAGES

- **Turkish** (native language)
- **English** – good command in reading, writing and speaking

REFERENCES

Available upon request